RESEARCH REPORT 2945-1

EVALUATION OF CATHODIC PROTECTION SYSTEMS FOR MARINE BRIDGE SUBSTRUCTURES

Leandro Etcheverry, David W. Fowler, Harovel G. Wheat, and David P. Whitney

CENTER FOR TRANSPORTATION RESEARCH
BUREAU OF ENGINEERING RESEARCH
THE UNIVERSITY OF TEXAS AT AUSTIN

DECEMBER 1998

Technical Report Documentation Page

1. Report No.	2. Government Accession No.	3. Recipient's Catalog No.
TX-00/2945-1		

4. Title and Subtitle	5. Report Date
EVALUATION OF CATHODIC PROTECTION SYSTEMS FOR MARINE BRIDGE SUBSTRUCTURES	December 1998
	6. Performing Organization Code
7. Author(s)	8. Performing Organization Report No.
Leandro Etcheverry, David W. Fowler, Harovel G. Wheat, and David P. Whitney	2945-1
9. Performing Organization Name and Address	10. Work Unit No. (TRAIS)
Center for Transportation Research The University of Texas at Austin 3208 Red River, Suite 200 Austin, TX 78705-2650	11. Contract or Grant No. 7-2945
12. Sponsoring Agency Name and Address	13. Type of Report and Period Covered
Texas Department of Transportation Research and Technology Transfer Section/Construction Division P.O. Box 5080 Austin, TX 78763-5080	Research Report (9/98 — 12/98)
	14. Sponsoring Agency Code

15. Supplementary Notes

Project conducted in cooperation with the Texas Department of Transportation.

16. Abstract

Four different cathodic protection systems were installed and evaluated in the reinforced concrete tie beams and footings of four bents at the Queen Isabella Causeway which links South Padre Island to the mainland of Texas. The types of cathodic protection systems installed and evaluated were impressed current sprayed zinc, sprayed titanium, titanium mesh with overlay and sacrificial sprayed zinc. The primary objectives of this study were to monitor and evaluate the installation of the different cathodic protection systems, to evaluate performance of the cathodic protection systems, to establish recommendations for full-scale application of cathodic protection for the Queen Isabella Causeway and to establish recommendations for the implementation of cathodic protection systems for marine bridge substructures in Texas. As part of this study, a pre-installation condition evaluation for the Queen Isabella Causeway was conducted. The purpose of the pre-installation evaluation was to assess the condition of the structure and the feasibility of cathodic protection as a rehabilitation option. The installation of the different cathodic protection systems was described, and the installation of the anode systems was evaluated using constructability, productivity, safety and environmental concerns, and aesthetics as the evaluation parameters. The preliminary performance of the cathodic protection systems was evaluated through field and remote monitoring. The field monitoring evaluations comprised visual inspection, delamination survey, half-cell potential measurements, corrosion rate measurements, chloride content determination, concrete permeability determination, rectifier and system component evaluation and polarization decay testing. As part of the performance evaluation, the variability of the sacrificial sprayed zinc system was studied with the remote monitoring capability. A simplified cost analysis was performed for the installed cathodic protection systems, which consisted in calculating the equivalent annual installation costs for a range of anode service lives. On the basis of the pre-installation condition evaluation, the field installation, the performance and the cost analysis, a cathodic protection system type was recommended for the Queen Isabella Causeway. Guidelines for the design, installation, monitoring and maintenance of the recommended system were provided as well as recommendations for the implementation of cathodic protection for marine bridge substructures in Texas.

17. Key Words	18. Distribution Statement
Bridge substructures, cathodic protection systems, installation, performance evaluation, Queen Isabella Causeway	No restrictions. This document is available to the public through the National Technical Information Service, Springfield, Virginia 22161.

19. Security Classif. (of report)	20. Security Classif. (of this page)	21. No. of pages	22. Price
Unclassified	Unclassified	180	

Form DOT F 1700.7 (8-72) Reproduction of completed page authorized

EVALUATION OF CATHODIC PROTECTION SYSTEMS FOR MARINE BRIDGE SUBSTRUCTURES

by

Leandro Etcheverry
David W. Fowler
Harovel G. Wheat
David P. Whitney

Research Report Number 2945-1

Research Project 7-2945
Project title: *A Performance Evaluation of Cathodic Protection Systems for Queen Isabella*

Conducted for the

TEXAS DEPARTMENT OF TRANSPORTATION

by the

CENTER FOR TRANSPORTATION RESEARCH
Bureau of Engineering Research
THE UNIVERSITY OF TEXAS AT AUSTIN

December 1998

DISCLAIMERS

The contents of this report reflect the views of the authors, who are responsible for the facts and the accuracy of the data presented herein. The contents do not necessarily reflect the official views or policies of the Texas Department of Transportation (TxDOT). This report does not constitute a standard, specification, or regulation.

There was no invention or discovery conceived or first actually reduced to practice in the course of or under this contract, including any art, method, process, machine, manufacture, design or composition of matter, or any new and useful improvement thereof, or any variety of plant, which is or may be patentable under the patent laws of the United States of America or any foreign country.

NOT INTENDED FOR CONSTRUCTION,
BIDDING, OR PERMIT PURPOSES

David W. Fowler, P.E. (Texas No. 27859)
Harovel G. Wheat, P.E. (Texas No. 78364)
R. L. Carrasquillo, P.E. (Texas No. 63881)
Research Supervisors

ACKNOWLEDGMENTS

Sincere appreciation is extended to the Texas Department of Transportation for its support in this project. Special thanks must be given to the project director, Ms. Robin Longwell; the construction project engineer, Mr. Armando Sandoval; the construction project inspector, Mr. Polo Ochoa; the Raymondville Area Engineer, Mr. Jacinto Garza; and, of course, the Pharr District Engineer, Mr. Amadeo Saenz, Jr.; and the Assistant District Engineer, Mr. I. Behoorz Badiozzamani. The authors thank Mr. Eduardo Gonzales and Mr. Jody Ellington of the Pharr District, who continue to provide support in the monitoring efforts. We also appreciate the contributions of C. W. Titus (CMD), who served on the project monitoring committee. Their hard work, close contact, and special considerations in this unfamiliar-technology construction and related-research project is what makes our interagency cooperative research agreements successful. Finally, we thank the technical people from Corrpro, Correxco, and Concorr. Without their considerable help in design, installation, and monitoring, the quality of this research project would be significantly diminished.

This report was prepared in cooperation with the Texas Department of Transportation.

SUMMARY

Four different cathodic protection systems were installed and evaluated in the reinforced concrete tie beams and footings of four bents at the Queen Isabella Causeway, which links South Padre Island to the mainland of Texas. The types of cathodic protection systems installed and evaluated were three impressed current types, including sprayed zinc, sprayed titanium, titanium mesh with overlay, and one sacrificial type of sprayed zinc. The primary objectives of this study were to monitor and evaluate the installation of the different cathodic protection systems, to evaluate performance of the cathodic protection systems, to establish recommendations for full-scale application of cathodic protection for the Queen Isabella Causeway, and to establish recommendations for the implementation of cathodic protection systems for marine bridge substructures in Texas.

As part of this study, a pre-installation condition evaluation for the Queen Isabella Causeway was conducted. The purpose of the pre-installation evaluation was to assess the condition of the structure and the feasibility of cathodic protection as a rehabilitation option. Overall, the structure was visually in good condition, though potentially in poor condition as evidenced by the chloride content and half-cell potential condition indicators. The condition of this structure made it an ideal candidate for cathodic protection.

The installation of the different cathodic protection systems is described, and the installation of the anode systems is evaluated using constructability, productivity, safety and environmental concerns, and aesthetics as the evaluation parameters. The application of the titanium mesh with overlay required adequate surface preparation to achieve bond to the substrate concrete. While sprayed zinc and the titanium mesh with overlay have colors similar to those of the surrounding concrete, titanium has a dark gold color with blue tints. The highest productivity in the installation of the anodes in the Queen Isabella Causeway was achieved for the sprayed zinc. The productivity was somewhat less for the sprayed titanium and substantially less for the titanium mesh with overlay.

The preliminary performance of the cathodic protection systems was evaluated through field and remote monitoring. The field-monitoring evaluations comprised visual inspection, delamination survey, half-cell potential measurements, corrosion rate measurements, chloride content determination, concrete permeability determination, rectifier and system component evaluation, and polarization decay testing. From the visual inspection, delamination survey, and half-cell potential surveys of the control members, it was evident that the progression of the deterioration was fairly rapid. This rapid progress of the deterioration was observed in a period of approximately 1 year. There were no signs of concrete deterioration in any of the bents protected with cathodic protection 9 months after installation. This observation confirmed the effectiveness of cathodic protection in arresting corrosion-induced concrete deterioration. Significant deterioration was observed in some of the anode materials. The sprayed titanium exhibited widespread minor disbondment of the anode material. The titanium mesh with overlay evidenced delaminations of the overlay. The increase in delaminated areas of the overlay over time was significant. The current density for the sprayed titanium was higher compared to the other impressed current systems. This difference was due to the low conductivity of the sprayed titanium anode and the

consequent higher applied current. This condition could result in accelerated electrochemical aging of the anode. Another indication of the low conductivity of the sprayed titanium system was the very low depolarization potentials for the reference cell that was located farthest from any of the two positive connections. The impressed current sprayed zinc exhibited adequate depolarization. The titanium mesh with overlay consistently had the highest depolarization values. Considering the sacrificial nature of the system, the galvanic sprayed zinc exhibited high depolarization values. The current readings for the sacrificial sprayed zinc readings were variable. The variability correlated well with changes in dew point between February and mid-April. Between mid-April and June, the correlation was not as good. A cyclic behavior for the current output during the course of a day was observed between mid-April and June. The higher temperatures and the solar radiation during the daytime hours could have resulted in drying of the concrete and, consequently, a decrease in the current output for the galvanic zinc.

On the basis of the simplified economic analysis conducted, the sprayed zinc systems were more cost effective than the sprayed titanium and titanium mesh with overlay anode systems for the Queen Isabella Causeway. A definitive selection could not be made between the impressed current and the sacrificial zinc systems based on the simplified economic analysis.

Based on the evaluation of the condition of the existing structure, the field installation, the performance, and the durability and cost analyses, the sacrificial sprayed zinc was the recommended cathodic protection system type for a full-scale installation at the Queen Isabella Causeway. The primary reasons for this selection rested on the installation simplicity, adequate performance to date, and both lower installation and projected costs with respect to any of the impressed current systems.

TABLE OF CONTENTS

CHAPTER 1. INTRODUCTION 1

1.1 Problem History 1
1.2 Objectives of Research Program 1
1.3 Organization 2

CHAPTER 2. CORROSION AND CATHODIC PROTECTION OF REINFORCING STEEL IN CONCRETE 3

2.1 Corrosion of Steel in Concrete 3
2.1.1 Protection of Steel in Concrete 3
2.1.2 Causes and Mechanisms of Corrosion 3
2.1.3 Corrosion Process 4
2.1.4 Microcell versus Macrocell Corrosion 5
2.1.5 Polarization 7
2.2 Cathodic Protection of Steel in Concrete 9
2.2.1 Principle 9
2.2.2 Impressed Current Systems 9
2.2.3 Sacrificial Systems 11
2.2.4 Impressed Current Versus Sacrificial Systems 12

CHAPTER 3. CATHODIC PROTECTION FOR BRIDGE SUBSTRUCTURES 13

3.1 Rehabilitation Strategies for Bridge Substructures 13
3.1.1 Patching 13
3.1.2 Encasement/Jacketing/Overlay 13
3.1.3 Steel Encapsulation 15
3.1.4 Deflection Systems 15
3.1.5 Coatings and Sealers 15
3.1.6 Corrosion Inhibitors 15
3.1.7 Electrochemical Techniques 16
3.2 Compatibility of Cathodic Protection and Other Rehabilitation Strategies 16
3.3 Cathodic Protection Systems for Bridge Substructures 16
3.3.1 Conductive Polymer Wire Mesh 17
3.3.2 Titanium Mesh with Overlay 18
3.3.3 Conductive Paint Coatings 18
3.3.4 Thermally Sprayed Metallic Coatings 19
3.3.5 Clamp-On Systems 20

CHAPTER 4. QUEEN ISABELLA CAUSEWAY 21

4.1 Structure Description 21
4.1.1 Overall Structure Description 21
4.1.2 Protected Members Description 21
4.2 Pre-installation Condition Evaluation 24
4.2.1 Visual Inspection 24
4.2.2 Delamination Survey 27
4.2.3 Concrete Cover Survey 27
4.2.4 Half-Cell Potential Measurements 27
4.2.5 Chloride Content Determination 29
4.2.6 Electrical Continuity 29
4.2.7 Conclusions from the Pre-installation Condition Evaluation 30
4.3 Components of the Cathodic Protection Systems 30
4.3.1 Rectifier and Remote-Monitoring Unit 30
4.3.2 Anodes 32
4.3.3 Monitoring Devices 33

CHAPTER 5. FIELD INSTALLATION 35

5.1 Installation of Generic Components 35
5.1.1 Scaffold and Work Platforms 35
5.1.2 Conduit and Wiring 36
5.1.3 Reference Cells 37
5.1.4 Null Probes 38
5.2 Concrete Preparation 40
5.2.1 Concrete Repairs 40
5.2.2 Surface Preparation 40
5.3 Installation of Anode Systems 40
5.3.1 Sprayed Zinc 40
5.3.2 Sprayed Titanium 44
5.3.3 Titanium Mesh with Overlay 47
5.4 Evaluation of Installation of Anode Systems 50
5.4.1 Constructability 50
5.4.2 Productivity 50
5.4.3 Safety and Environmental Concerns 51
5.4.4 Aesthetics 52
5.4.5 Conclusions 52

CHAPTER 6. PERFORMANCE EVALUATION 53

6.1 Introduction 53
6.2 Energization 53
6.3 Field Evaluation 55

6.3.1 Visual Inspection 55
6.3.2 Delamination Survey 60
6.3.3 Half-Cell Potential Measurements 61
6.3.4 Corrosion Rate Measurements 64
6.3.5 Chloride Content Determination 64
6.3.6 Concrete Permeability Measurement 65
6.3.7 Rectifier and System Component Evaluation 66
6.3.8 Polarization Decay Testing 68
6.4 Remote Monitoring 71
6.4.1 Remote-Monitoring Operation 71
6.4.2 Data Collection Process 71
6.4.3 Periodic System Check 71
6.4.4 Current Output Variability for Sacrificial Sprayed Zinc System 71
6.5 Conclusions from Performance Evaluation 74

CHAPTER 7. DURABILITY AND COST ANALYSES 77

7.1 Durability for Installed Systems 77
7.2 Estimated Installation Costs 77
7.3 Cost Analysis 78
7.4 Conclusions from Durability and Cost Analyses 82

CHAPTER 8. CONCLUSIONS AND RECOMMENDATIONS 85

8.1 Conclusions 85
8.1.1 Pre-installation Condition Evaluation 85
8.1.2 Field Installation 85
8.1.3 Performance Evaluation 85
8.1.4 Durability and Cost Analyses 87
8.2 Recommendations 87
8.2.1 Recommendations for Future Research 87
8.2.2 Cathodic Protection System Selection for the Queen Isabella Causeway 88
8.2.3 Guidelines for Full-Scale Installation 88
8.3 Cathodic Protection for Marine Bridge Substructures in Texas 93

APPENDICES

Appendix A: Pre-installation Condition Evaluation Corrosion Potential Mapping 95
Appendix B: Energization Polarization Development Testing 109
Appendix C: Field Evaluation Corrosion Potential Mapping 113
Appendix D: Field Evaluation Corrosion Rate Data 123
Appendix E: Field Evaluation Chloride Content 127
Appendix F: Field Evaluation As-Found Conditions 131

Appendix G: Field Evaluation Electrical Continuity Data *137*
Appendix H: Field Evaluation AC Resistance Data *147*
Appendix I: Field Evaluation Null Probe Data *153*
Appendix J: Field Evaluation Polarization Decay Testing *157*

REFERENCES 165

CHAPTER 1. INTRODUCTION

1.1 PROBLEM HISTORY

Bridges are deteriorating at an alarming rate. The Federal Highway Administration (FHWA), in a recent report to Congress, reported that 39 percent of the total bridges were deficient, and 23 percent were structurally deficient (Ref 1). Deficient bridges require repairs but can remain open until they reach an unsafe condition. Structurally deficient bridges are closed or in need of repair to remain open. It is estimated that $91 billion is needed to repair the damage and deterioration of the nation's bridge infrastructure (Ref 2). Deterioration on most of these bridges is caused by corrosion of steel in concrete.

Cathodic protection is one of the many rehabilitation strategies available to combat corrosion. The FHWA stated in 1982 that cathodic protection was the only proven method to stop corrosion of steel in concrete (Ref 3).

The Queen Isabella Causeway Demonstration Project is an attempt to determine which of a number of cathodic protection technologies is most effective in stopping corrosion in bridge substructures in marine environments.

1.2 OBJECTIVES OF RESEARCH PROGRAM

The Queen Isabella Causeway Demonstration Project consisted of installing four different cathodic protection systems in a bridge substructure in a marine environment and evaluating installation and performance of the systems. The primary objectives for this project were to:

- Monitor and evaluate the installation of the different cathodic protection systems
- Evaluate the performance of the different cathodic protection systems
- Establish recommendations for full-scale application of cathodic protection in the Queen Isabella Causeway
- Establish recommendations for the implementation of cathodic protection systems for bridge substructures in Texas

Secondary objectives were to:

- Assess the condition of the structure and the feasibility of cathodic protection as a rehabilitation option by means of a pre-installation condition evaluation
- Assess the methods used to evaluate the performance of the cathodic protection systems
- Perform a simplified comparative economic analysis of the cathodic systems installed at the Queen Isabella Causeway

While the performance of the systems will be evaluated over approximately 2 years and 9 months, this report reflects only the first 9 months of service. Although 9 months is not sufficient time to reach definitive conclusions on the systems, preliminary observations on performance will be made.

It is anticipated that as a result of this study, recommendations will be developed for the effective and efficient use of cathodic protection for bridge substructures. Research results and findings will be implemented immediately as a result of troubleshooting and maintenance operations of the installed systems in the Queen Isabella Causeway or in new installations of cathodic protection systems in other existing bridge substructures in marine environments in the state of Texas.

1.3 ORGANIZATION

This report is organized into eight chapters. Chapter 2 presents the theory of corrosion and cathodic protection of reinforcing steel in concrete. Presented in Chapter 3 is a description of the different rehabilitation strategies available for repair and rehabilitation of concrete bridge substructures and the compatibility of cathodic protection systems with other repair and rehabilitation strategies. A brief description, history of installations, and advantages and disadvantages of different types of cathodic protection systems for concrete bridge substructures are also provided in Chapter 3. Chapter 4 presents a description of the Queen Isabella Causeway, the results of the pre-installation condition evaluation, and a description of the designed and installed components of the cathodic protection systems. Chapter 5 presents the installation sequence as well as a comparative evaluation of the installation of the different cathodic protection systems for the Queen Isabella Causeway. Chapter 6 presents a preliminary evaluation of the performance of the different cathodic protection systems installed. Presented in Chapter 7 is a cost analysis for the different cathodic protection systems installed. The conclusions from this research study and the recommended cathodic protection system type for a full-scale installation at the Queen Isabella Causeway are presented in Chapter 8. Guidelines for the design, installation, monitoring, and maintenance of the recommended system are also provided in Chapter 8 as well as recommendations for the implementation of cathodic protection for marine bridge substructures in Texas.

CHAPTER 2. CORROSION AND CATHODIC PROTECTION OF REINFORCING STEEL IN CONCRETE

2.1 CORROSION OF STEEL IN CONCRETE

The most serious deterioration process affecting concrete is caused by corrosion of the reinforcing steel (Ref 4). The deterioration of concrete structures is a worldwide problem and its costs are substantial. It becomes important, therefore, to fully understand the theory and mechanisms of corrosion of steel in concrete.

2.1.1 Protection of Steel in Concrete

Portland cement concrete provides an ideal environment for reinforcing steel. The high alkalinity (pH 12.5–13.5) of concrete causes the reinforcing steel to form a passivating film. The precise nature of this film is unknown, but it isolates the steel from the environment and thus delays the onset of corrosion (Ref 5).

The Pourbaix diagram, which is an electrical potential versus pH diagram, describes the electrochemical behavior of iron in an aqueous environment (Figure 2.1). Iron will not corrode in the pH range from 8 to 13.5 (Ref 6). The alkalinity of concrete helps to prevent the corrosion of steel in concrete.

2.1.2 Causes and Mechanisms of Corrosion

There are two main mechanisms that nullify the effects of the protective passivating film and lead to corrosion: carbonation and chloride contamination.

Carbonation results from atmospheric carbon dioxide diffusing through concrete and decreasing the alkalinity of concrete. Factors that influence the ability of concrete to resist carbonation are: adequate concrete cover, sound concrete with no cracking, high cement content, and good compaction. Carbonation is common in old structures and poorly constructed buildings but is rare in modern highway structures (Ref 5).

Chloride contamination attacks the passivating layer around the reinforcing steel but unlike carbonation there is less of a drop in pH (Ref 7). Chlorides can be cast into concrete or can penetrate concrete. Cast-in chlorides come from the addition of chloride accelerators, seawater, or contaminated aggregates. Chlorides that penetrate concrete can come from contact with seawater or sea salt spray, deicing salts, and various chemicals. The degree of chloride contamination of concrete that will activate the corrosion process, also known as the corrosion threshold level, is estimated at 1.7 lb of acid-soluble chloride per cubic yard of concrete (1 kg/m^3) (Ref 8). The main factor influencing the ability of concrete to resist chloride contamination is adequate cover of reinforcing steel by sound, crack-free, impermeable concrete.

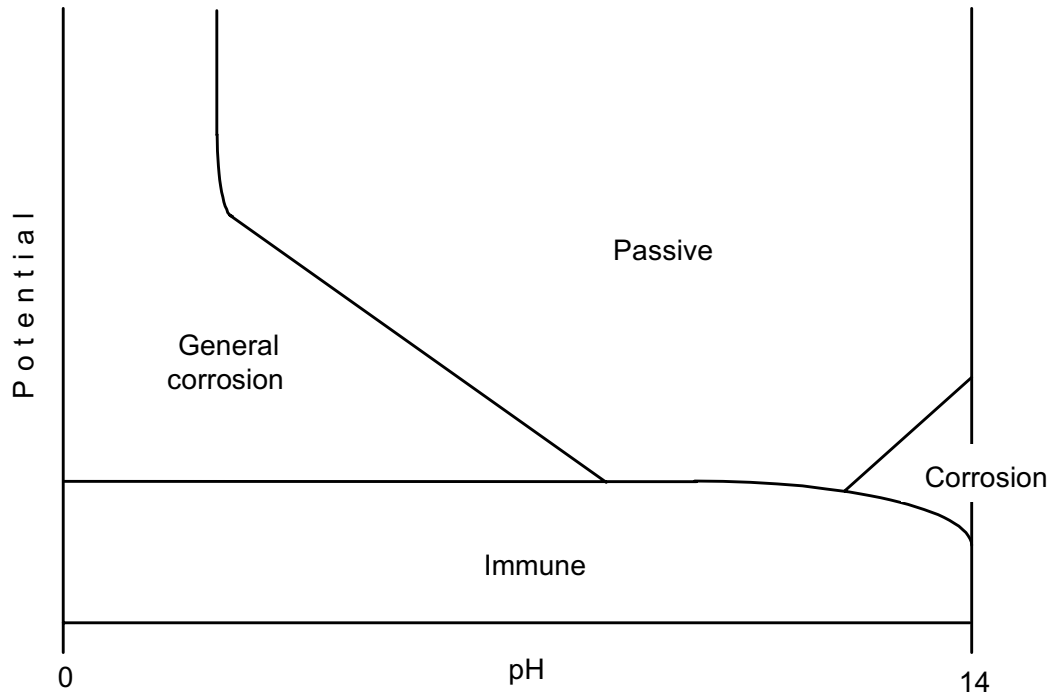

Figure 2.1: Schematic Pourbaix diagram for iron

Chloride contamination is the most common cause for premature reinforcing steel corrosion in concrete (Ref 6). Chloride-induced corrosion is very common for highway structures exposed to seawater or deicing salts. Long before carbonation becomes a problem for these structures, chlorides cause corrosion (Ref 7).

2.1.3 Corrosion Process

Once the passivating layer is nullified by chlorides or carbonation, corrosion ensues. Corrosion is an electrochemical reaction that occurs in the presence of oxygen and water. An anodic and a cathodic reaction are present when a corrosion cell exists. The anodic reaction involves the loss of electrons by the iron atom (iron oxidation):

$$Fe \rightarrow Fe^{2+} + 2e^{-}$$

The cathodic reaction involves the consumption of water and oxygen. This reaction generates hydroxyl ions that increase the alkalinity at the cathode.

$$2e^{-} + H_2O + \tfrac{1}{2}O_2 \rightarrow 2OH^{-}$$

The anodic reaction — the dissolution of iron — is the first in a series of reactions. The end product of these reactions is hydrated ferric oxide ($Fe_2O_3H_2O$), commonly known as rust. Rust is several times larger in volume than the original iron. This encapsulated expansion causes tensile stresses in the concrete that lead to cracking, delamination, and spalling.

2.1.4 Microcell versus Macrocell Corrosion

The anodic and cathodic reactions described above take place at the anode and the cathode, respectively. Currents flow through concrete from the cathode to the anode by ion flow and through the reinforcing steel from the anode to the cathode by electron flow.

Two types of corrosion cells develop within concrete: microcells and macrocells. When a microcell develops within concrete, the anode is very close to the cathode on the same reinforcing bar (Figure 2.2) (Ref 5). Carbonation-induced corrosion usually occurs on a microcell (Ref 7). When a macrocell develops, the anode and cathode are often well separated (Figure 2.3) (Ref 5). Chloride-induced corrosion is prone to the development of macrocells (Ref 7).

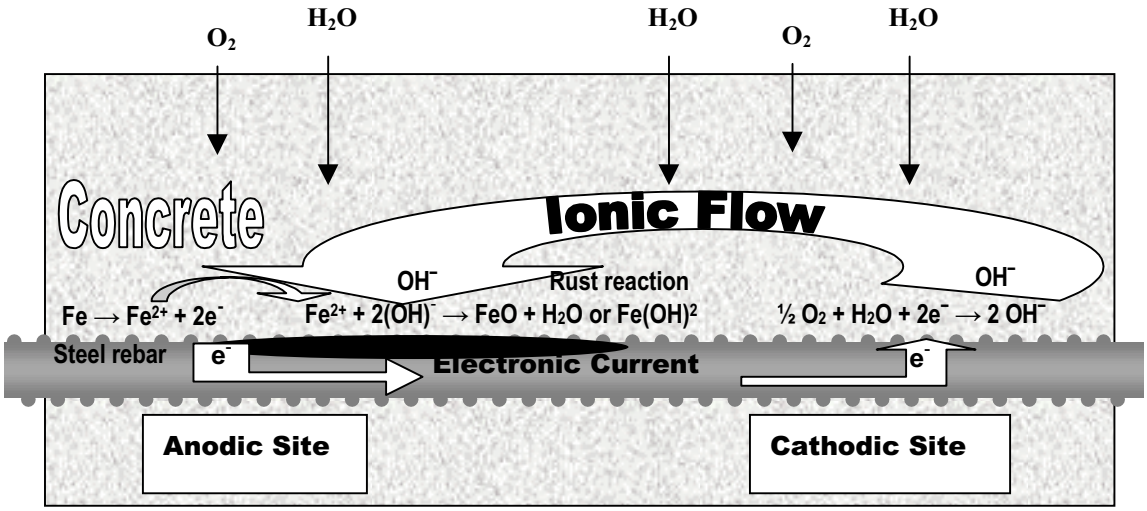

Figure 2.2: Microcell corrosion: Activity in proximity on same rebar

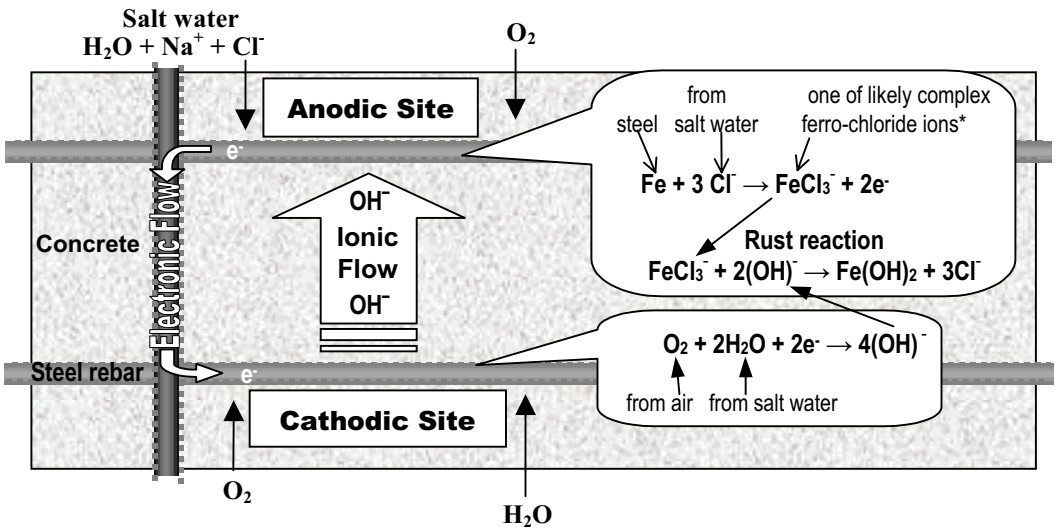

Figure 2.3: Macrocell activity with chloride ions in steel reinforced concrete (*Note: Several possible complex ferro-chlorides can form and compete for available reactive ions. Their instability in the presence of oxygen results in various expansive oxidation products of iron, as shown in Figure 2.4).

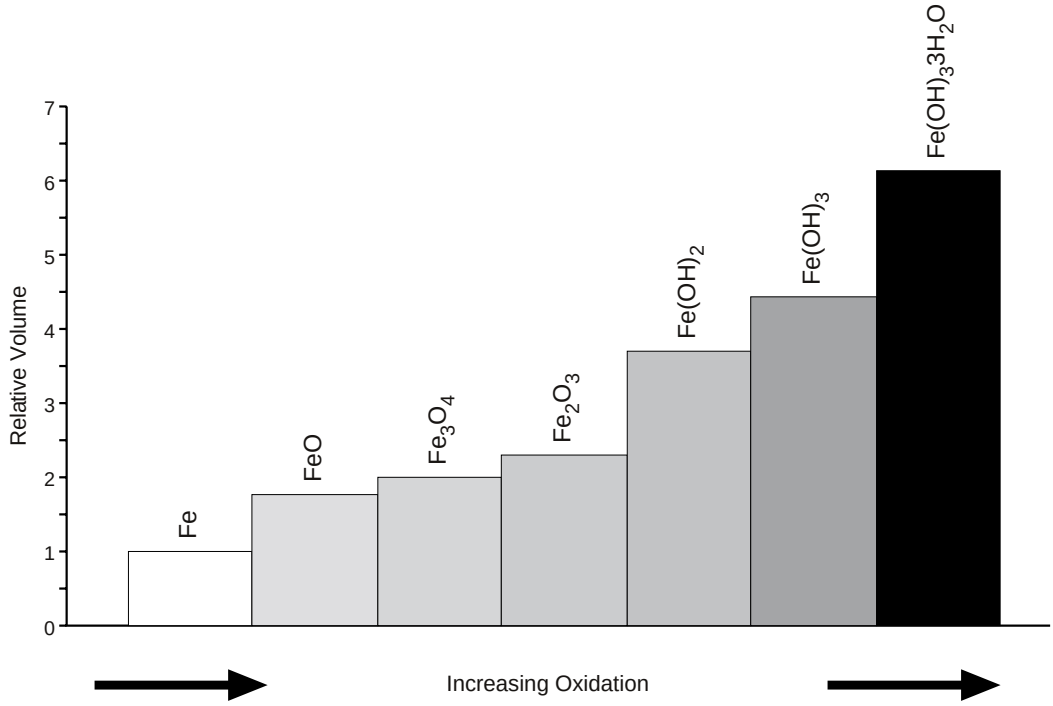

Figure 2.4: Relative volumes of iron oxidation products

2.1.5 Polarization

A simplified graphic representation of a corrosion cell for reinforcing steel in concrete is shown in Figure 2.5 (Ref 9). The electrochemical characteristics of each reaction can be studied by examining the confined half-cell reactions. The resulting polarization, also known as activation polarization, in the absence of other effects, is governed by the following relationship:

$$\eta = a + b(\log I) \qquad \text{(Equation 2.1)}$$

where

η = Activation polarization

a = Potential intercept

b = Tafel constant

I = Current

The anodic and cathodic half-cells polarize to a common corrosion potential E_{corr}. This potential is also called mixed potential because the resulting potential is the combination of the half-cell potentials for the anodic and cathodic reactions. The corrosion current, I_{corr}, is directly proportional to the corrosion rate. I_{corr} and E_{corr} are represented in Figure 2.5 by the intersection of the anodic and the cathodic curves.

Two other types of polarization affect the corrosion of steel in concrete. Cathodic diffusion is associated with concentration polarization by which the rate of oxygen diffusion through concrete influences the corrosion rate. As shown in Figure 2.6, the higher the oxygen diffusion (as shown in Curve 2), the higher the corrosion rate. The other type of polarization is ohmic polarization. Because concrete is not a very conductive medium, the resistance of concrete influences the corrosion rate. As shown in Figure 2.7, the higher the resistance, the smaller the corrosion rate.

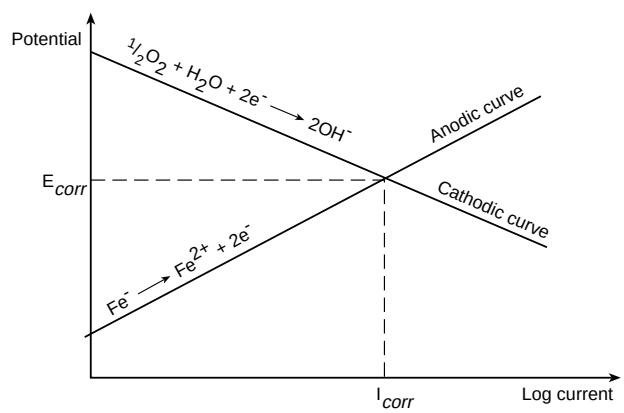

Figure 2.5: Simplified representation of a corrosion cell of steel in concrete

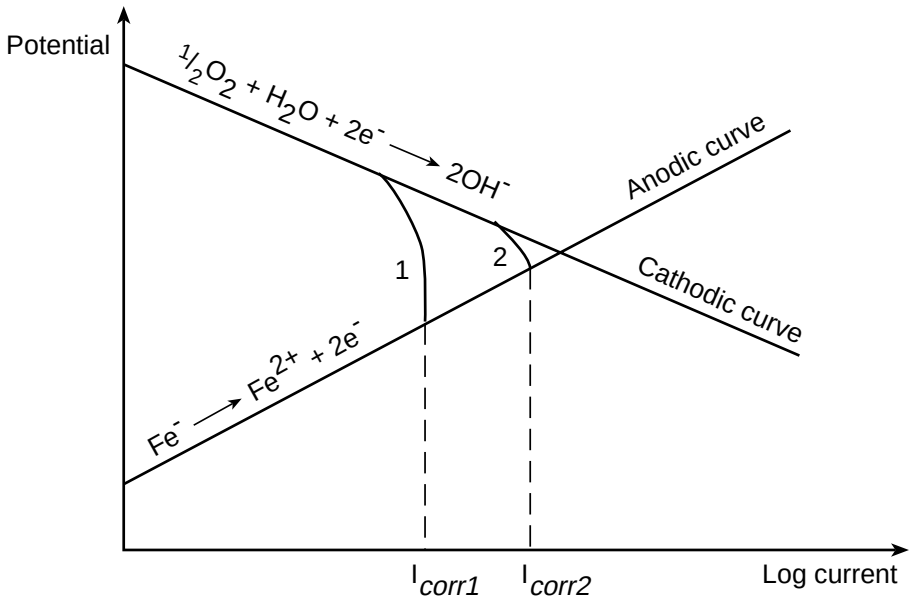

Figure 2.6: Effect of cathodic diffusion on polarization

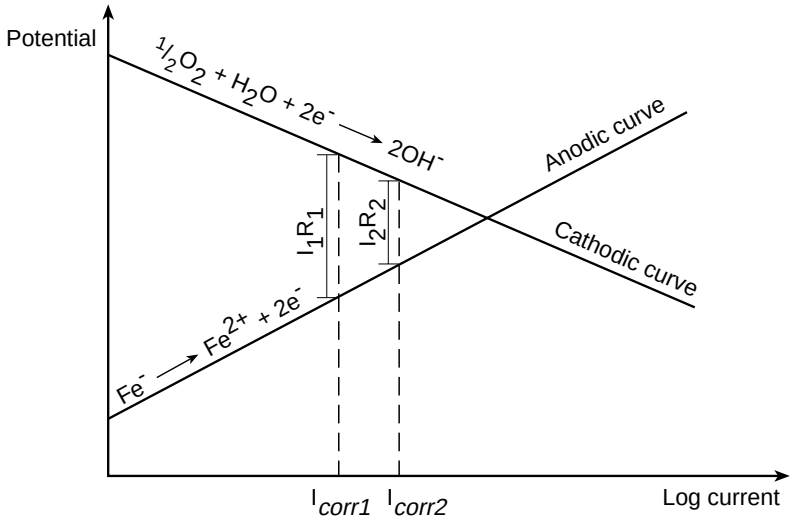

Figure 2.7: Effect of concrete resistance on polarization

2.2 CATHODIC PROTECTION OF STEEL IN CONCRETE

2.2.1 Principle

Cathodic protection reduces the corrosion rate by cathodic polarization of the reinforcing steel in concrete. The rationale behind cathodic protection is to prevent the reinforcing steel from giving up electrons so that corrosion does not occur. This retention of steel electrons is achieved by supplying the electrons from another source. Consider the corrosion half-cell reactions introduced in Section 2.1.3:

$$Fe \rightarrow Fe^{2+} + 2e^-$$
$$2e^- + H_2O + \tfrac{1}{2} O_2 \rightarrow 2OH^-$$

If there is an excess of electrons, the rate of the anodic reaction decreases. On the other hand, an excess of electrons will increase the rate of the cathodic reaction. There are two main methods of supplying the electrons: by applying an impressed current or by introducing a sacrificial anode.

2.2.2 Impressed Current Systems

In impressed current cathodic protection systems, a small direct current is passed from a permanent anode to the reinforcing steel. An external power supply needs to be connected between the anode and the steel with the appropriate polarity and voltage to prevent the reinforcing steel from giving up electrons. Figure 2.8 shows an impressed current system schematically and the reactions involved.

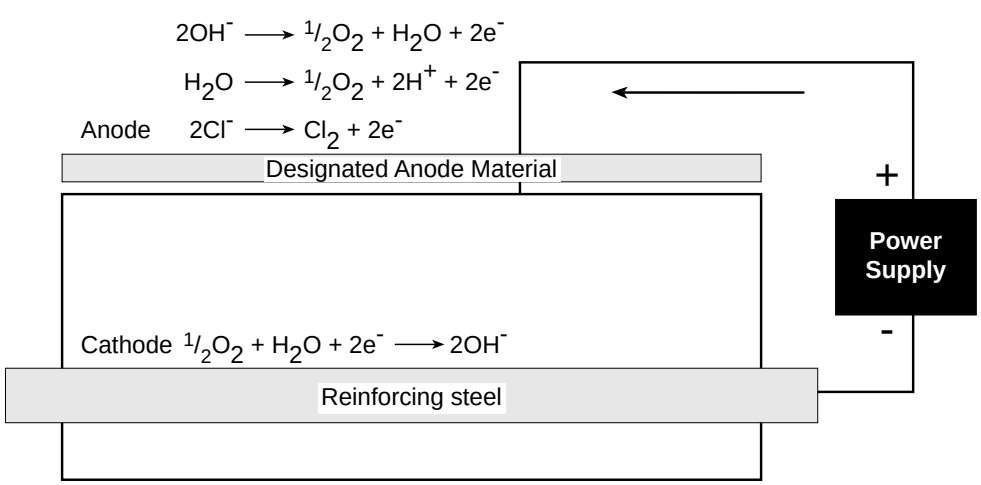

Figure 2.8: Impressed current system

If the current applied is enough to stop the anodic reaction from occurring, the only reaction at the cathode should be:

$$2e^- + H_2O + ½\ O_2 \rightarrow 2OH^-$$

If the potential gets too negative, which means the current applied is excessive, the hydrogen evolution reaction can occur.

$$H_2O + e^- \rightarrow H + OH^-$$

The monatomic hydrogen migrates into the steel metal lattice, reducing the strength and resulting in failure under load. This phenomenon is known as *hydrogen embrittlement*. Hydrogen embrittlement is not a problem for conventional reinforcing steel but may be a problem for certain high-strength steels. Caution is justified for cathodic protection installations on structures containing prestressed or post-tensioned steel.

Both possible reactions at the cathode, described above, lead to the production of hydroxyl ions, which restore the passivating film broken down by chloride attack. Chloride ions are driven away from the reinforcing steel. Because the chloride ion is negatively charged, it is repelled from the now-cathodic reinforcing steel and moves towards the installed anode.

$$Cl^- \rightarrow Cl^2 + 2e^-$$

Another reaction that occurs at the cathode is the consumption of the hydroxyl ions formed at the cathode to produce oxygen. Water is then oxidized to give rise to hydrogen ions leading to acid etching of the concrete. If the potential gets too negative, the acidification around the anode increases.

$$2OH^- \rightarrow H_2O + {}^1/_2O_2 + 2e^-$$
$$H_2O \rightarrow {}^1/_2\ O_2 + 2H^+ + 2e^-$$

The electrochemical principle of impressed current cathodic protection can be explained by the polarization curves of the reactions involved. Figure 2.9 shows the polarization of the two reactions involved.

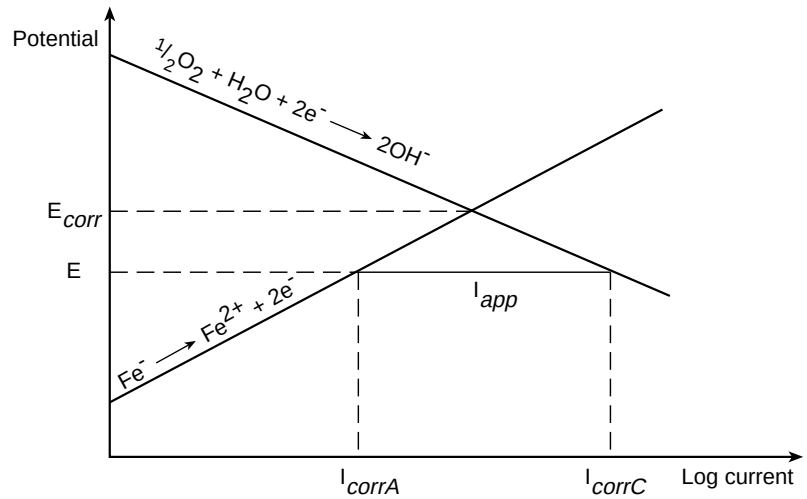

Figure 2.9: Electrochemical principle of impressed current systems

When an electric current is supplied, I_{app}, the potential shifts in the direction from E_{corr} to E owing to the excess of metal electrons supplied at the metal surface (Ref 10). The rate of the anodic reaction, corrosion rate, is reduced to I_{corrA}.

2.2.3 Sacrificial Systems

Another method of providing cathodic protection to a structure is by introducing a sacrificial anode, also called galvanic anode. The sacrificial anode corrodes preferentially producing electrons. Sacrificial anodes need to be more active than iron to protect the reinforcing steel. Typical anodes are zinc, aluminum, magnesium, and their alloys. Figure 2.10 shows a sacrificial system schematically and the reactions involved.

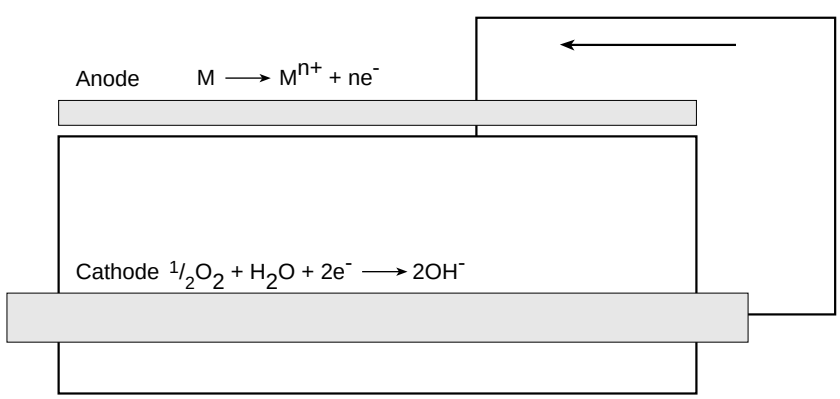

Figure 2.10: Sacrificial system

The reaction at the anode is the consumption of the anode to produce the electrons that the steel would be otherwise giving up.

$$M \rightarrow M^{n+} + ne^-$$

The resistance of the concrete electrolyte is the crucial element to determine whether the use of sacrificial anodes is viable. In cases where the electrolyte resistance is too high, the effective potential difference between the steel and the anode may not be sufficient to adequately protect the structure. Thus, sacrificial anodes are very common for structures exposed to seawater and to other electrolytes that decrease the concrete resistivity.

The electrochemical principle of sacrificial anode protection can be explained by the polarization curves of the reactions involved. Figure 2.11 shows the polarization of the two reactions involved.

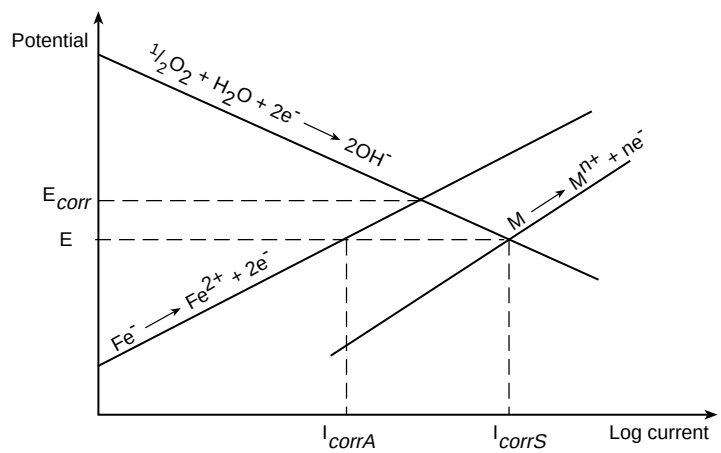

Figure 2.11: Electrochemical principle of sacrificial systems

When a sacrificial anode is used, the reinforcing steel and the sacrificial anode are polarized to the same potential E. The corrosion rate for the reinforcing steel is reduced to I_{corrA}. The rate of consumption of the sacrificial anode is given by I_{corrS}.

2.2.4 Impressed Current versus Sacrificial Systems

The main advantage of sacrificial systems over impressed current systems is that they do not require a power supply. Impressed current systems require more monitoring than sacrificial anode systems. Sacrificial anode systems are, however, limited in the current and voltage that they can produce. For concrete with high resistivity, as found in atmospheric concrete, the energy output is generally not sufficient to achieve protection. In other environments, such as contact with seawater or seawater splash, protection may be achieved with the use of sacrificial anodes. Impressed current systems provide greater flexibility because the current or output can be easily adjusted. While sacrificial anodes corrode, requiring periodic replacement, the service life of the anodes used for impressed current systems is usually much longer.

CHAPTER 3. CATHODIC PROTECTION FOR BRIDGE SUBSTRUCTURES

3.1 REHABILITATION STRATEGIES FOR BRIDGE SUBSTRUCTURES

Concrete bridge substructures, which are often exposed to deicing salts and seawater, are especially vulnerable to chloride-induced corrosion deterioration. And among bridge substructures, bridge decks have received much attention in terms of rehabilitation strategies. Bridge substructure repair has the following additional challenges with respect to bridge deck repair (Ref 11):

- The protection system must provide protection from the elements.
- Vertical and overhead surfaces are the surfaces to be protected.
- Portions of the concrete may have varied moisture contents and/or chloride concentrations because of contact with water or damp soil.

There are several repair techniques that are used for repair and rehabilitation of concrete bridge substructures. The emphasis is on rehabilitation of corrosion-induced deterioration caused by chloride contamination because this corrosion mechanism is the most common for bridges. Rehabilitation strategies for bridge substructures can be classified according to Figure 3.1.

3.1.1 Patching

Patching is the cheapest, fastest, and most widely used repair technique. The objective of patching is to restore the original characteristics of the concrete with respect to strength and durability. Some of the possible application methods for patching are shotcrete, hand-applied, dry-pack, preplaced aggregate, form and pump form, and cast-in-place.

The most commonly used patching materials are portland cement concrete, quickset hydraulic mortar/concrete, and polymer mortar/concrete (Ref 8). Admixtures can be added to improve durability, setting-time, and workability. For compatibility considerations, the use of portland cement concrete is often recommended.

When patching, one must recognize the incipient anode effect. Patching a structure with extensive chloride attack may accelerate corrosion elsewhere owing to electrochemical incompatibility. Corrosion along a reinforcing steel bar may be caused by the dissimilar environment introduced with the repair material (Ref 12).

3.1.2 Encasement/Jacketing/Overlay

Encasements, jacketing, and overlays are used to restore the structural capacity or to delay or prevent deterioration in bridge substructures. The term *encasement* is applicable for columns, piers, or piles while *jacketing* is applicable to abutments or wing walls (Ref 8).

Installation involves demolition of the deteriorated concrete, addition of reinforcement, and placement of concrete through a shutter around the member (Ref 7). *Overlay*, a general term that is most often applied to bridge decks, can also be applied to certain elements of the bridge substructure.

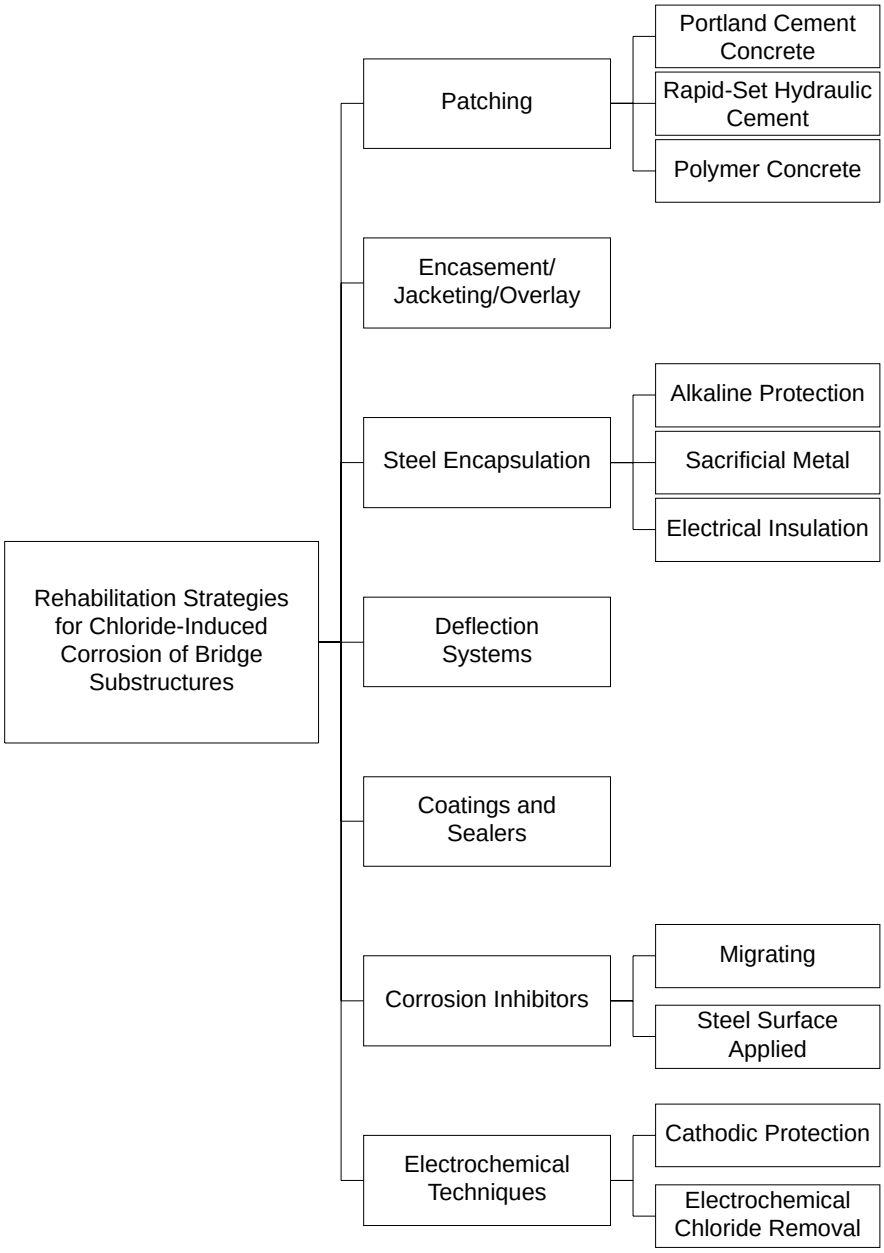

Figure 3.1: Rehabilitation strategies for chloride-induced corrosion of bridge substructures

3.1.3 Steel Encapsulation

By encapsulating the steel, it is possible to protect the steel in concrete. There are three main ways of providing steel encapsulation: alkaline protection, sacrificial metal, and electrical insulation (Ref 4). Alkaline protection can be achieved by coating the reinforcing steel bar with alkaline slurry or by patching around the steel. A sacrificial metal used to coat the reinforcing steel corrodes preferentially, leaving the steel uncorroded. The most common material used to coat the reinforcing steel is zinc. Electrical insulation is achieved with the use of fusion-bonded epoxy-coated bars. Controversy exists on the effectiveness of epoxy-coated reinforcement.

3.1.4 Deflection Systems

A very effective way of reducing chloride-induced corrosion deterioration in bridge substructures is to deflect water away from the bridge deck so that it does not come in contact with the bridge substructure. This water could be contaminated with chlorides from deicing salts. Deflection can usually be achieved with adequate guttering and drainage from the deck away from the bridge substructure.

3.1.5 Coatings and Sealers

Coatings and sealers are applied to the surface of the concrete to exclude external sources of chlorides from concrete. There are a great variety of proprietary coatings and sealers. None of these proprietary materials is fully impermeable to chlorides, nor can they stop corrosion once chlorides have penetrated concrete. Coatings are one- or two-component organic liquids. Organic coating materials are normally epoxies, acrylics, and urethanes (Ref 8).

A sealer is a solvent-based or water-based liquid. There are two types of sealers: penetrating sealers and surface sealers. Penetrating sealers are typically silanes and siloxanes (Ref 8). They react with the pore walls of the hardened cement paste to create a nonwettable surface. Surface sealers block pores in the concrete surface. Surface sealers are typically linseed oil or epoxy (Ref 8).

3.1.6 Corrosion Inhibitors

Corrosion inhibitors are chemical compounds that cause a shift of potential of reinforcing steel in concrete. There are two types of corrosion inhibitors: anodic and cathodic. Anodic corrosion inhibitors restore the passivating film broken down by chlorides. The most popular corrosion inhibitor in the United States, calcium nitrite, is an anodic corrosion inhibitor. Cathodic corrosion inhibitors retard the cathodic reaction of the corrosion cell. Corrosion inhibitors can be applied on the concrete surface, where they are referred to as migrating corrosion inhibitors, or on the surface of the exposed steel.

Corrosion inhibitors have not been fully tested, and their impact on the service life of reinforced concrete is unknown (Ref 4).

3.1.7 Electrochemical Techniques

There are two main electrochemical techniques for rehabilitation: cathodic protection and electrochemical chloride removal. The theory of cathodic protection has been covered in Chapter 2 and is the focus of this research effort. The rationale behind electrochemical chloride removal is similar to that of cathodic protection. The main differences are that in electrochemical chloride removal, the anode application is temporary and the current output is much higher. The same equations discussed in Section 2.2.1 are valid. The most common anodes used in electrochemical chloride removal are titanium mesh and steel. An electrolyte is circulated along the surface of the concrete. The electrolyte is where the ionic current flows. It needs to be alkaline to prevent the circulated solution from getting too acidic and ,thereby, etching the concrete. Electrochemical chloride removal has been mainly used in piers and columns of bridge substructures.

3.2 COMPATIBILITY OF CATHODIC PROTECTION AND OTHER REHABILITATION STRATEGIES

The concrete substrate or repair materials for the element to be subjected to cathodic protection should have low resistivity. High resistivity patching materials, such as polymer or epoxy materials, with resistivities in excess of 1,600 Ωft (500 Ωm) are incompatible with cathodic protection (Ref 13). Patching materials with metal or carbon fibers are also unacceptable. Ionic conductivity is required, not electrical conductivity. Excessive electrical conductivity may in fact lead to uneven levels of protection within a structure or an electrical short.

Concrete encasements, jacketing, and overlays with high additions of silica fume are incompatible with cathodic protection, especially galvanic cathodic protection systems. Higher additions of silica fume result in higher concrete resistivities.

Bonding agents need to be cementitious materials. Epoxy-based bonding agents should be avoided (Ref 13). Crack injection is done with materials that are for the most part incompatible with cathodic protection. If extensive crack repairs need to be performed, the cracks should be routed and sealed with cementitious materials rather than injected with epoxy.

3.3 CATHODIC PROTECTION SYSTEMS FOR BRIDGE SUBSTRUCTURES

Sir Humphrey Davy (Ref 13) discovered cathodic protection in 1824. It was first used to protect metallic fittings in wood sailing vessels (Ref 14). The first application of cathodic protection for reinforced concrete was on a bridge deck in California in 1974. It was not until the early eighties that cathodic protection was used by another state. At that time, the Minnesota Department of Transportation used cathodic protection on a reinforced concrete

pavement (Ref 13). The first application of cathodic protection system for a bridge structure in Texas was installed on the deck of US 87 Missouri-Pacific Railroad Overpass in Big Spring, Texas (Ref 15). This was an experimental project, which involved the installation of five different cathodic protection systems.

Cathodic protection for bridges had been installed on 9,000,000 ft^2 (840,000 m^2) of surface area of bridges according to a 1988–1989 survey (Ref 16). According to this survey, 99 percent of these applications were on bridge decks. Even though most of the applications of cathodic protection have been targeted towards bridge decks, there have been a number of installations for bridge substructures.

The types of cathodic protection systems available for rehabilitation of bridge substructures are classified into the following:

- Conductive polymer wire mesh
- Titanium mesh with overlay
- Conductive paint coatings
- Thermally sprayed metallic coatings
- Clamp-on systems

Each type of cathodic protection system for bridge substructures is described, and the advantages and disadvantages are presented. In addition, a history of application is provided for each system. The history of application, rather than being an extensive review of all the applications of the different systems, presents selected published installations in North America as well as some other applications.

3.3.1 Conductive Polymer Wire Mesh

System Description. Conductive polymer wire mesh is made of copper wires that are coated with a conductive polymer material (Ref 10). The mesh is flexible and adheres to vertical and overhead surfaces. The manufacturer is Raychem, and the product name is Raychem Ferex (Ref 13). Installation involves fastening the mesh with non-metallic fasteners and encapsulating it with a concrete overlay. The use of this anode material is very limited today (Ref 13).

The main advantage of this system is the ease of installation owing to the light weight and flexibility of the anode (Ref 10). The system provides uniform distribution of the anode to the surface. The main disadvantages are anode degradation and embrittlement (Ref 13). Damage to the anode can occur during construction, and this may lead to corrosion of the copper core. As with any system that involves the application of an overlay, concern about debonding of the overlay exists.

History of Application and Performance. Conductive polymer wire mesh was installed in a column of the Burlington Bay Skyway in Burlington, Ontario, in 1983 (Ref 17). The total surface area installed was 430 ft^2 (40 m^2). Seven months after installation, the system was functioning satisfactorily in terms of cathodically protecting the structure. However, the areas of delaminated overlay were significant.

3.3.2 Titanium Mesh with Overlay

System Description. The mesh is diamond-shaped and is made up of Grade 1 titanium. It is packaged in rolls for transport and storage. The mesh distributes the current across the surface to be protected. Elgard is the manufacturer of the mesh. Installation involves fastening the titanium mesh with nonmetallic fasteners and encapsulating the system with a concrete overlay.

Titanium is inert and very long lasting. The mesh is lightweight and flexible, and this facilitates installation. Titanium mesh anodes provide adequate electrical redundancy so performance is not affected by localized damage to the titanium mesh during installation or during the life of the system. Most failures for bridge substructure applications have occurred because of debonding of the concrete overlay.

History of Application and Performance. In 1985, a cathodic protection system using titanium mesh was installed on the substructure of the Leslie Street/401 Bridge in Toronto, Ontario (Ref 18). Two columns with a total surface area of 80 ft^2 (7.4 m^2) were protected. Depolarization tests performed approximately 1 year after installation indicated very good levels of cathodic protection. A titanium mesh anode was cast into structural concrete for the rehabilitation of a 3,390-ft^2 (305-m^2) installation in the substructure of the Verle Allyn Pope Bridge on Highway 206 over the Intercoastal Waterway at Crescent Beach, Florida (Ref 19). Throughout the 3-year evaluation period, the cathodic protection systems had achieved good levels of cathodic protection. A pier of the Howard Frankland Bridge in Tampa Bay, Florida was also protected with this system (Ref 19). The installation covered a total of 1,700 ft^2 (158 m^2) including columns, footings, and struts. Delaminations of the shotcrete overlay were observed shortly after installation (Ref 19). Periodic testing performed over a 3-year period indicated that the cathodic protection was providing good protection to the structure (Ref 19).

3.3.3 Conductive Paint Coatings

System Description. The anode consists of carbon-dispersed paint. The primary anode is usually platinized wire, platinized niobium copper wires, or carbon fibers (Ref 7). Installation consists of mechanically fastening the wire to the concrete surface and painting the surface with conductive paint.

The main advantage of this system is the ability to apply it to complicated geometries that are prevalent in bridge substructures. The application and the materials are relatively low cost. The system is, however, very susceptible to electrical short-circuits; the conductive paint may penetrate the concrete and come in contact with the reinforcing steel (Ref 10). Several failures have been reported in wet, freezing and thawing, and splash zone environments as a result of debonding of the paint layer (Ref 13).

History of Application and Performance. In 1983, a cathodic protection system using conductive paint coating was installed in the caps, piers, footings, and columns beneath the eastbound lanes of the Kennedy Expressway Overpass above the northbound lane of River Road in Rosemont, Illinois (Ref 20). Approximately 1 year after installation, a condition

evaluation of the Rosemont pier was performed. Minor areas of the coating had scaled from the concrete (Ref 20). The cathodic protection systems provided adequate protection to the structure (Ref 20). In 1985, a conductive paint anode system for cathodic protection was installed on the James River Bridge on IH 95 in Richmond, Virginia (Ref 21). A total of 83,000 ft^2 (7,700 m^2) of concrete was protected at the substructure of this bridge. This has been the largest application of conductive paints to date. Depolarization tests indicated good protection to the structure (Ref 21).

3.3.4 Thermally Sprayed Metallic Coatings

System Description. Thermally sprayed coatings consist of a thin layer of metal applied to the concrete surface. There are two main types of equipment for applying the metallic coating: arc spray and flame spray. For arc spray equipment, an electric arc continually feeds two electrically charged wires into an arc, melting the wire. The molten metal is then propelled by compressed air. Flame-spray guns melt a single wire, which is atomized and deposited on the concrete surface.

Zinc has been the most widely metallized sprayed anode. It can be used as an impressed current or sacrificial anode. It was developed by CALTRANS, and there are no proprietary rights on the material.

Sprayed titanium anode is a relatively new material. Elgard owns the rights to this system. The rationale behind the development of this system was to create a material with the effectiveness of the titanium mesh with overlay but without the susceptibility of the overlay to debond. The anode requires a catalyst, which prevents the titanium from passivating and forming an oxide that prevents the flow of current (Ref 22).

The latest experimental metallizing material is aluminum zinc. This is a galvanic system in its developmental stage.

The main advantage of any metallized anode is that it can be applied to any surface geometry or orientation. Metals are good conductors, so efficient distribution of the current is achieved. The greatest disadvantage of sprayed zinc has been the production of corrosion products that result in an increase in circuit resistance with time (Ref 7). Metallized titanium and aluminum have not been in service long enough to assess the advantages and disadvantages of these systems.

History of Application and Performance. In 1983, a metallized zinc was installed in two columns at Pier 4 of the Richmond-San Rafael Bridge located in the northern half of San Francisco Bay on Route 17 (Ref 11). A total surface area of 210 ft^2 (19.5 m^2) was installed on each column. This was the first structure to receive a sprayed zinc metallized system. In the 3 years of monitoring, the columns evidenced zinc corrosion products, and limited duration depolarization tests performed indicated adequate performance of the sprayed zinc coating. In 1989, five columns of the Niles Channel Bridge in the Florida Keys were coated with sprayed zinc (Ref 23). This was one of the first applications of cathodic protection on a structure with epoxy-coated rebars. Approximately 210 days after energization, the structure exhibited acceptable depolarization potentials. The Oregon Department of Transportation has made two very large applications of zinc-sprayed systems: the Yaquina Bay Bridge and

the Cape Creek Bridge (Ref 7). The Yaquina Bay Bridge has an impressed current sprayed zinc that was applied to diverse areas of the substructure, which included the deck soffit, diaphragm, columns, and piers, encompassing a total of 151,000 ft^2 (14,000 m^2).

Very recently, a total of 3,015 ft^2 (280 m^2) of the new catalyzed sprayed titanium were sprayed on the Depoe Bay Bridge in Depoe Bay, Oregon (Ref 24). Sacrificial sprayed aluminum zinc was sprayed in a limited area of 60 ft^2 (5.6 m^2) in the Bryant Patton Bridge at St. George Island, Florida (Ref 25).

3.3.5 Clamp-On Systems

System Description. There are several types of clamp-on systems, which include conductive rubber mats with zinc metal and wood, wood or recycled clamps with zinc, and stay-in-place fiberglass forms. The systems are prefabricated and fastened to the concrete structure on site. Bulk zinc anodes are often used in conjunction with these systems. A new variation of these systems consists of a zinc sheet with an adhesive backing. The adhesive is a hydrogel, which adheres to the concrete surface. The new system is used sacrificially and was developed by 3M.

The main advantage of these systems is prefabrication. This allows for ease of installation, especially considering the accessibility restrictions of marine bridge substructures. These systems are for the most part sacrificial, which minimizes the monitoring demands. The use of this type of systems is limited to simple geometries.

History of Application and Performance. In 1986, conductive rubber system jackets were installed on the bents of the B. B. McCormick Bridge in Jacksonville, Florida, which spans the Intercoastal Waterway (Ref 19). After 5 years of operation, the systems produced potentials that met or exceeded the criteria for acceptable levels of cathodic protection (Ref 19).

In 1992, a cathodic protection system was installed for the first time on prestressed concrete pilings (Ref 26). The site in at St. George Island, Florida, was the Bryant Patton Bridge, which spans the Apalachicola Bay in Franklin County. A perforated zinc sheet was used as the anode. Depolarization tests performed indicated acceptable levels of cathodic protection to the structure.

The zinc hydrogel system was applied at the Long Key Bridge located in the middle Florida Keys (Ref 27). In the evaluation period of 4 months after installation, the zinc hydrogel system had performed satisfactorily.

CHAPTER 4. QUEEN ISABELLA CAUSEWAY

4.1 STRUCTURE DESCRIPTION

4.1.1 Overall Structure Description

The Queen Isabella Causeway, shown schematically in plan in Figure 4.1, is located in the southernmost tip of the state of Texas, latitude 26.15° north and longitude 97.10° west. It is a 2.5-mi (4.02-km) bridge structure that links South Padre Island to the mainland of Texas at Port Isabel spanning the Laguna Madre (Figure 4.1).

The east-west structure consists of four lanes, two lanes running in each direction. The structure has 150 spans: three continuous steel plate girder spans and 147 simple prestressed concrete girder spans. The spans are supported by 151 bents numbered from 1 to 151 from west to east. Figure 4.2 shows a view of the Queen Isabella Causeway from the south side of the west end. Construction for this structure was completed in 1973.

4.1.2 Protected Members Description

The members of the structure selected for this study are the tie beam and the three footings in each of Bents 19 through 24. For identification purposes, the footings are designated north, center, and south. The typical bent is shown in Figure 4.3. Bent 19 is located approximately 1,200 ft (366 m) away from the west end of the causeway. The bents are separated approximately 70 ft (21 m) from each other. All bents had similar geometry to the typical bent except for seven bents, which consisted of prestressed piles supporting the bent cap.

The tie beam and three footings of Bents 19 through 22 were each protected with a different cathodic protection system:

- Bent 19 with sprayed zinc impressed current system
- Bent 20 with sprayed titanium impressed current system
- Bent 21 with titanium mesh with overlay impressed current system
- Bent 22 with sprayed zinc galvanic system

On Bents 23 and 24 no cathodic protection systems were installed. Bent 23 was scheduled to be protected with a galvanic aluminum zinc anode, but due to a spraying problem, it was never installed. Therefore, Bents 23 and 24 served as the controls.

For each bent where a cathodic protection system was installed, all of the surfaces of the tie beam and the footings were covered with an anode material with the exception of the bottom surface of the footings. The total surface area covered was approximately 1,320 ft^2 (123 m^2) per bent.

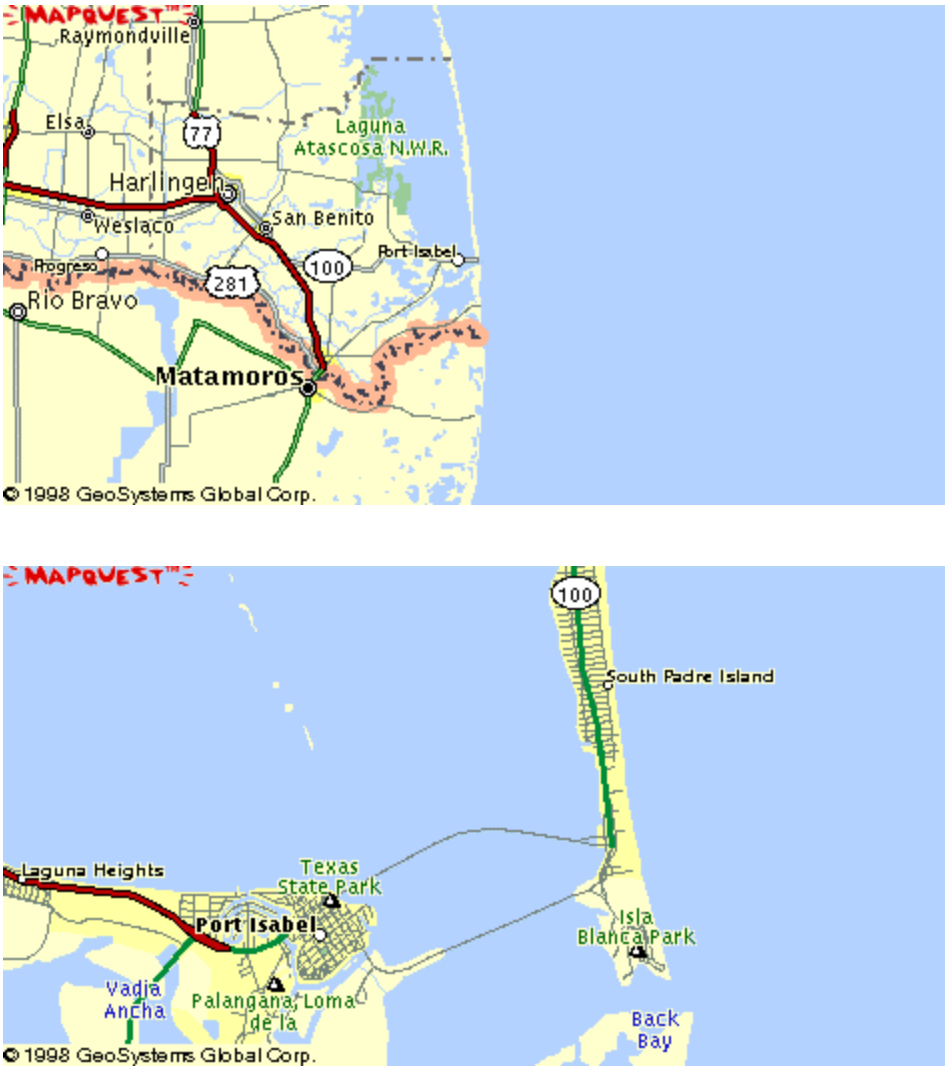

Figure 4.1: Plan and location of Queen Isabella Causeway

Figure 4.2: View of Queen Isabella Causeway

Figure 4.3: Typical bent

The footings are 10.5 ft (3.20 m) long by 10.5 ft (3.20 m) wide by 3.5 ft (1.07 m) high (Figure 4.4). Footings are cast in place and are supported by four batter piles. The steel reinforcement consists of a single layer of No. 10, No. 9 and No. 6 bars in all six surfaces. Construction drawings showed the steel to have 5-in. (127-mm) cover.

The tie beams are 54 ft (16.46 m) long by 4 ft (1.22 m) wide by 3 ft (0.91 m) high (Figure 4.4). The tie beams are precast except for sections at the ends and the center where they support three cast-in-place columns. The construction joints at the interface of the precast and the cast-in-place sections are denoted in Figure 4.4. The longitudinal steel reinforcement for the tie beams consists of a single layer of No. 11 bars on all four longitudinal surfaces. Construction drawings showed the steel to have 4.25-in. (108-mm) cover.

4.2 PRE-INSTALLATION CONDITION EVALUATION

A pre-installation condition evaluation was performed on the six bents (Bents 19 through 24) involved in this study. The pre-installation condition survey was conducted in the course of five site visits in March and April 1997. The purpose of the pre-installation condition survey was to assess the condition of the structure and the feasibility of cathodic protection as a rehabilitation strategy (Ref 7). The condition evaluation included the following: visual inspection, delamination survey, cover survey, half-cell potential measurements, and total chloride content determination. The underside of the tie beam was excluded from the survey because of access limitations.

4.2.1 Visual Inspection

The visual inspection involved measurement of cracks and spalls by marking a grid on the concrete surface of the footings and tie beams. The condition of the tie beam and footings in each of the different bents was found to be similar.

The footings exhibited cracks and spalls, which for most bents were predominant in the south footings. Crack widths recorded ranged from 0.030 in. (0.8 mm) to 0.125 in. (3.2 mm). The crack lengths were greater in the south footing, as shown in Table 4.1, reaching densities of up to 10 ft/100 ft^2 (32 m/100 m^2). Spalls were mostly located on the side faces of the footings. A typical spall on the side of a footing is shown in Figure 4.5. The spalled areas were for the most part greater in the south footing, as shown in Table 4.1, reaching a density of up to 14 ft^2/100 ft^2 (46 m^2/100 m^2).

The tie beams exhibited mostly cracks, which were predominant in areas in the proximity of the construction joint. Crack widths recorded ranged from 0.030 in. (0.8 mm) to 0.125 in. (3.2 mm). Cracks in the proximity of a construction joint are shown in Figure 4.6. The crack lengths were greater in Bents 23 and 24, as shown in Table 4.2, reaching a density of up to 3 ft/100 ft^2 (10 m/100 m^2). No major spalled areas were found in the tie beams.

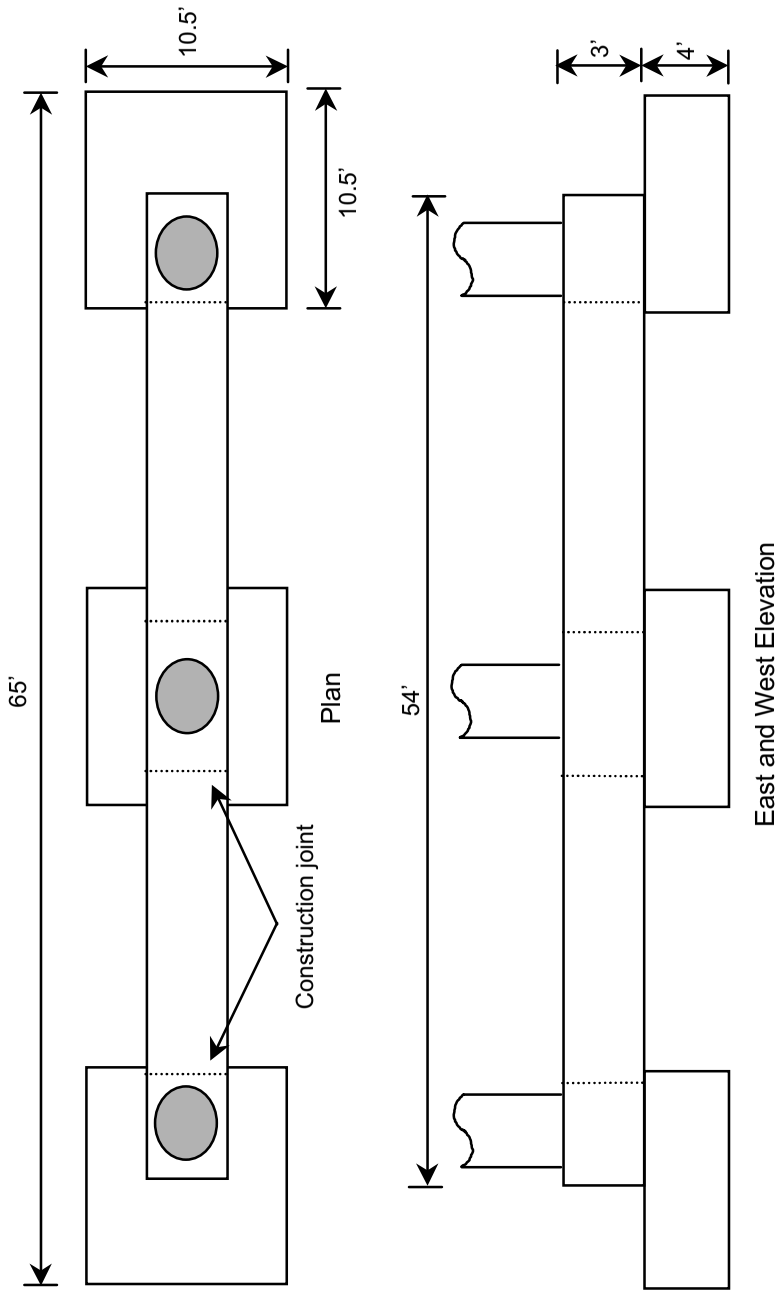

Figure 4.4: Geometry of footings and tie beams

Table 4.1: Results for visual survey for footings

Visual Inspection	Footing																	
	North						Center						South					
	19	20	21	22	23	24	19	20	21	22	23	24	19	20	21	22	23	24
Total Crack Length (ft)	6	0	0	4	0	7	0	0	14	5	14	11	22	22	6	17	15	9
Crack Density (ft/100 ft^2)	3	0	0	2	0	3	0	0	7	2	7	5	10	10	3	7	7	4
Spalled Area (ft^2)	0	0	0	0	2	0	0	0	0	0	3	0	7	0	6	14	4	0
Spall Density (ft^2/100 ft^2)	0	0	0	0	1	0	0	0	0	0	1	0	3	0	3	6	2	0

Figure 4.5: Typical spall in a footing

Table 4.2: Results for visual survey for tie beams

Visual Inspection	Tie Beam					
	19	20	21	22	23	24
Total Crack Length (ft)	4	8	8	4	16	16
Crack Density (ft/100 ft^2)	1	1	1	1	3	3
Spalled Area (ft^2)	3	5	7	5	2	0
Spall Density (ft^2/100 ft^2)	1	1	1	1	0	0

Figure 4.6: Crack in the proximity of tie beam construction joint

4.2.2 Delamination Survey

The delamination survey consisted of hammer sounding at various locations of the tie beams and footings. No delaminations were detected.

4.2.3 Concrete Cover Survey

The concrete cover survey involved measurement of concrete cover by means of a Soiltest Inc. Micro Covermeter. At all locations measured, the concrete cover exceeded 3.5 inches (89 mm).

4.2.4 Half-Cell Potential Measurements

The half-cell potential measurements were conducted on the footings and tie beams of every bent by forming a grid on the surface of the top and sides of the footings and tie beams. The equipment consisted of a copper/copper-sulfate electrode (CSE) cell, a Fluke 87 meter, and a reel of wire. By convention, the positive terminal of the voltmeter was connected to the steel and the negative terminal through the reel of wire to the half-cell (Figure 4.7). Moving the standard CSE along the concrete surface, the condition of the steel below the moving CSE cell was detected. Readings more positive than -200 mV CSE indicate 90 percent probability of no corrosion, readings between -200 mV CSE and -350 mV CSE indicate uncertainty, and readings less than -350 mV CSE indicate 90 percent probability corrosion activity. The half-cell potential measurements for Bents 19 through 24 are shown in Appendix B. At most locations, high probability of corrosion-activity areas correlated well with the presence of cracks, construction joints, or spalls.

Table 4.3 summarizes the results for the footings. The percentage of readings indicating 90 percent probability of corrosion activity for Bent 19 was higher than that of other bents. The south footing for most bents had a higher percentage of readings representing high probability of corrosion activity than the center and north footings.

Table 4.4 summarizes the results for the tie beams. The sum of the percentages in the uncertain range and in the 90 percent probability of corrosion activity range was higher for Bent 19 than for other bents. In the proximity of construction joints, the half-cell potential readings increased, indicating higher probability of corrosion activity.

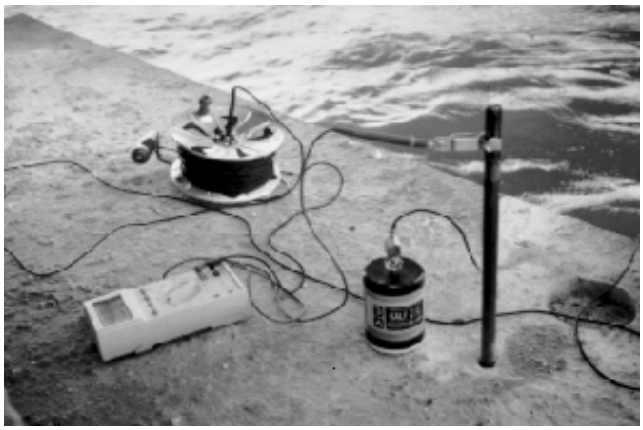

Figure 4.7: Setup for half-cell potential measurements

Table 4.3: Percentage of readings within the specified range for footings

Potential Ranges (mV)	**Footing**																	
	North						**Center**						**South**					
	19	**20**	**21**	**22**	**23**	**24**	**19**	**20**	**21**	**22**	**23**	**24**	**19**	**20**	**21**	**22**	**23**	**24**
More positive than -200	0	86	92	86	86	61	25	91	84	59	47	72	14	72	72	67	56	58
-200 to -350	86	14	6	14	14	36	75	9	9	34	44	25	58	27	14	31	28	33
More negative than -350	14	0	2	0	0	3	0	0	7	7	9	3	28	1	14	2	16	9

Table 4.4: Percentage of readings within the specified range for tie beam

Potential Ranges (mV)	Tie Beam					
	19	**20**	**21**	**22**	**23**	**24**
More positive than -200	43	95	91	91	98	84
-200 to -350	54	5	7	5	2	16
More negative than -350	3	0	2	4	0	0

4.2.5 Chloride Content Determination

The total chloride content was determined at various locations on the top surface of the footings and tie beams. Penetration of chloride ions into the structure was determined using a CL-1000 chloride test system marketed by James Instruments. Powdered samples were collected between the depths of 0.065 and 0.5 in. (1.6 and 12.7 mm) and every 0.5 in. (12.7 mm) thereafter until the level of the reinforcing steel was reached. Measurements were then converted into percent chloride ion content using a mathematical model presented in American Association of State Highway and Transportation Officials (AASHTO) T 260, *Sampling and Testing for Total Chloride Ion in Concrete and Concrete Raw Materials*, Procedure C (Ref 28). Assuming a concrete density of 4,000 lb/yd^3 (2,370 kg/m^3), the chloride percentage was translated into chloride content in pounds of chloride per cubic yard.

The distribution of chlorides with depth, from the surface to the level of the reinforcing steel, was consistent with the penetration of chlorides from the marine environment. The chloride contents at the level of the reinforcing steel for the different bents at various locations are presented in Figure 4.8. The chloride contents taken in the proximity of cracks and spalls in the footings and cracks and construction joints in the tie beams were extremely high, very much above the corrosion threshold level. The maximum chloride content obtained, 22.04 lb/yd^3 (13.07 kg/m^3), was recorded at a location of a crack on the east side of the top of the south footing of Bent 22. The maximum chloride content at the tie beams was 13.09 lb/yd^3 (209.68 kg/m^3) and was recorded at the northernmost construction joint of Bent 22.

4.2.6 Electrical Continuity

As per the specifications, electrical continuity testing was performed for the members in question. The equipment used for the electrical continuity test consisted of a Fluke 87 meter, test leads, and a wire reel. The test involved measuring voltage drop between reinforcing steel at different locations within a bent. Electrical continuity was tested at ten locations per bent. If the voltage drop was less than 1.0 mV, continuity was verified. Electrical continuity was found in all but one location. Electrical discontinuity was found between the north footing and the tie beam in Bent 20.

4.2.7 Conclusions from the Pre-installation Condition Evaluation

A very strong correlation was found between the existence of cracks, construction joints or spalls, chloride contents, and half-cell potentials indicative of corrosion activity. The source of the chlorides was the seawater from the Laguna Madre.

At the footings, more indications of corrosion activity were found in the south footings than in other footings. This was due to the prevailing south wind and wave action in the area. The tie beams were found to be in better condition than the footings. This was due to the fact that the footings were in the splash/evaporation zone. At the tie beams, the construction joint was responsible for the deterioration as evidenced by the existence of cracks and high chloride contents. It was observed that at times of severe weather, the cast-in-place portion of the tie beam was subjected to seawater spray from waves striking the footings.

Electrical continuity was verified in all but one location. Electrical continuity is a prime concern for cathodic protection performance. The discontinuous location should be made continuous. The concrete cover found at random locations within the structure, in excess of 3.5 in. (8.9 mm) allows for the installation of the cathodic protection systems without electrical shorts.

Overall, the structure was visually in good condition but potentially in poor condition as evidenced by the chloride content and half-cell potential condition indicators. The condition of this structure made it an ideal candidate for cathodic protection because a substantial economic advantage can be enjoyed for cathodic protection in structures that can accommodate cathodic protection prior to major concrete remedial repairs being required (Ref 13).

4.3 COMPONENTS OF THE CATHODIC PROTECTION SYSTEMS

The components for the cathodic protection systems installed at the Queen Isabella Causeway are shown schematically in Figure 4.9 (Ref 7). The main components of the cathodic protection systems are described in this section. Components described in this section are the rectifier and remote-monitoring unit, the anodes, and the monitoring devices. Details on the installation of the components of the cathodic protection systems are provided in Chapter 5.

4.3.1 Rectifier and Remote- Monitoring Unit

The rectifier was model CAAYSA 24-5 manufactured by Good-All Electric. The rectifier was a saturable reactor constant current type with the ability to change constant current control to constant voltage. The rectifier had three separately controlled circuits, one for each impressed current system installed. The three impressed current cathodic protection systems were installed in Bents 19, 20 and 21; the cathodic protection systems installed in these bents were sprayed zinc, sprayed titanium and titanium, mesh with overlay, respectively.

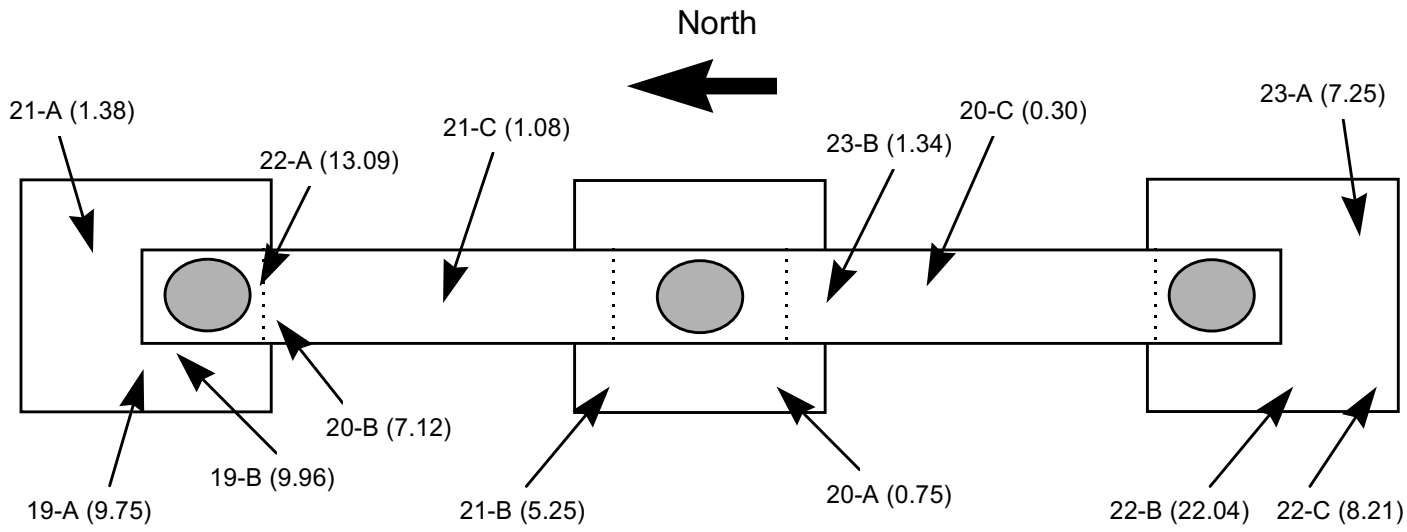

Notes:
First number represents bent location where chlorides were taken
Letter next to first number is the sample identification for a given bent
Number in parentheses are the chloride contents at the level of the reinforcing steel expressed in lb/yd^3

Figure 4.8: Total chloride contents at the level of the reinforcing steel

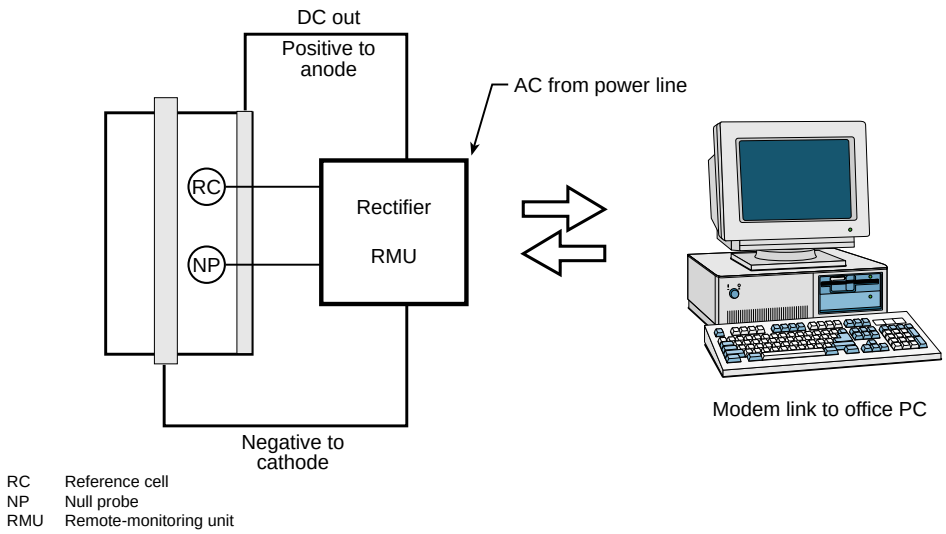

Figure 4.9: Components of the cathodic protection systems for the Queen Isabella Causeway

The rated DC output of each circuit was 24 volts and 5 amperes. The rectifier was connected to the AC power line and converted AC current to DC current. The positive terminal was connected to the anode and the negative terminal (system ground connection) to the cathode (reinforcing steel).

The remote-monitoring unit (RMU) was a CORD-2 manufactured by COREXCO. The remote-monitoring unit was connected via modem to an office personal computer. The purpose of the remote-monitoring unit was to transfer data to a remote office personal computer.

4.3.2 Anodes

Four different anode systems were installed in the Queen Isabella Causeway. The systems were impressed current sprayed zinc (Bent 19), impressed current sprayed catalyzed titanium (Bent 20), impressed current titanium mesh with overlay (Bent 21), and galvanic sprayed zinc (Bent 22). Two grounds or negative connections were installed in each of these bents.

Sprayed Zinc. Sprayed zinc was the anode for the impressed current and the sacrificial systems for Bents 19 and 22, respectively. Each of the two anode connectors, or primary anodes, consisted of a zinc disk, galvanized stud, and nut and washer. The zinc disks were 3.5 in. (89 mm) in diameter and 0.125 in. (3.17 mm) thick. The zinc coating thickness applied was 0.02 in. (0.51 mm) +/- 0.004 in. (0.10 mm). Zinc splicers were installed at the corners between the tie beam and the footings to ensure electrical continuity between the coating in the tie beam and the footings. The zinc splicers consisted of 2-in. (51-mm) by 2-in. (51-mm) by 1-ft (0.30-m) zinc angles. The sprayed zinc was coated with a single-component moist curing aliphatic urethane.

Sprayed Titanium. Sprayed titanium was the anode used for the impressed current system in Bent 20. Each of the two current distributor plates consisted of a titanium disk,

titanium stud, and stainless steel nut and washer. The titanium disks were 4 in. (102 mm) in diameter and 0.125 in. (3.17 mm) thick. Titanium splicers were installed at the corners between the tie beam and the footings. The titanium splicers consisted of 2-in. (51-mm) by 2-in. (51-mm) by 1-ft (0.30-m) titanium angles. The sprayed titanium was coated with a catalyst.

Titanium Mesh with Overlay. Titanium mesh with overlay was the anode used for the impressed current system in Bent 21. The anode consisted of a titanium mesh of Grade 1 titanium designated ELGARD 210 and manufactured by the ELGARD Corporation. The titanium mesh was secured to the concrete surface by means of plastic fasteners. The primary current conductor was solid Grade 1 titanium strip, which was 0.5 in. (13 mm) wide by 0.035 in. (0.89 mm) thick. The conductor was welded to the titanium mesh. The titanium mesh was encapsulated in a concrete overlay. Three different applications of the titanium mesh with overlay were attempted. The final application involved shotcrete application of the concrete overlay.

4.3.3 Monitoring Devices

Reference Cells. Silver/silver-chloride reference cells were permanently embedded in the concrete. The silver/silver-chloride reference electrodes were model CB and are manufactured by Electrochemical Devices. Three reference cells were installed per bent (bents 19 through 24). Two reference electrodes were located in the footings and one reference electrode was located in the tie beam of each bent. The reference electrodes were placed in the most anodic areas of the footings and tie beams as found in the half-cell potential survey performed as part of the pre-installation condition evaluation.

Figure 4.10 shows a diagram of the reference cell and its connections. Each reference cell had a ground wire that was connected to the reinforcing steel. A pair of wires, one corresponding to the reference cell and one corresponding to the reference cell ground were spliced to a pair of wires in a junction box at the location of each reference cell and routed to the rectifier through the conduit.

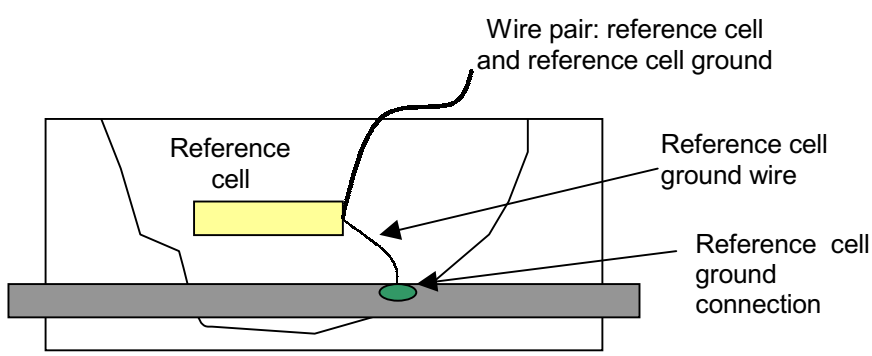

Figure 4.10: Reference cell and its wire connections

Null Probes. A piece of reinforcing bar was isolated at an anodic site within the structure. The isolated rebar was connected to the rebar mat. With the system in the de-

energized condition, a strong galvanic current develops, which indicates that the null probe is corroding. When the system is energized, the current reverses indicating that the null probe is not corroding and that sufficient level of protection has been achieved.

Two null probes were installed in each of the three impressed current systems. One null probe was located in the tie beam, and one null probe was located in the footing of each of these bents. The null probes were placed in the most anodic areas of the footings and tie beams as found in the half-cell potential survey performed as part of the pre-installation condition evaluation.

Figure 4.11 shows a diagram of the null probe and its connections. The null probe ground wire was connected to the continuous reinforcing steel and the null probe wire is connected to the isolated piece of reinforcing steel. These wires were spliced to a pair of wires in each null-probe junction box and were routed to the rectifier through the conduit.

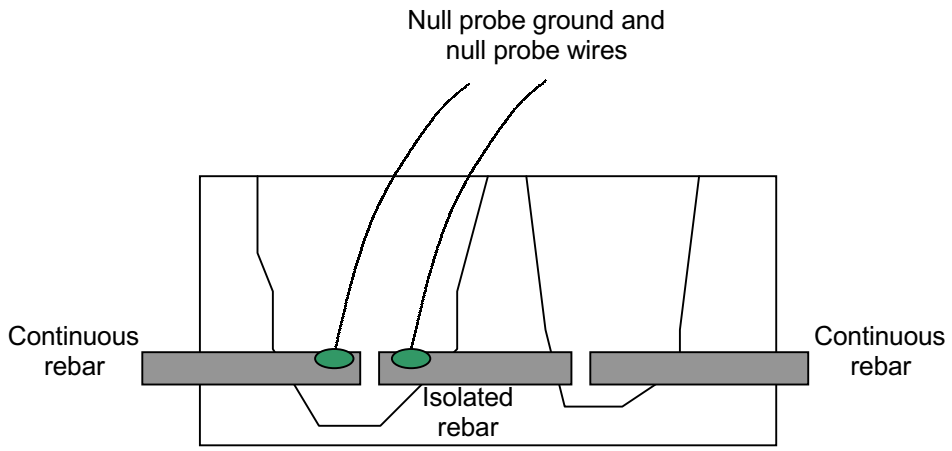

Figure 4.11: Null probe and its wire connections

CHAPTER 5. FIELD INSTALLATION

5.1 INSTALLATION OF GENERIC COMPONENTS

5.1.1 Scaffold and Work Platforms

A scaffold was installed around the perimeter of each bent. The installation of the scaffold resulted in a number of delays. The scaffold consisted of a wooden frame on which plywood was secured. The wood frames rested on steel truss-beams that were secured to the underside of the footings. Strong wind and wave action from occasional cold fronts resulted in the destruction of the scaffold. Two such occurrences prompted the modification of the original scaffold design. The wood frame and the plywood were tied to cables secured to a structure beam and were lowered at the start of the workday and raised at the end of the workday (Figure 5.1).

A platform was also installed for heavy equipment and storage. The platform was anchored in position by means of a pile that could be driven into the underwater bed. The platform could be hauled by boat to different locations.

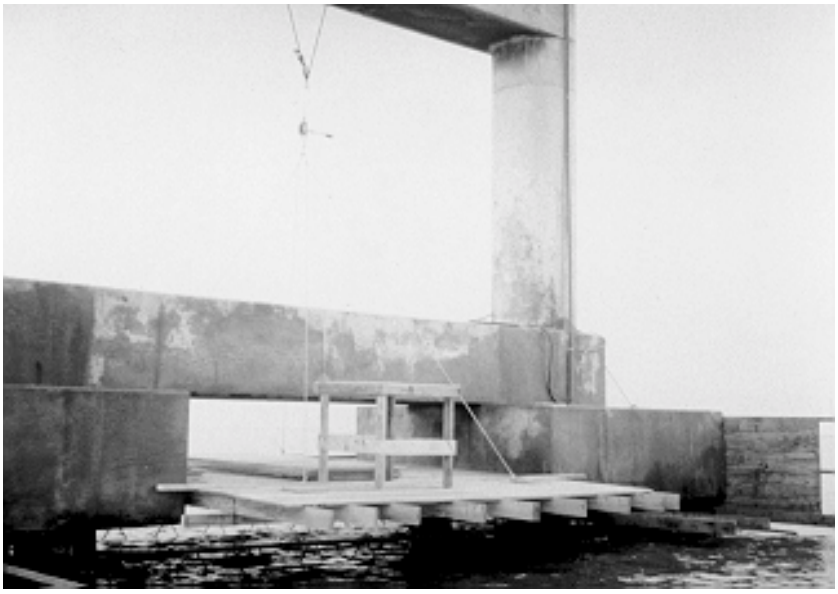

Figure 5.1: Modified scaffold design in raised position

5.1.2 Conduit and Wiring

The main conduit was secured along the south side of the bridge at the face of the outermost beam supporting the concrete deck. A rolling scaffold hanging to the side of the bridge deck was used to install the conduit (Figure 5.2). One traffic lane was blocked off during the installation of the conduit and wiring.

Figure 5.2: Conduit installation

The crew consisted of one laborer on the concrete deck in charge of providing conduit segments, tools, and other supplies, and two workers on the scaffold in charge of securing the conduit to the side of the bridge. The conduit was held against the concrete with plastic clamps secured to the concrete surface by means of Grade 304 stainless steel bolts. The 2.5-in. (63.5-mm) diameter PVC conduit was delivered in 10-ft (3.05-m) segments. The conduit-to-conduit connection was achieved with a female-male coupling with epoxy cement. An expansion joint was installed every two or three conduit segments. A junction box was installed at every bent at the level of the conduit in which a cathodic protection system was installed.

The installation of the conduit proceeded from east to west. Between Bent 24 and Bent 19, the installation of the conduit proceeded at a slower pace because a junction box was installed at the location of each bent. Down each bent from the main conduit, 1.25-in. (31.7-mm) PVC conduit was installed. The installation of conduit for the three workers proceeded at the rate 30 ft/hr (9.1 m/hr) between Bents 24 and 19 and at the rate of 150 ft/hr (45.7 m/hr) between Bent 19 and the western end of the bridge.

A continuous rope was threaded through the conduit as the installation of the conduit proceeded. Liquid soap was added to the inside surfaces of the conduit for lubrication. Once installation of the conduit was completed, wires were pulled from one end of the conduit to the other. Within the 2.5-in. (63.5-mm) diameter PVC conduit, the following were installed: one 1.5-in. (38.1-mm) diameter black jacket, three red No. 10 AWG with HMWPE

insulation, and one black No. 10 AWG with HMWPE insulation. The 1.5-in. (38.1-mm) diameter jacket comprises thirty-five pairs of No. 16 AWG shielded lead wire in twisted pairs. These wires were for the reference cells and null probes connections. The three red wires delivered current independently from the rectifier to the three impressed current systems. The black wire served as the ground connection for the impressed current systems. At the location of the junction box at each bent, five pairs of No. 16 AWG shielded lead wires in twisted pairs in a vinyl jacket were spliced to five pairs of the 1.5-in. (38.1-mm) diameter jacket. Wire splicing was a very time-consuming process. Each wire was peeled, coupled with a copper sleeve, and then protected with a heat-shrinkable cable.

5.1.3 Reference Cells

The location of the reference cells was determined based on the results of the half-cell potential survey described in Chapter 4. The location for the reference cells was chosen among the most anodic areas in the bent and is presented in Table 5.1. In each zone, one reference cell was installed in the tie beam and two were installed in the footings. One reference cell in the footing was placed in the proximity of the reinforcing steel top mat and the other in the proximity of the bottom mat.

The concrete at the site of the reference electrode was removed. The reference cell was connected to the steel with a thermite weld, which consists of igniting a powder with a flint gun to provide the connection. Figure 5.3 shows a reference cell and ground connections.

Connections were covered with epoxy. The reference cell electrode and corresponding ground wires were then spliced to a pair of shielded lead wires in the junction box and routed in the conduit to the rectifier unit. The cavity where the reference cell was placed was patched with Sikatop 123.

Figure 5.3: Reference cell

Table 5.1: Reference cell locations

Zone	Reference Cell	Location
1	1	South Tie Beam
	2	Bottom Mat/North Footing
	3	Top Mat/North Footing
2	1	Bottom Mat/South Footing
	2	Top Mat/South Footing
	3	North Tie Beam
3	1	South Tie Beam
	2	Top Mat/Center Footing
	3	Bottom Mat/Center Footing
4	1	South Tie Beam
	2	Bottom Mat/Center Footing
	3	Top Mat/Center Footing
5	1	South Tie Beam
	2	Top Mat/Center Footing
	3	Bottom Mat/South Footing
6	1	Bottom Mat/South Footing
	2	Top Mat/South Footing
	3	Center Tie Beam

5.1.4 Null Probes

The location of the null probes was determined based on the results of the half-cell potential survey described in Chapter 4. The location for the null probes was chosen among the most anodic areas in the bent and is presented in Table 5.2. In each of Zones 1 through 5, one null probe was installed in the tie beam and one was installed in the footings.

A 6-in. (152-mm) section of reinforcing steel was isolated and determined to be discontinuous from the rest of the reinforcing steel. At the two ends of the reinforcing steel selected for isolation, the concrete was removed to access the reinforcing steel (Figure 5.4). An effort was made to remove as little concrete as possible. Enough concrete was removed, however, to sawcut the segment of reinforcing steel.

Table 5.2: Null probe locations

Zone	Null Probe	Location
1	1	South Footing
	2	North Tie Beam
2	1	South Tie Beam
	2	North Footing
3	1	Center Footing
	2	North Tie Beam
4	1	South Footing
	2	North Tie Beam
5	1	South Footing
	2	North Tie Beam

Figure 5.4: Null probe

Once the reinforcing steel bar was isolated, the areas around the two cuts were thoroughly cleaned. One tap hole was drilled on one of the ends of the isolated reinforcing bar. A pan head stainless steel screw was drilled at that location for the wire connection. The connection at the continuous reinforcing bar was made either with the same method or a thermite weld. Epoxy filler was used to cover all connections. The connections at the isolated segment and the continuous reinforcing bar were then spliced to a pair of shielded

lead wires in the junction box and routed in the conduit to the rectifier unit. The cavity for the installation of the null probe was patched with Sikatop 123.

5.2 CONCRETE PREPARATION

5.2.1 Concrete Repairs

The areas of spalled concrete and areas around some cracks were identified for Bents 19 through 23. Jackhammers were used to remove the deteriorated concrete in these areas. Concrete removal areas and routed cracks were patched with Sikatop 123 with Armatec corrosion inhibiting admixture. Sikatop 123 is a two-part polymer-modified mortar used for concrete repair. The compatibility of Sikatop 123 with cathodic protection was not investigated.

5.2.2 Surface Preparation

The surface preparation common to Bents 19 through 23 was sandblasting. Bent 21 required additional surface preparation, discussed in Section 5.3.3. The equipment used for sandblasting was a 600-lb (272-kg) capacity sandblasting machine with a 375-cfm (10.6-m^3/min) air compressor. The productivity for three workers, one at the nozzle and two others feeding sand, was 200 ft^2/hr (18.6 m^2/hr), which is equivalent to 1.5 mhr/100ft^2 (0.16 mhr/m^2). Owing to environmental concerns, it became imperative to enclose the area so as to prevent sand and debris from dropping into the water.

All treated bents were subjected to metallizing with the exception of Bent 21. For the bents treated with metallizing, the surface preparation was the same. Resulting exposed aggregate profile and density was comparable to CSP-3 according to the International Concrete Repair Institute guideline *Selecting and Specifying Concrete Surface Preparation for Sealers, Coatings and Polymer Overlays* (Ref 29). The concrete surface in these bents was clean and textured but with minimal exposed aggregate.

5.3 INSTALLATION OF ANODE SYSTEMS

5.3.1 Sprayed Zinc

Equipment. The equipment used for zinc spraying was the Thermion Bridgemaster arc spray system (Figure 5.5) with an inverter power source. Electric arc equipment works by continually feeding two electrically charged wires into the arc, melting the wire, and spraying it onto the concrete surface. Two spools of wires are placed at the body of the equipment and are fed through the lead wires to the tip of the gun. At the tip of the gun, shown in Figure 5.6, there are two electrodes at the extremes of the gun that provide the electric arc, two openings through which the zinc wires are fed, and an opening located at the center through which the compressed air is propelled. The compressed air propels the molten metal onto the

concrete surface. Compressed air was set at a pressure of 80 psi (5,624 kg/m^2) for this application.

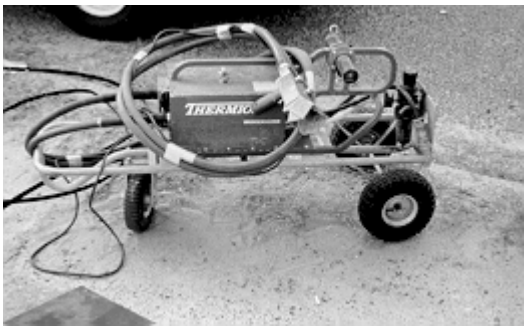

Figure 5.5: Arc spraying equipment

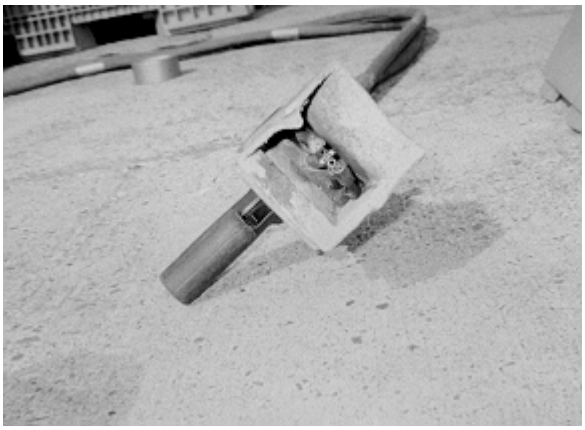

Figure 5.6: Arc spraying gun

Zinc Wire. The zinc wire selected was alloy 1030, which contains a minimum of 99.99 percent pure zinc. Its density is 0.258 lb/in^3 (7,140 kg/m^3). The wire was 0.125 in. (3.18 mm) in diameter.

Application. The primary anodes for the zinc systems consisted of 3.5-in. (89-mm) diameter circular plates, which served as current distributors. Each current distributor plate was secured to the concrete surface by means of a galvanized stud. The galvanized stud was inserted in a drilled hole with epoxy. In two instances, an excess of epoxy was placed in the drilled hole. The excess epoxy deposited between the current distributor plate and the concrete surface nullified the current distribution. Figure 5.7 shows one of the current distribution plates where excessive epoxy was placed. The plate had to be removed, and the area under the plate was sandblasted to remove the excess epoxy.

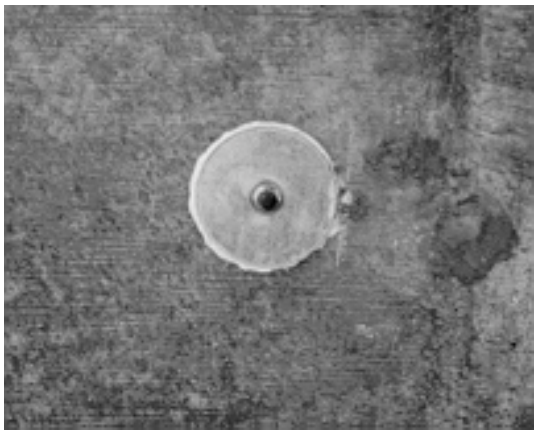

Figure 5.7: Excessive epoxy under a current distributor plate

The target thickness for the zinc was 0.02 in. (0.51 mm) +/- 0.004 in. (0.10 mm). This range was achieved for all areas tested. The actual thickness was measured by placing a piece of tape on the concrete, removing the tape once the zinc was sprayed, and measuring the zinc coating thickness with a micrometer. The problem with this method for measuring zinc thickness is that from the applicator's standpoint there is an incentive to do an acceptable job at a location where the tape is placed. A nondestructive device, the Positector 100-Zn2, manufactured by the DeFelsko Corporation was also used to measure zinc thickness. The readings in this trial were neither accurate nor consistent. Later, it was found that the measuring device had malfunctioned.

The method selected for spraying zinc was arc spray (Figure 5.8). The zinc consumption rate when using arc spray was 0.90 lb/ft^2 (4.39 kg/m^2), which is equivalent to a theoretical zinc thickness of 0.024 in. (0.61 mm). The actual thickness was less as a result of metal and wind action losses. The American Welding Society has published a *Guide for the Protection of Steel with Thermal Sprayed Coatings of Aluminum and Zinc and their Alloys and Composites* (Ref 30). In this document, the nominal feedstock required when using arc spray to apply a 0.02-in. (0.51-mm) coating (assuming a deposit efficiency of 60 percent to 65 percent) is estimated at 1.08 lb/ft^2 (5.27 kg/m^2). The lower consumption rate for this job indicates higher than average productivity or deposit efficiency.

Figure 5.8: Zinc arc spraying

The machine productivity (productivity measured while the gun is spraying) was measured at 130 ft^2/hr (12.08 m^2/hr). The actual productivity rate for each of the two applicators per bent was 92 ft^2/hr (8.55 m^2/hr). This is equivalent to 3.3 mhr/100ft^2 (0.36 mhr/m^2), given that there were three workers per set of arc spray equipment. The nominal productivity rate is provided in *Zinc Thermal Coatings for Reinforced Concrete,* an unpublished standard of the American Welding Society. Assuming 60 to 65 percent deposit efficiency, the nominal productivity was calculated to be 80 ft^2/hr (7.43 m^2/hr) for a coating thickness and zinc wire diameter, as specified for this project.

The average adhesion strength was 156 psi (109,700 kg/m^2) and 151 psi (106,200 kg/m^2) for Bents 19 and 22, respectively. The standard deviation for the adhesion strength measurements was 34 psi (23,900 kg/m^2) and 84 psi (59,000 kg/m^2) for Bents 19 and 22, respectively. The target adhesion strength was 150 psi (105,500 kg/m^2). The adhesion strength tests were performed with an Elchometer 106 Adhesion Tester (Figure 5.9).

Figure 5.9: Adhesion tester

Workers wore a respirator at all times during the spraying. It became important during installation for the applicator to proceed from the windward to the leeward end to avoid excessive inhalation of zinc fumes. Excessive inhalation of zinc fumes can lead to a condition known in the field as "zinc fever." Its symptoms include fever, dry-mouth, sore throat, rapid respiration, and chest tightness, the severity of which depends on the degree of exposure.

Enclosures were used to prevent zinc debris from polluting the surrounding water. The enclosure material allowed clean air to flow in but prevented zinc dust from flowing out.

Once the zinc spraying was completed, a single 0.003-in. (0.08-mm) protective topcoat of moist-cured polyurethane was roller-coated onto the sprayed zinc surface. It took five workers 3 hours to apply the coating, a rate equivalent to 1.1 mhr/100ft^2 (0.12 mhr/m^2).

Upon completion of the installation of zinc anode, the impressed current system was energized with a temporary rectifier. A short circuit was detected between the anode and the reinforcing steel. An Infometrics 525 infrared camera was used to detect the location of the short. To remove solar loading, the test was conducted between 2 and 3 a.m. A 12 V battery charge was used to apply current to the zinc anode in Bent 19 for 2 hours so as to increase the concrete temperature. Infrared images were captured and a *hot spot* was located on the top southern end of the tie beam in the proximity of the column. The short circuit was caused by a piece of metal, which was later removed.

5.3.2 Sprayed Titanium

Equipment. The equipment used for the titanium spraying was a Type 14E flame spray gun (Figure 5.10) manufactured by Sulzer Metco. In flame spray equipment, the wire is pulled into the gun by wire drive rolls and gears. The mechanism by which the drive rolls and gears grip and release the wire can be controlled by the wire grip. Acetylene gas and oxygen are directed to the siphon plug and nozzle assembly located in the gas head where they are ignited. Air is directed through the air cap where it surrounds the flame and

concentrates the flame over the tip of the titanium wire. The molten metal is wiped away by the air, producing the resulting metal spray.

Figure 5.10: Flame-spray gun

The flame spray setup consisted of connecting the fuel and oxygen cylinders to the gas flowmeter and the air supply to the air control unit and to the air flow meter. The input settings were set at 95 ft^3/hr (2.69 m^3/hr) for the oxygen, 50 ft^3/hr (1.41 m^3/hr) at 15 psi (10,546 kg/m^2) for the acetylene gas, and 30 ft^3/hr (0.85 m^3/hr) at 100 psi (70,306 kg/m^2) for the air. The gun was then hooked to the meter by means of standard 15-ft (4.57-m) long hoses.

Titanium Wire. The wire specified for use was 0.0937-in. (2.378-mm) diameter annealed Grade 1 titanium wire. Grade 1 titanium is a high-purity commercial grade of titanium that contains 0.2 percent iron and 0.18 percent oxygen.

Application. The primary anodes for the bent sprayed with titanium were titanium 3.5-in. (89-mm) diameter circular plates. It was essential that titanium plates and studs be used so as to avoid galvanic corrosion.

The method selected for spraying the titanium was flame spray (Figure 5.11). The machine productivity for the titanium was 45 ft^2/hr (4.2 m^2/hr). The actual production rate was 33 ft^2/hr (3.1 m^2/hr), a rate equivalent to 9.1 mhr/100ft^2 (0.98 mhr/m^2), given that there were three workers per set of flame-spray equipment.

Figure 5.11: Titanium flame spraying

If arc spraying had been used, the application could have proceeded faster. Titanium, however, because it is not as ductile as other metals such as zinc, abrades the tip and lead liners of the arc spray equipment, resulting in a need for periodic equipment repair and replacement (Ref 24). For the Depoe Bay Bridge, Oregon, the arc spraying method was used with 0.125- m^2/hr in. (3.175-mm) diameter titanium wire (Ref 23). The reported machine production rate was 81.7 ft^2/hr (7.59 m^2), and the actual production rate was 40 ft^2/hr (3.72 m^2/hr) (Ref 23). The machine production rate for the Depoe Bay Bridge application was higher than that for the Queen Isabella Causeway application, though the actual productivity rates were comparable.

The procedure used to verify whether an adequate amount of titanium had been sprayed consisted in measuring the titanium resistance. The resistance of the titanium coating was measured with a Nilsson 400 AC resistance meter and a resistance measuring probe. The resistance-measuring probe has an outer row of spring-loaded pins at two opposite sides that are used to pass a constant current through the titanium coatings. There are two inner pins that measure the voltage drop through the coatings. These two pins are connected to the Nilson 400 AC resistance meter. Approximately thirty measurements were taken while the titanium was sprayed. Titanium was applied until the resistance was less than 0.25 ohm/square. The target resistance in the field was in the range of 0.15 to 0.20 ohm/square. In order to meet the target resistance range, the titanium consumption rate was set to approximately 0.15 lb/ft^2 (0.73 kg/m^2). Calibrating the equipment to the consumption rate that would meet the AC resistance requirements was time consuming and required several interruptions of the spraying operation.

A proprietary catalyst coating was applied on the titanium anode. Pure titanium without the catalyst would not function as an anode; it would passivate, and no current would pass through it until the breakdown potential was reached (Ref 24). The catalyst was sprayed onto the titanium anode. It took three workers 5 hours to apply the coating, which is equivalent to 1.1 mhr/100 ft^2 (0.12 mhr/m^2). As part of the application procedure for the

catalyst, once the catalyst was applied, a temporary rectifier was used to supply current to the system for a day.

5.3.3 Titanium Mesh with Overlay

Application. The first step in the application of the titanium mesh with overlay was the installation of the titanium mesh. The titanium mesh was shaped to the geometry of the members and was secured to the concrete surface by means of plastic fasteners (Figure 5.12). The holes for the plastic fasteners were drilled, and the plastic fasteners were hammered in place. In several instances, the mesh caught in the grooves of the fasteners while we were securing the fasteners. This could have forced the mesh into contact with the reinforcing steel, creating a short. While the titanium mesh was being installed, the continuity of the titanium mesh with the reinforcing steel was checked at all times. One fastener was installed every 1 ft^2 (0.09 m^2). At locations where there were bends in the mesh or where the mesh was installed in vertical or overhead orientation, the density of the fasteners was increased. Adjacent segments of titanium mesh were superimposed approximately 5 in. (127 mm) to achieve continuity.

Figure 5.12: Titanium mesh secured with plastic fasteners

Once the titanium mesh was secured in place, the titanium strip was installed. The titanium strip serves as the conductor, and the titanium mesh distributes the current. The titanium strip was wrapped around the sides of the footings and tie beams. The titanium strip was then spot-welded to the titanium mesh every 1 in. (25.4 mm). A spot welder capable of delivering 5,000 A over a 1-ft (0.30-m) segment was used (Figure 5.13). The productivity rate of the four workers involved in the installation of the titanium mesh and the titanium strip was 15.3 m^2/hr (165 ft^2/hr), which is equivalent to 0.6 mhr/100 ft^2 (0.06 mhr/m^2).

Figure 5.13: Spot welding of titanium strip to titanium mesh

The installation of the concrete overlay was performed three times, with the overlay and the mesh removed the first two times the overlay was installed. The first application involved trowel-applied Sikatop 123. This product is intended for patch repair rather than overlay application. It is the same material that was used for the repairs on the bents. Two days after the application of the system, the overlay evidenced very severe cracking and was removed.

The second application involved trowel-applied Emaco S88-CA manufactured by Master Builders. Emaco S88-CA is a one-component, cement-based shrinkage-compensating mortar. It took five concrete finishers 40 hours to trowel-apply the 1-in. (25.4-mm) concrete overlay. The productivity for the five concrete finishers was 33 ft^2/hr (3.06 m^2/hr), which is equivalent to 15.1 mhr/100 ft^2 (1.62 mhr/m^2). Two days after the application of the overlay, hammer sounding was performed to test for delaminations. Delaminated areas amounted to 25 percent of the concrete overlay. Seven days later, the delamination areas had risen to 75 percent and were prevalent in the vertical and overhead orientations. This overlay was also removed.

The main reason for the failure of the second trial was inadequate surface preparation. Bonding of the overlay to the substrate was complicated by the presence of the titanium mesh, which acts as a bond breaker, and by the vertical and overhead orientation, which hinders proper consolidation. The surface preparation for the first two trials on Bent 21 was identical to the surface preparation selected for the bents where metallizing was used. Using a rough profile with exposed aggregate to achieve interlock of the overlay with the aggregate would have prevented premature failure of the overlay in this trial.

The surface preparation for the third trial included scabbling with handheld milling machines in addition to sandblasting, which was a procedure common to all bents. It took five workers, each equipped with one scabbler, 32 hours to achieve the desired profile and density. The productivity for the scabbling operation was 41 ft^2/hr (3.8 m^2/hr), which is equivalent to 12.2 mhr/100 ft^2 (1.3 mhr/m^2). The exposed aggregate profile and density achieved were comparable to CSP-6, according to the International Concrete Repair Institute

guideline *Selecting and Specifying Concrete Surface Preparation for Sealers, Coatings and Polymer Overlays* (Ref 29). Figure 5.14 shows a graphic comparison of the surface preparation for the first two trials and the last trial.

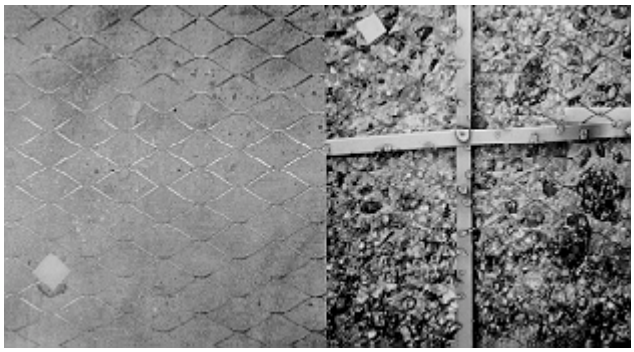

Figure 5.14: Concrete surface preparation comparison. Figure on left represents the lightly sandblasted surface used in the first two trials. The right figure shows exposed aggregates from heavier sandblasting used in the third trial.

The concrete overlay was dry-mix shotcrete applied for the third trial (Figure 5.15). The equipment consisted of an Allentown N2 shotcrete machine and a model 900 rig. The equipment was mounted on the bridge deck, and traffic on one lane was blocked for this purpose. The crew consisted of six workers: one applicator and a helper, two concrete finishers, and two laborers who loaded the shotcrete machine. The productivity for the shotcrete operation was 63 ft^2/hr (5.8 m^2/hr), which is equivalent to 9.5 mhr/100 ft^2 (1.02 mhr/m^2).

Figure 5.15: Shotcrete application of titanium overlay

5.4 EVALUATION OF INSTALLATION OF ANODE SYSTEMS

5.4.1 Constructability

The application of the zinc anode was simple: The equipment used for the spray is light and portable, and the measurement of the zinc thickness with the tape method was rudimentary. Readings from the nondestructive device were found to be inaccurate and inconsistent because of equipment malfunction. Sprayed zinc can be readily accommodated to complex shapes found in bridge substructures.

The application of the titanium mesh with overlay was the most problematic. With adequate surface preparation from the outset, the difficulties for this project could have been avoided. Especially when applying the overlay in vertical or overhead orientations or for complicated geometries, a clean concrete surface with exposed aggregate of the appropriate density and profile should be specified. Otherwise, no bond between the concrete overlay and the substrate will be achieved.

The titanium spray application was complicated. Calibrating the equipment to the consumption rate that would meet the AC resistance requirements was time consuming and required several stoppages in the work.

5.4.2 Productivity

The productivity for the application of the anode systems was measured in man-hours for every 100 ft^2 (9.3 m^2). The main work items were included for the evaluation of productivity for the different anode systems. These work items are presented in Table 5.3 through Table 5.5. Work items common to the three systems were not included as part of the productivity comparison. Scabbling was included for the titanium mesh with overlay because this was an additional surface preparation work item that prevented premature failure for this system.

Table 5.3 presents the main work items for the application of the sprayed zinc anode. The overall productivity was 4.4 mhr/100 ft^2 (0.47 mhr/m^2). This was the anode system with the highest productivity rating.

Table 5.4 presents the main work items for the application of the sprayed titanium anode. The overall productivity was 10.2 mhr/100 ft^2 (1.09 mhr/m^2). The true differences in actual productivity between flame spraying and arc-spraying titanium should be studied further.

Table 5.5 presents the main work items for the installation of the titanium mesh with overlay anode. Delays caused by inadequate surface preparation were not included in the productivity calculation. The productivity for the trowel-applied overlay was included in the evaluation because, with proper surface preparation, this application would not have resulted in premature failure. The overall productivity was 27.9 mhr/100 ft^2 (3.00 mhr/m^2) for the trowel-applied overlay and 22.3 mhr/100 ft^2 (2.40 mhr/m^2) for the shotcrete-applied overlay. The faster turnaround achieved with the shotcrete application versus the trowel application

prevented the concrete from being exposed to the elements for a long time once the surface preparation was completed.

5.4.3 Safety and Environmental Concerns

The application of sprayed zinc raises some safety and environmental concerns. Workers exposed to zinc fumes can suffer from "zinc fever." Controversy exists regarding the toxicity of sprayed zinc to aquatic life. In applications in Oregon, the environmental controls have been very stringent requiring complete containment and air filtration (Ref 7). In Florida, the controls have not been so stringent (Ref 7). The environmental controls in the Queen Isabella Causeway were similar to the controls typically imposed in Florida.

The application of sprayed titanium requires enclosures, though the implications for safety and the environment are minimal.

The environmental concerns associated with the application of the titanium mesh with overlay are the same as those associated with any concrete installation in a marine environment.

Table 5.3: Productivity measurements for sprayed zinc

Work Item	**Productivity (mhr/100 ft^2)**
Zinc spraying	3.3
Polyurethane coating	1.1
Overall productivity	4.4

Table 5.4: Productivity measurements for sprayed titanium

Work Item	**Productivity (mhr/100 ft^2)**
Titanium spraying	9.1
Catalyst application	1.1
Overall productivity	10.2

Table 5.5: Productivity measurements for titanium mesh with overlay

Work Item	Productivity (mhr/100 ft^2)
Surface preparation scabbling	12.2
Titanium mesh and strip installation	0.6
Overlay trowel application	15.1
Overlay shotcrete application	9.5
Overall productivity, trowel applied	27.9
Overall productivity, shotcrete applied	22.3

5.4.4 Aesthetics

Both sprayed zinc and titanium have the ability to conform to any geometry. While sprayed zinc has a color similar to that of the surrounding concrete, titanium has a dark gold color with blue tints. The titanium mesh with overlay color matches well with the surrounding concrete.

5.4.5 Conclusions

The application of the titanium mesh with overlay requires adequate surface preparation in bridge substructures having vertical or overhead surfaces or complicated geometries. A clean concrete surface with exposed aggregate of the appropriate density and profile should be specified. Otherwise, the overlay and the concrete substrate will not bond.

The highest productivity in the installation of the anodes was achieved for the sprayed zinc. The productivity was somewhat less for the sprayed titanium and substantially less for the titanium mesh with overlay. The true differences in actual productivity between flame spraying and arc-spraying titanium should be studied further.

The application of sprayed zinc raises some safety and environmental concerns. As indicated earlier, workers exposed to zinc fumes could be susceptible to zinc fever. In addition, zinc dust could be toxic to aquatic life.

Sprayed zinc and titanium can conform to any type of surface. Whereas the color of both the sprayed zinc and the titanium mesh are similar to that of the surrounding concrete, titanium has a dark gold color with blue tints.

CHAPTER 6. PERFORMANCE EVALUATION

6.1 INTRODUCTION

Upon installation of the cathodic protection systems (Figure 6.1) in September 1997, the impressed current systems were energized, and the performance of the different cathodic protection systems was evaluated by field and remote monitoring. Energization and part of the field evaluation were conducted from the rectifier and the remote-monitoring unit shown in Figures 6.2 and 6.3, respectively.

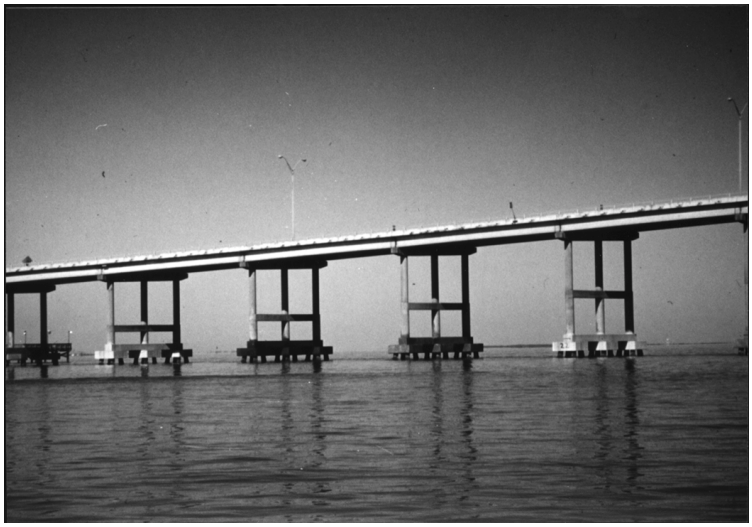

Figure 6.1: Completed installation of cathodic protection systems

6.2 ENERGIZATION

The energization of the impressed current cathodic protection systems was conducted on October 7, 1997. Polarization development was the method used to energize the systems. Instant-off potentials were measured with a Fluke 87 meter using the manual current-interrupt technique for each of the embedded silver/silver-chloride reference cells. The current settings were established by increasing the current output for the impressed current systems stepwise until all the embedded reference cells in a given zone polarized around 100 mV. The data are presented in Appendix C.

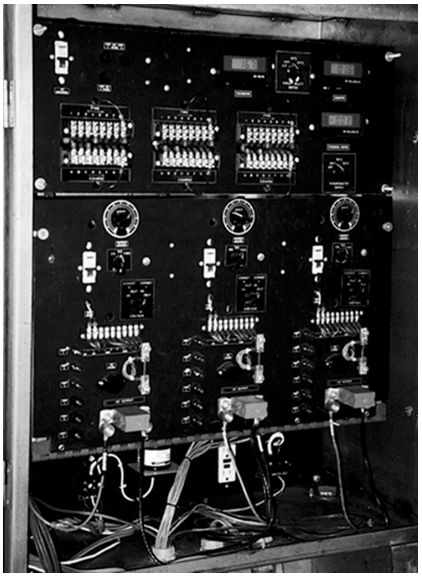

Figure 6.2: Rectifier unit

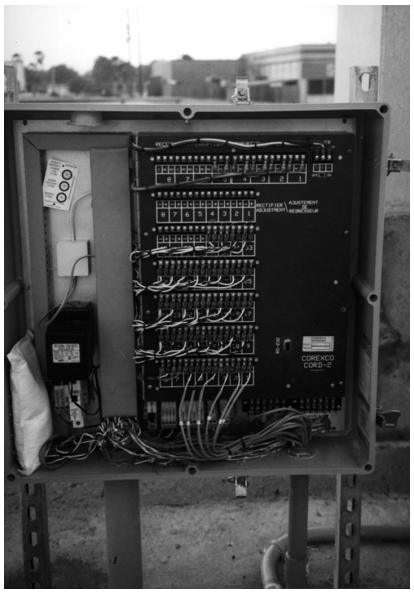

Figure 6.3: Remote-monitoring unit

The rectifier was set to constant current mode. Activation current settings were 1.5 A for Zone 1, 3.0 A for Zone 2, and 1.5 A for Zone 3. Throughout the energization, Reference Cell 1 in Zone 1 was not functioning properly. The null probes were not used for the energization because the polarity reversed with the first current increment. Thus, null probe readings were discontinued once the reversal of polarity was confirmed.

6.3 FIELD EVALUATION

The field evaluation was performed in a series of site visits that were made approximately every 2 months. Four field evaluation visits were conducted for the purpose of evaluating preliminary performance of the cathodic protection systems. Presented in Table 6.1 is the schedule of Queen Isabella Causeway field evaluation visits, which were conducted for the purpose of evaluating performance of the cathodic protection systems.

Table 6.1: Schedule of field evaluation visits

Field Evaluation Number	Evaluation Dates	Days from Energization
1	December 17–19, 1997	71
2	February 9–12, 1998	125
3	April 1–4, 1998	176
4	June 3–6, 1998	239

Besides the members protected with cathodic protection, two control members were included in the field evaluation program. The control members were Bents 23 and 24. Bent 23 was patch-repaired with Sikatop 123 and Bent 24 was left untreated.

The field monitoring evaluations included visual inspection, delamination survey, half-cell potential measurements, corrosion rate measurements, chloride content determination, concrete permeability determination, rectifier and system component evaluation, and polarization decay testing. The rectifier and system component evaluation and the polarization decay testing were conducted on every field evaluation.

6.3.1 Visual Inspection

A visual inspection of the bents protected with cathodic protection and the control bents was conducted on the second and the fourth field evaluations. A visual inspection of the cathodic protection system components was also performed.

During the second field evaluation, a visual inspection was conducted for the bents subjected to cathodic protection. The bents sprayed with zinc, Bents 19 and 22, showed no signs of deterioration or anode consumption. The sprayed titanium in Bent 20 exhibited disbondment of the titanium coating at the south end of the tie beam and the sides of the footings. The total debonded area was approximately 0.50 ft^2 (0.19 m^2). The largest debonded area was a 0.25-ft^2 (0.09-m^2) area at the top of the south end of the tie beam (Figure 6.4). The titanium mesh with overlay in Bent 21 exhibited corrosion products at the edges of the footings and the tie beam at locations where wire was used to secure the forms to the titanium mesh at the time of installation (Figure 6.5). The corrosion of the wire was unsightly but was not of serious consequence. No additional observations were made in the fourth evaluation for the members protected with cathodic protection. Although evidence of deterioration in some of the installed cathodic protection systems was observed, no signs of deterioration were detected in the concrete substrate in the bents where cathodic protection systems were installed.

The control members in Bents 23 and 24 were inspected during the second and fourth evaluations. The results of the visual survey for Bents 23 and 24 performed in the second and fourth evaluations are presented in Tables 6.2 and 6.3, respectively.

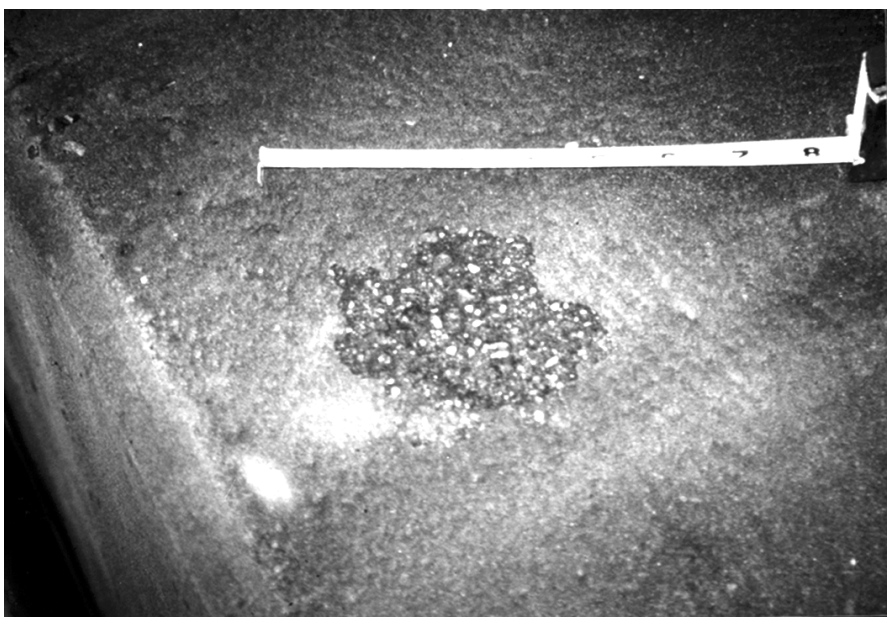

Figure 6.4: Sprayed titanium debonded

Figure 6.5: Corrosion of wire ties for Bent 21

Table 6.2: Visual inspection of Bents 23 and 24 (second evaluation)

Visual Inspection	**Footing**						**Tie Beam**	
	North		**Center**		**South**			
	23	**24**	**23**	**24**	**23**	**24**	**23**	**24**
Total Crack Length (ft)	2	7	10	26	10	20	5	36
Crack Density (ft/100 ft^2)	1	3	5	12	4	9	1	7
Spalled Area (ft^2)	0	0	0	0	0	2	0	0
Spalled Density (ft^2/100 ft^2)	0	0	0	0	0	1	0	0

Table 6.3: Visual inspection of Bents 23 and 24 (fourth evaluation)

Visual Inspection	Footing						Tie Beam	
	North		Center		South			
	23	24	23	24	23	24	23	24
Total Crack Length (ft)	2	7	11	31	15	28	8	41
Crack Density (ft/100 ft^2)	1	3	5	14	7	12	1	7
Spalled Area (ft^2)	2	0	3	0	2	2	2	0
Spalled Density (ft^2/100 ft^2)	1	0	1	0	1	1	0	0

All the spalls and some of the cracks found at the time of the pre-installation condition evaluation for Bent 23 were repaired during installation and no deterioration was observed in the repair areas. However, several feet of new cracks had appeared for Bent 23 in areas that were not repaired during installation. The total crack length at the time of the second field evaluation in Bent 23 was 27 ft (8 m). Bent 24, the untreated control, had deteriorated significantly with respect to the pre-installation visual survey. The total crack length for Bent 24 doubled between the pre-installation and the second evaluations. The percent increase in total crack lengths between the second and fourth evaluation for Bents 23 and 24 was 33 percent and 20 percent, respectively.

The growth rate per year in crack lengths and spalled areas was computed between the second and the fourth evaluations for both control bents and between the pre-installation and the second evaluations for Bent 24. The growth rate per year was not computed between the pre-installation and the second evaluations for Bent 23 because this bent underwent repairs subsequent to the pre-installation condition evaluation. The data are presented in Tables 6.4 through 6.6. For the purposes of the calculation of growth rate of crack lengths and spalled areas, it was assumed that the pre-installation condition evaluation was performed on March 31, 1997.

The greatest increases in crack lengths for both bents occurred in the south footings and in the proximity of the construction joint of the tie beams. There was no growth in crack lengths in the north footings in any of the two control bents. Spalled areas increased significantly between the second and fourth evaluations for Bent 23. Even though the crack and spall density in the control members was not serious, the increase in crack lengths and spalled areas over time was indicative of an accelerated deterioration process.

Table 6.4: Growth rate in visual inspection parameters between second and fourth evaluations for Bent 23

Growth Rate	Footing			Tie Beam
	North	Center	South	
Total Crack Length (ft/yr)	0.0	17.3	12.7	23.1
Spalled Area (ft^2/yr)	0.0	0.0	0.0	0.0

Table 6.5: Growth rate in visual inspection parameters between pre-installation and second evaluations for Bent 24

Growth Rate	Footing			Tie Beam
	North	Center	South	
Total Crack Length (ft/yr)	0.0	3.2	16.0	9.6
Spalled Area (ft^2/yr)	6.4	9.6	6.4	0.0

Table 6.6: Growth rate in visual inspection parameters between second and fourth evaluations for Bent 24

Growth Rate	Footing			Tie Beam
	North	Center	South	
Total Crack Length (ft/yr)	0.0	16.0	25.6	16.0
Spalled Area (ft^2/yr)	0.0	0.0	0.0	0.0

A visual inspection of other cathodic protection system components was also performed. The rectifier stainless steel box showed signs of corrosion pitting (Figure 6.6). Two conduit segments running along the south side of the bridge, through which the system component wires were routed, had become disjointed at the male/female coupling (Figure

6.7). This was probably due to a lack of a sufficient number of expansion joints at that location. The remaining cathodic protection system components were in good condition.

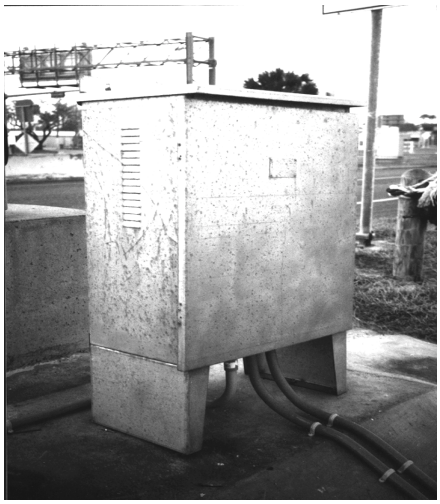

Figure 6.6: Corrosion of the rectifier box

Figure 6.7: Disjointed conduit segments

6.3.2 Delamination Survey

Delamination surveys were conducted in Bents 19 through 24 using the hammer sounding technique in the second and fourth evaluations.

A 1.5 ft^2 (0.13 m^2) delaminated area of the overlay in Bent 21 was found on the top of the north end of the tie beam during the second evaluation. By the fourth evaluation, the total delaminated area in the overlay for Bent 21 had risen to 15 ft^2 (1.4 m^2). The delaminated

areas were carefully delineated and marked with spray paint. The increase in the delaminated area of the overlay in Bent 21 over time was very significant. It is noteworthy that the delaminations detected in Bent 21 represented deterioration of the anode overlay and not of the concrete substrate. Owing to the presence of the overlay in Bent 21, the concrete substrate could not be sounded for delaminations. No delaminations were detected in any of the other bents subjected to cathodic protection.

Delaminations were detected for the control members in the second and fourth evaluations. The delaminations remained unchanged between the second and fourth evaluations. Bent 23 exhibited a total of 9 ft^2 (0.8 m^2) of delaminated area, which was found in the footings. Bent 24 exhibited a total of 18 ft^2 (1.7 m^2) of delaminated area, which was roughly equally distributed between the footings and the tie beam. No delaminations had been detected at the time of the pre-installation condition evaluation in any of the control bents.

6.3.3 Half-Cell Potential Measurements

Half-cell potential measurements were conducted on the footings and tie beams of Bents 23 and 24 on the second and fourth evaluations. The measurements were collected following the same procedure as described in Section 4.2.4. The half-cell potential measurements for Bents 23 and 24 recorded in the second and fourth field evaluations are shown in Appendix D. Tables 6.7 and 6.8 summarize the results for the control bents collected in the second and fourth evaluations, respectively. Figures 6.8 and 6.9 present the percentage of corrosion potentials in each range obtained at the pre-installation condition evaluation, the second evaluation, and the fourth evaluation for Bents 23 and 24, respectively.

In Bent 23, an increase in the percentage of readings in the uncertain range and a decrease in the percentage of readings in the high probability range was evident with respect to the pre-installation condition evaluation. The decrease in readings in the high probability of corrosion range was the result of the repairs performed during installation. At repair locations, a significant decrease in the half-cell potential was noticed. The repairs were performed at locations where the damage was visually obvious, which correlated well with half-cell potentials in the high probability of corrosion range at the time of the pre-installation condition evaluation. The percentage increase in readings in the uncertain range was an indication of an increase in areas with incipient corrosion.

In Bent 24, a significant shift towards potentials indicating higher probabilities of corrosion activity was observed between the pre-installation condition evaluation and the second evaluation. This same phenomenon was observed in both control bents between the second and fourth evaluations.

Table 6.7: Percentage of readings within specified range (second evaluation)

Potential Ranges (mV)	Bent 23				Bent 24			
	Footing			Tie Beam	Footing			Tie Beam
	North	Center	South		North	Center	South	
More positive than -200	61	31	47	73	61	47	28	66
-200 to -350	39	69	45	7	31	41	53	34
More negative than -350	0	0	8	0	8	12	19	0

Table 6.8: Percentage of readings within specified range (fourth evaluation)

Potential Ranges (mV)	Bent 23				Bent 24			
	Footing			Tie Beam	Footing			Tie Beam
	North	Center	South		North	Center	South	
More positive than -200	61	22	28	86	47	41	19	61
-200 to -350	36	78	58	14	44	53	58	36
More negative than -350	3	0	14	0	9	6	23	3

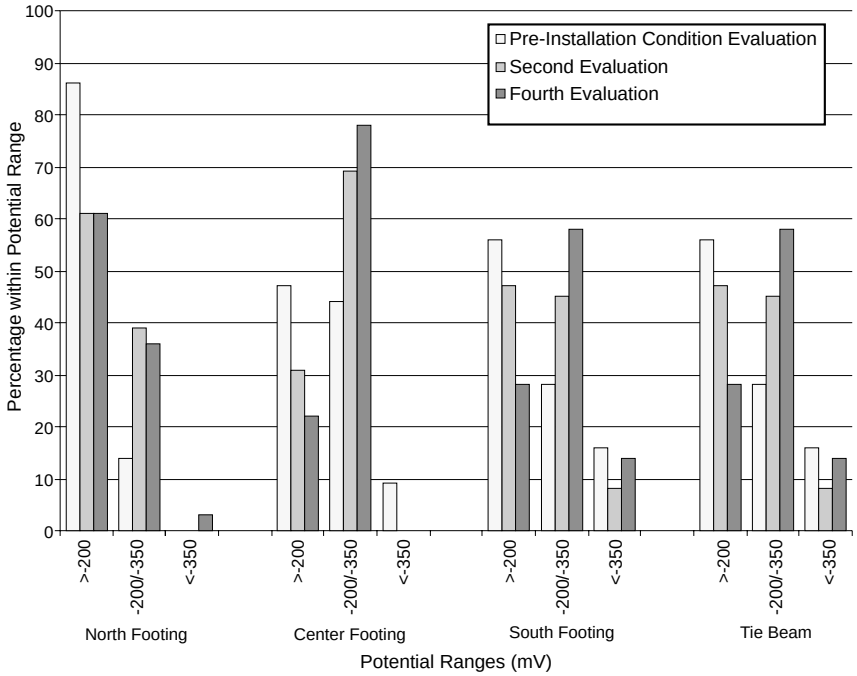

Figure 6.8: Corrosion potential ranges in different evaluations for Bent 23

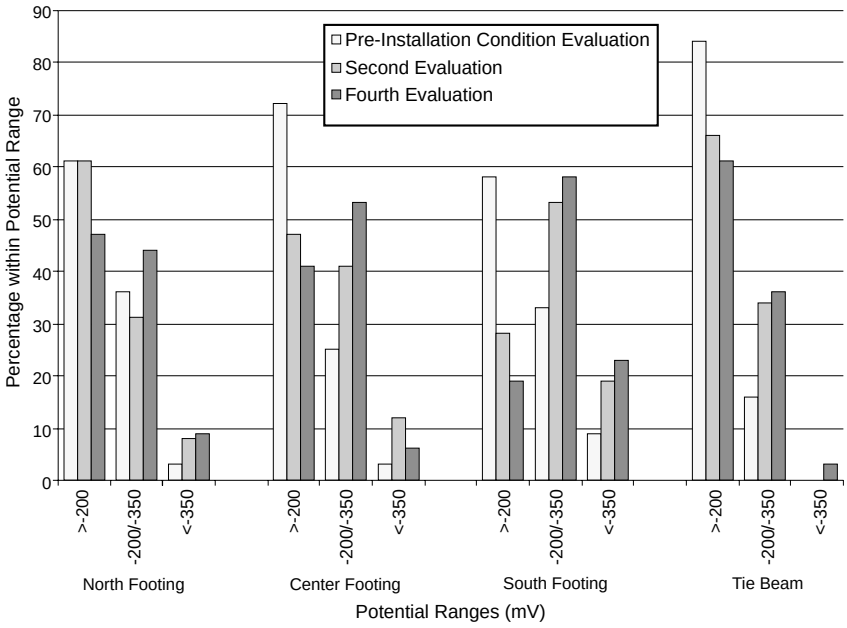

Figure 6.9: Corrosion potential ranges in different evaluations for Bent 24

6.3.4 Corrosion Rate Measurements

Corrosion rate tests were conducted with a 3LP Corrosion Rate device at selected locations in Bent 24 on the second and fourth evaluations. The guidelines for interpreting corrosion rate data obtained with the 3LP device are presented in Table 6.9.

Corrosion rate data obtained in the second and fourth evaluations are presented in Appendix E. The values obtained for both visits were in the 1.0 to 10.0 mA/ft^2 (11 to 108 mA/m^2) range, which translated into a predicted time-to-damage between 2 and 10 years. The predicted time-to-damage does not constitute an estimate of the remaining service life of the tie beams and footings.

Table 6.9: Guidelines for interpreting corrosion rate data

I_{corr} (mA/ft^2)	**Predicted Time to Damage**
Less than 0.2	None
0.2 to 1.0	10 to 15 years
1.0 to 10.0	2 to 10 years
Greater than 10.0	Less than 2 years

6.3.5 Chloride Content Determination

In the second field evaluation, five 2-in. (51-mm) diameter cores were collected, one each from Bents 19 through 24. The cores were collected from areas on the top surface of the footings that were found to be sound in the pre-installation condition evaluation. Powdered samples were collected from each core every 0.5 in. (12.7 mm). The powdered samples were analyzed for total chloride ion content in accordance with AASHTO T 260, and all results are presented in Appendix F. The interpolated chloride contents at the level of the reinforcing steel were around the chloride threshold for every core. The chloride contents obtained were comparable to the chloride contents obtained in sound areas during the pre-installation condition evaluation. From the limited survey conducted, no significant difference in chloride levels between protected and unprotected bents or between bents protected with different cathodic protection systems could be found.

6.3.6 Concrete Permeability Measurement

Concrete permeability measurements were collected in the second field evaluation. The values were probably representative of the concrete permeability for all bents. Three 4-in. (102-mm) diameter cores were collected from Bent 24 for concrete permeability testing. Rapid permeability tests were performed in accordance with the procedure of AASHTO T 277, *Resistance of Concrete to Chloride Ion Penetration* (Ref 31). Table 6.10 presents the chloride permeability as a function of charge passed as per AASHTO T 277.

One core was extracted from the south footing and two cores were extracted from the top of the south end of the tie beam in Bent 24. At the tie beam, one core was collected from the precast section and the other from the cast-in-place section in the proximity of the southernmost column. The two cores collected in the tie beam were 10 in. (254 mm). The concrete permeability data are presented in Table 6.11.

There was a significant difference between the permeability obtained in the precast and cast-in-place portions of the tie beam in Bent 24. The difference in permeability could have exacerbated the deterioration process at the tie beam by creating a corrosion cell between the areas of high and low permeability. The concrete permeability of the footer was low in comparison with the permeability in the precast portion of the tie beam.

Table 6.10: Chloride permeability versus charge passed

Charge Passed (coulombs)	**Chloride Permeability**
Greater than 4,000	High
Between 2,000 and 4,000	Moderate
Between 1,000 and 2,000	Low
Between 100 and 1,000	Very Low
Less than 100	Negligible

Table 6.11: Concrete permeability data obtained in Bent 24

Core	**Location**	**Charge Passed (coulombs)**
1	Tie beam at top of the precast section in the proximity of the southernmost column	1,620
2	Tie beam at top of the cast-in-place section in the proximity of the southernmost column	4,110
3	South footing	1,550

6.3.7 Rectifier and System Component Evaluation

Rectifier data were recorded in the as-found condition, and all system components were evaluated. Electrical continuity and AC resistance data were collected after the power was turned off. The current flow in the null probes in each of the zones was measured with the power on and off. In the first field evaluation, limited data could be gathered for the galvanic system in Zone 4 because the current-interrupt feature for this zone could not be identified.

A 10-ohm resistor was installed in the remote-monitoring unit in between the null probe and the null probe ground terminals in the first evaluation. This resistor served as a shunt to measure millivolt drop between the two terminals.

As-Found Conditions. As-found conditions were recorded at the start of every site evaluation. The rectifier as-found data are presented in Appendix G. The rectifier output voltage, output current, and back emf for each zone were measured with an external Fluke 87 meter. The voltage and current outputs were also recorded from the built-in rectifier LCD meter. The current output was measured as a millivolt drop across a shunt and converted to current units. The shunts for the impressed current systems were 50 mV/8 A, and the shunt for the galvanic sprayed zinc system was 0.1 ohm. Based on the current output, the current density was computed using the total square feet of concrete surface subjected to cathodic protection.

The readings obtained with the built-in meter were found to be accurate when compared with the readings obtained with the external meter. The current density values for Zones 1 and 3 were in the range generally encountered in impressed current cathodic protection systems (1.0 to 1.5 mA/ft^2 [10.8 to 16.1 mA/m^2]). The current density for Zone 2, however, was higher. This was due to the low conductivity of titanium sprayed anode. At energization, the high current output required to achieve 100-mV polarization for Zone 2 was twice that of other zones.

The galvanic sprayed zinc in Zone 4 produced substantial current output. The current readings in the four field evaluations were widely variable, ranging between 0.24 A and 0.46 A.

The back emf values for the impressed current systems were in an acceptable range. The back emf is the sum of the anode and the rebar polarization. Low back emf values indicate the possibility of an electrical short, and high back emf values indicate excessive polarization of the anode, rebar, or both.

Electrical Continuity Testing. The electrical continuity testing was performed to determine the presence of electrical shorts between the different anodes and the system ground and to verify the adequacy of the instrumentation. Appendix H presents electrical continuity test results for all components in each of the zones gathered in the four field evaluations. All testing was conducted using DC techniques. The presently accepted criteria used to evaluate DC continuity data include the following (Ref 32):

- DC resistance measured between the two locations should be less than 1 ohm.

- DC resistance in opposite directions (i.e., with meter connections reversed) should differ by less than 1 ohm.
- Potential difference between the two locations should be less than 1 mV.

The anode-to-system ground data indicated that there were no shorts between the anode and the reinforcing steel for the impressed current systems in Zones 1 through 3. The Reference Cell 1 in Zone 1 showed unstable readings in the first two evaluations. The problem was an open connection that was fixed sometime between the second and third evaluations.

Based on the continuity check criteria, the data presented in Appendix H indicated that the reference cell grounds and null probe grounds were discontinuous with their respective system grounds. The currently accepted criteria used to evaluate DC electrical continuity are under revision (Ref 33). In lieu of this and the adequate behavior of the reference cells and null probes, the reference cell grounds and the null probe grounds were deemed continuous to their respective system grounds.

AC Resistance Measurements. AC resistance measurements were collected as another measurement of electrical continuity and to check the stability of the reference cells; these measurements are presented in Appendix I. The AC resistance between the anode and the system ground for each zone, between the embedded reference cells and their respective grounds, and between the null probe and their respective grounds was measured with a Nilsson 400 resistivity meter configured as a two-point probe.

Guidelines for categorizing electrical continuity based on AC resistance test results are presented in SHRP-S-337 (Ref 13):

- If the AC resistance is less than 0.10 ohm, electrical continuity is highly probable.
- If the AC resistance is between 0.10 and 0.50 ohm, electrical continuity is uncertain.
- If the AC resistance is greater than 0.50 ohm, electrical discontinuity is highly probable.

On the basis of these guidelines, the anode and the system grounds and the null probe and the null probe grounds were found to be discontinuous.

The stability of the reference cells was also measured. AASHTO limits the AC resistance for the reference cell to 10,000 ohm (Ref 32). Reference cells with AC resistance in excess of 25,000 ohm have been found to exhibit adequate behavior, and the resistance limit for reference cell stability is currently under revision. The highest AC resistance measured was 11,000 ohm. The AC resistance measured for most reference cells was under 10,000 ohm. Therefore, all reference cells were deemed stable based on the AC resistance measurements.

Null Probe Testing. Null probe testing was conducted in the first, second, and fourth field evaluations. The current flow in the null probes in each of the zones was measured across a 10-ohm resistor with the system in the energized and the de-energized conditions. The data are presented in Appendix I. When the positive lead of the Fluke 87 meter was

connected to the null probe and the negative lead was connected to the null probe ground, a negative reading indicated that the null probe was corroding. As expected, all null probes showed positive millivolt drop readings with the system in the energized condition and a reversal or a decrease with the system off.

The concept of null probes was found to be of limited use in determining level of protection by cathodic protection. Having observed the installation of the null probes, which was typical of the installation of null probes in other projects, the reproducibility of null probe measurements was found to be questionable. Concrete and rebar condition at the location of the null probe as well as amount of concrete removed to isolate the rebar segment were some of the many variables that limit the reproducibility of null probe measurements. The use of null probes for assessment of cathodic protection performance should be limited to checking reversal or changes in the millivolt drop as the system is energized or de-energized. Limited information can be obtained from the magnitude of the changes in millivolt drop.

6.3.8 Polarization Decay Testing

Polarization decay testing was performed in accordance with the National Association of Corrosion Engineers (NACE) Standard RP0290-90, *Cathodic Protection of Reinforcing Steel in Atmospherically Exposed Concrete Structures* (Ref 34). In the first evaluation, polarization decay testing could not be performed for the galvanic system in Zone 4 because the current-interrupt feature for this zone could not be identified.

Instant-Off Potential Measurement. Instant-off potentials for the embedded reference cells were measured using a Fluke 87 meter. Because the Good-All Electric was a full-wave rectifier, the instant-off potential could be measured with the manual current-interrupt technique or the peak-hold technique. The manual current-interrupt technique was used in the first field evaluation, and the peak-hold technique was used in the second and third evaluations. Both the manual current-interrupt and the peak-hold techniques were used in the fourth evaluation. The readings obtained using both techniques are presented in Appendix J. From the study of the waveform for the different reference cells using a Fluke 97 50 MHz Scopemeter in the fourth evaluation, it was concluded that the instant-off measurements were corrupted by electrical noise pick up in some reference cells. Because of the nature of the waveforms found, the electrical noise affected the peak-hold instant-off measurements more than the current-interrupt measurements. Electrical noise does not affect the operation of the cathodic protection systems, but it hampers the ability to monitor the cathodic protection systems.

The instant-off potential data are shown in Appendix J. No instant-off potentials were found to be more negative than -1,100 mV. An unpublished CEN European document in its final draft form establishes this limit for plain reinforcing steel (Ref 35).

Polarization Decay Testing. Once static potential data were obtained using the embedded reference cells, depolarization potentials were computed. The data are presented in Appendix J.

In the first field evaluation, the 100-mV depolarization criterion was satisfied for all reference cells in 4 hours, with the exception of Reference Cell 1 in Zone 2.

In the second field evaluation, the instant-off potential measurement for Reference Cell 3 in Zone 2 was probably corrupted by electrical noise, and so the 1-hour static potential was used in lieu of the instant-off potential for calculation of depolarization potentials. Several reference cells in the impressed current zones that satisfied the 100-mV depolarization criterion in 4 hours in the first evaluation did not satisfy the criterion in the second evaluation. Depolarization values could be obtained for the galvanic sprayed zinc cathodic protection system in Zone 4 in this field evaluation. Reference Cell 1 and Reference Cell 2 in Zone 4 did not satisfy the 100-mV depolarization criterion in 4 hours. Reference Cell 2, however, depolarized 95 mV. Reference Cell 1 depolarized in excess of 100 mV in the first hour but polarized in the remaining 3 hours to a depolarization value of 65 mV after 4 hours.

A more extensive depolarization test was performed in the third evaluation. Static potential readings were collected at 15 minutes, 30 minutes, 1 hour, 2 hours, 3 hours, 4 hours, and 17.5 hours. The corresponding depolarization potentials were computed. Because the instant-off measurement for several references was corrupted by possible electrical noise pick up, the depolarization potentials were computed using the 15-minute static potential in lieu of the instant-off potential for these reference cells. Upon current interruption, Reference Cell 1 in Zone 1 showed polarization in the first hour and exhibited depolarization behavior thereafter. Only Reference Cell 1 in Zone 2 did not satisfy the 100-mV depolarization criterion in 17.5 hours.

For the fourth evaluation, the depolarization potentials were computed using the instant-off potentials obtained using the manual-current technique. Static potentials were collected at 15 minutes, 30 minutes, 1 hour, 2 hours, 4 hours, and 22 hours. The corresponding depolarization potentials were computed. Reference Cell 1 showed slow depolarization at the outset but adequate depolarization potentials in 22 hours. Only Reference Cell 1 in Zone 2 did not satisfy the 100-mV depolarization criterion in 22 hours.

Figure 6.10 presents the 4-hour depolarization potentials obtained in the four field evaluations for all reference cells in all zones. The depolarization potential for the first two evaluations is not presented for Reference Cell 1 in Zone 1, since this reference cell gave unstable readings owing to an open connection. Readings for the first evaluation for the galvanic sprayed zinc system in Zone 4 are not presented because the current-interrupt feature for this reference cell could not be identified in this evaluation. The depolarization potentials presented for several reference cells used static potentials in lieu of instant-off potentials as a result of electrical noise.

From the depolarization testing in the four field evaluations, it could be gathered that the sprayed titanium in Zone 2 had consistently very low depolarization potentials for Reference Cell 1. The two anode positive connections for Zone 2 were located in the west side face of the tie beam approximately 15 ft (4.6 m) from each end of the tie beam. Reference Cell 1 in Zone 2 was located in the bottom mat of the south footing. Reference Cell 1 was the reference cell located farthest from any of the two positive connections in Zone 2. The low depolarization of Reference Cell 1 in Zone 2 was another manifestation of

the low conductivity of the catalyzed titanium spray coating. The high resistivity of the coating resulted in a decrease in protection in areas located far from the positive connections. This would also indicate that two positive connections for this installation were not sufficient.

The impressed current sprayed zinc in Zone 1 exhibited adequate depolarization. The behavior of Reference Cell 1 was not normal and was probably affected by electrical noise. The titanium mesh with overlay in Zone 3 had consistently the highest depolarization values. Considering the sacrificial nature of the system in Zone 4, the sacrificial sprayed zinc exhibited high depolarization values.

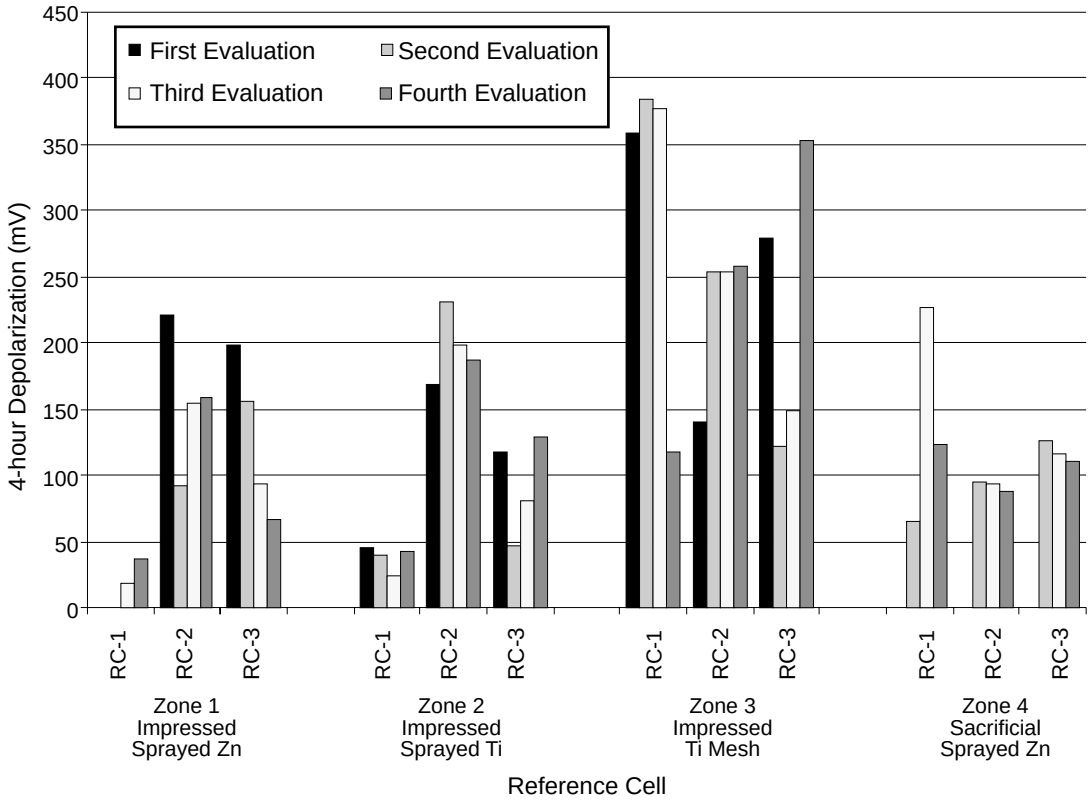

Figure 6.10: Four-hour depolarization for all reference cells

6.4 REMOTE MONITORING

6.4.1 Remote-Monitoring Operation

Remote monitoring was performed using a personal computer equipped with a modem. There were several problems with the remote monitoring that limited the collection of data. The first problem observed was that when the systems were turned off temporarily from a remote station to obtain instant-off potentials, the AC breaker for the impressed current systems went off, resulting in an interruption in cathodic protection for the bents with impressed current systems. This problem was resolved in January 1998.

Another problem was that the software required to access the remote-monitoring unit was incompatible with Windows 95. At the time of this study, a new version of the remote-monitoring unit software was expected.

6.4.2 Data Collection Process

The remote monitoring data were accessed via "direct talk" to the remote-monitoring unit. A direct call was placed with Hyperterminal using Windows 95. Each time the remote monitoring unit was accessed, the readings were obtained for the thirty-six channels of the CORD-2. The instant-off potentials and the power-off readings for the null probes were also obtained remotely in each session. The remote-monitoring data were collected from February to June 1998.

Immediately following the collection of data remotely, a World Wide Web Internet site providing on-time weather information was accessed. The weather information recorded included temperature, relative humidity, dew point, and wind speed.

6.4.3 Periodic System Check

The remote-monitoring system was used to check the operation of the different cathodic protection systems. Periodically, readings for the thirty-six channels in the CORD-2 unit were collected. No anomalies were found between February and June 1998 in the operation of the cathodic protection systems.

6.4.4 Current Output Variability for Sacrificial Sprayed Zinc System

The variability of the current output for the sacrificial sprayed zinc system was studied with the remote-monitoring capability. The galvanic zinc current output obtained using the remote-monitoring ranged from 18.4 mA to 59.3 mA. This is equivalent to 0.14 to 0.45 mA/ft^2 (1.51 to 4.84 mA/m^2), respectively.

The correlation of temperature, relative humidity, dew point, and wind speed with the current output of the galvanic system was investigated. The rationale behind the selection of wind speed as one of the variables was that higher wind speeds resulted in more wave action,

which could affect current output. The correlation coefficients between the different climactic variables and current output are presented in Table 6.12.

Table 6.12: Coefficient of determination between weather variables and current

Variable	Period		
	February to mid-April	**mid-April to June**	**February to June**
Dew Point	0.90	0.53	0.57
Relative Humidity	0.59	0.21	0.44
Temperature	0.23	0.26	0.16
Wind Speed	0.00	0.15	0.00

The coefficient of determination was obtained between February and mid-April, between mid-April and June, and between February and June. Very good correlation was found between dew point and current between February and mid-April. The coefficient of determination between dew point and current output in this period was 0.90. Presented in Figure 6.11 is the graph of current output versus dew point between February and mid-April. The coefficient of determination between dew point and current throughout the data collection period (February through June) was the highest among the variables studied.

From mid-April to June, a decrease in the output current was observed during the daytime hours. At any given dew point, the current values were lower between mid-April and June than between February and mid-April. During the night hours, for any given dew point, the output current was comparable to the levels obtained between February and mid-April.

Because the tie beams were not in the splash/evaporation zone, the current output from the galvanic sprayed zinc in this area was very much dependent on the atmospheric conditions. The dependency of the galvanic current in this area was higher than that in the footings, where the concrete moisture content was relatively high and constant. The results of an investigation in which the relationship between relative humidity and galvanic current was studied for laboratory specimens indicated that surface wetting might increase the fraction of the anode in contact with concrete surface and, therefore, the current delivery would increase (Ref 36). Another similar factor could be dew point, which is a measure of the total amount of moisture in the air. It is defined as the temperature to which air must be cooled to reach its saturation point. Between mid-April and June, the higher temperatures and the solar radiation present during the daytime hours could have resulted in the drying of concrete and, consequently, a decrease in the currents measured. The cyclic behavior of current over a 24-hour period is presented in Figure 6.12. The current measurements were collected every hour over a 24-hour period for 6 days in May and June 1998. The lowest current readings occurred between 4 and 7 p.m., and the highest readings occurred between 5 and 8 a.m. The highest current readings occurred following or during cloudy days.

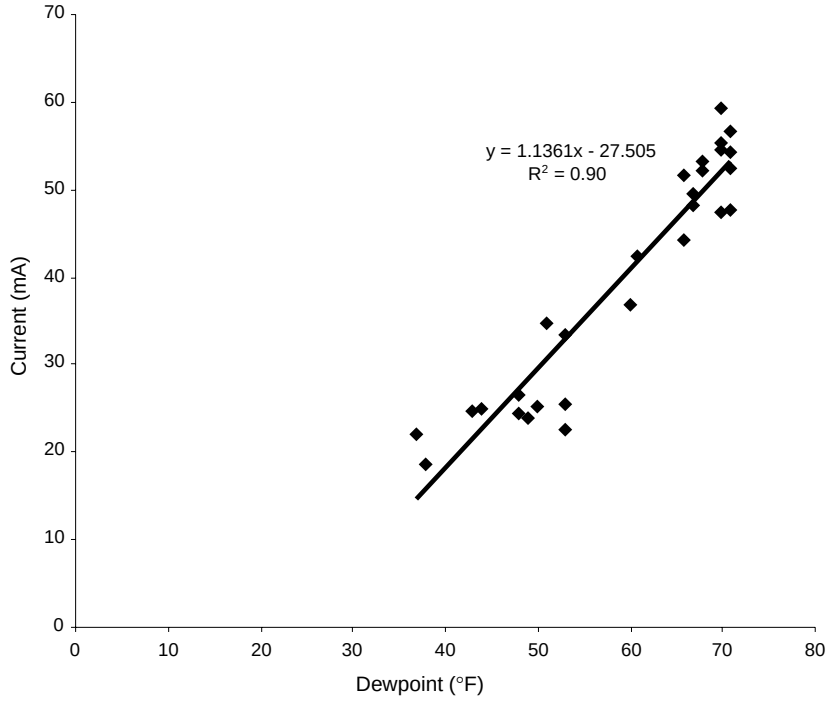

Figure 6.11: Dew point versus current between February and mid-April

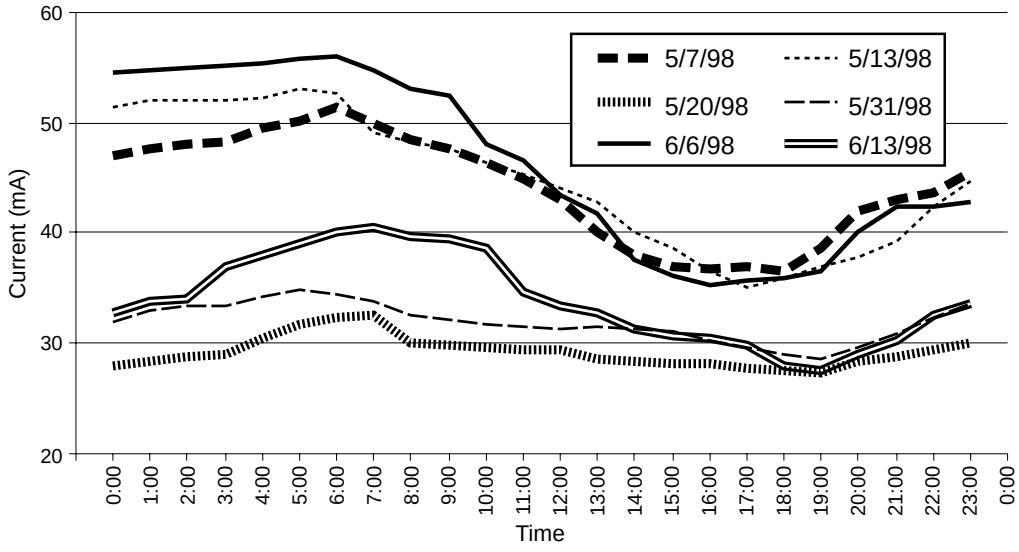

Figure 6.12: Cyclic current behavior

6.5 CONCLUSIONS FROM PERFORMANCE EVALUATION

From the visual inspection, delamination survey, and half-cell potential of the control members, it was evident that the progression of the deterioration was fairly rapid. This rapid progress of the deterioration was observed in a period of approximately 1 year. Corrosion rate data collected at several locations for the untreated control members translated into a predicted time-to-damage between 2 and 10 years.

The deterioration, as was also observed in the pre-installation condition evaluation, was most prevalent in the south footings and in the proximity of the construction joint for the tie beam. There was a significant difference between the permeability obtained in the precast and cast-in-place portions of the tie beam. The difference in permeability could have created a macrocell between the areas of high and low permeabilities in the proximity of the construction joint. This could have exacerbated the deterioration process at this location.

There were no signs of concrete deterioration in any of the bents protected with cathodic protection. This confirmed the effectiveness of cathodic protection in arresting corrosion-induced concrete deterioration. Deterioration was observed, however, in some of the anode materials. The sprayed titanium exhibited widespread minor disbondment of the anode material. The titanium mesh with overlay evidenced delaminations of the overlay. The increase in delaminated areas of the overlay over time was very significant.

From the rectifier and system component evaluation of the cathodic protection systems, it was gathered that the methods to evaluate cathodic systems take the form of guidelines from a variety of sources. There is not a single updated source for information on how to evaluate cathodic protection systems. Many guidelines are under revision or are documents in progress.

The benefit from the use of null probes was found to be extremely limited. Having observed the installation of the null probes that was typical of the installation of null probes in other projects, the reproducibility of null probe measurements was found questionable. The use of null probes for assessment of cathodic protection performance should be limited to checking reversal or changes in the millivolt drop as the system is energized or de-energized. Limited information can be obtained from the magnitude of the changes in millivolt drop. The benefit from the use of null probes was also found questionable for the energization of the cathodic protection systems because polarity reversed with the first current increment.

The high voltages required to achieve the desired current levels in the impressed current systems were indicative of high resistivity concrete. This was confirmed by the low permeability measured in the footings and in the precast areas of the tie beams. The current density values for the impressed current sprayed zinc and the titanium mesh with overlay were in the range generally encountered in impressed current cathodic protection systems. The current density for the sprayed titanium, however, was higher. This was due to the low conductivity of the sprayed titanium anode.

Another indication of the low conductivity of the sprayed titanium system was the very low depolarization potentials for the reference cell that was located farthest from either of the two anode positive connections. This would indicate that two positive connections for this installation were not sufficient.

The impressed current sprayed zinc exhibited adequate depolarization. The titanium mesh with overlay had consistently the highest depolarization values. The sacrificial sprayed zinc exhibited high depolarization values considering the galvanic nature of this system.

The galvanic sprayed zinc produced substantial current output. The current readings in the four field evaluations were variable. The variability correlated well with changes in dew point between February and mid-April. Between mid-April and June, the correlation was not as good. A cyclic behavior for the current output during the course of a day was observed between mid-April and June. The higher temperatures and the solar radiation occurring during the daytime hours could have resulted in the drying concrete and, consequently, a decrease in the current output for the galvanic zinc.

CHAPTER 7. DURABILITY AND COST ANALYSES

7.1 DURABILITY FOR INSTALLED SYSTEMS

The *durability* or *service life* of the cathodic protection systems installed at the Queen Isabella Causeway are terms meant to identify the number of years that the cathodic protection systems would provide adequate protection to the substrate concrete. The information available for durability of cathodic protection systems is scarce. The advertised durability of the cathodic protection systems often exceeds the age of systems in place.

Sprayed zinc anode durability is estimated in the literature to range between 10 and 15 years (Refs 7, 5) for impressed current systems. After more than 4.5 years, a number of sacrificial sprayed zinc bridge substructures installed in subtropical environments in Florida had shown physical integrity and adequate performance in harsh marine environments (Ref 36). The ground connection for these bridge substructures was achieved by direct contact of the sprayed zinc anode to the reinforcing steel. The limiting factor for the service life of impressed current and sacrificial sprayed zinc systems has been the accumulation of metal dissolution products at the zinc anode interface. The accumulation of zinc corrosion products results in an increase in circuit resistance and debonding of the zinc coating.

The service life of the titanium mesh with overlay is estimated to range between 20 and 35 years (Refs 7, 5). The main problem with this anode system for bridge substructures has been debonding of the concrete overlay.

The sprayed titanium is a relatively new system. The estimated service life of the system ranges from 20 to 40 years (Refs 7, 24).

Findings from the preliminary performance evaluation presented in Chapter 6 could impact the durability of the systems studied. Disbondment of the sprayed titanium was observed in the performance evaluation. In addition, the low conductivity of the sprayed titanium and the consequent higher applied current could result in accelerated electrochemical aging of the anode. Electrochemical aging of sprayed titanium in laboratory studies resulted in a friable anode and a reduction in bond strength to the substrate concrete (Ref 37). In the case of the titanium mesh with overlay anode, premature and progressive delamination of the concrete overlay was observed. No observations that could potentially impact durability were made for the sprayed zinc systems in the preliminary performance evaluation.

7.2 ESTIMATED INSTALLATION COSTS

The installation costs for the cathodic protection systems are presented in Table 7.1. The costs were divided into three categories: generic components, anode installation for the different bents, and rectifier/remote monitoring. Owing to the small scale and experimental nature of this project, the installation costs might not be representative of typical installations.

The costs presented were estimated costs or bid costs used for pricing and payment of the installation work.

Actual costs could not be obtained. Substantial discrepancies between estimated and actual installation costs were expected, especially for the titanium mesh with overlay system. As reported in Chapter 5, in two instances there were failures of the overlay that required removal of the entire overlay. Surface preparation was another source of possible discrepancies. The actual costs for the surface preparation of the final application of the titanium mesh with overlay system were expected to be significantly higher than those for other bents based on the productivity data presented in Chapter 5.

The costs of the generic components, presented in Table 7.1, were the costs for materials and installation of the scaffold, instrumentation, negative and positive connections, concrete repairs, and sandblasting surface preparation. The cost of gaining access to the bents by means of the scaffold was high and represented a substantial proportion of the total cost for the installation of each system. The costs would have decreased substantially if the bents had been accessed from a barge, especially in the case of a larger scale application.

For comparison purposes, the estimated initial costs unique to each system were computed. The estimated initial costs and the estimated initial costs per unit area are presented in Table 7.2. The costs for the rectifier and the remote-monitoring unit were equally divided among the three impressed current systems. Even though remote monitoring was also used for the sacrificial sprayed zinc in Bent 22, the ability to monitor remotely was deemed of greater importance for impressed current than for sacrificial systems. Therefore, no costs associated with the rectifier/remote-monitoring unit were apportioned to the sacrificial sprayed zinc system in Bent 22.

The unique initial cost per unit area for the sprayed titanium anode in Bent 20 was \$71/ft^2 (\$760/m^2). This is equivalent to 4 times the cost of the titanium mesh with overlay anode in Bent 21, 10 times the cost of the impressed current sprayed zinc anode in Bent 19 and 35 times the cost of the sacrificial sprayed zinc anode in Bent 22. The sacrificial sprayed zinc anode system in Bent 22 had the lowest cost per unit area at \$2/ft^2 (\$22/m^2).

7.3 COST ANALYSIS

A simplified cost analysis was used to compare the annual costs of the different cathodic protection systems. The annual costs were computed through a range of service lives because of the uncertainty in estimating the service life of the cathodic protection systems installed in the Queen Isabella Causeway. Ironically, the two anode systems with the highest service life in the literature showed premature deterioration in the performance evaluation.

On the basis of the service lives presented in the literature for the different cathodic protection systems and the preliminary observations gathered in the performance evaluation, a range of service lives for the different anode systems was determined to compute equivalent annual costs. For the titanium mesh with overlay and the sprayed titanium systems, the range of service lives was from 10 years to the highest estimate in the literature presented in Section 7.1.

Table 7.1: Estimated installation costs for the cathodic protection systems

Work Item	Cost ($)
Generic Components Per Bent	
Scaffold installation	20,000
Negative and positive connections	1,000
Reference cell/null probe installation	1,450
Wiring	1,200
Concrete repairs	2,900
Sandblasting	1,400
Bent 19 (Impressed Sprayed Zinc)	
Zinc spraying and topcoat	2,750
Total for Bent 19	30,700
Bent 20 (Impressed Sprayed Titanium)	
Titanium spraying	84,950
Catalyst application	2,000
Total for Bent 20	114,900
Bent 21 (Impressed Ti Mesh with Overlay)	
Mesh and wiring installation	5,650
Concrete overlay	5,600
Total for Bent 21	39,200
Bent 22 (Sacrificial Sprayed Zinc)	
Zinc spraying and topcoat	2,750
Total for Bent 22	30,700
Rectifier/Remote Monitoring	
Conduit to rectifier/remote monitoring	32,000
Wiring to rectifier/remote monitoring	20,000
Rectifier/remote monitoring	20,200

Table 7.2: Estimated initial costs for the anode systems

Work Item	Cost ($)	Cost ($/ft^2)
Bent 19 (Impressed Sprayed Zinc)		
Zinc spraying and topcoat	2,750	
Rectifier/remote-monitoring unit	6,750	
Total	9,500	7
Bent 20 (Impressed Sprayed Titanium)		
Titanium spraying	84,950	
Catalyst application	2,000	
Rectifier/remote-monitoring unit	6,750	
Total	93,700	71
Bent 21 (Impressed Titanium Mesh with Overlay)		
Mesh and wiring installation	5,600	
Concrete overlay	9,200	
Rectifier/remote-monitoring unite	6,750	
Total	21,550	16
Bent 22 (Sacrificial Sprayed Zinc)		
Zinc spraying and topcoat	2,750	
Total	2,750	2

The only costs considered in the simplified economic analysis were the initial costs of anode installation, presented in Table 7.2 for each bent, and the cost of sandblasting surface preparation ($1,400 per bent). The equivalent annual costs were computed for every 5-year increment in the range of service lives determined for each system. A discount rate of 7 percent was used to obtain the equivalent annual costs for the different service lives.

It was assumed that, throughout the service life of the cathodic protection systems, the same level of protection would be afforded by the cathodic protection systems to the treated

members. For the purposes of the comparative simplified economic analysis, the costs of monitoring and maintenance were assumed to be equivalent for the different systems.

Tables 7.3 and 7.4 present the equivalent annual costs and equivalent annual costs per 9.29 m^2 (100 ft^2) for the different systems. The sacrificial and impressed current sprayed zinc systems had lower equivalent annual costs per square foot than the other two systems. Even if the titanium mesh with overlay and the sprayed titanium reached the upper end of the service life in the literature, the annual cost would still be higher than that of the other systems.

It was assumed that at the end of the service life, the different anode systems could be re-installed. The costs of re-installation were assumed to be equal to the costs of installation minus the costs of the rectifier/remote monitoring, if applicable. The costs of gaining access to the bents were not considered because it was assumed that the costs of using a barge would be a fraction of the cost associated with installing a scaffold.

Assuming a 35-year economic analysis and that both the sprayed titanium and titanium mesh with overlay systems reached a 35-year service life, the sprayed zinc systems would have to be replaced at the end of their service life several times to reach the 35-year life. Because there would be no need to re-install the rectifier in the impressed current sprayed zinc system, the costs of re-applying the anode would be the costs of sandblasting and zinc spraying; essentially, the costs of re-installation would be the same for the impressed current and the sacrificial zinc systems. If both the impressed current and the sacrificial sprayed zinc were replaced at the 5-year equivalent annual cost of the sacrificial sprayed zinc, the equivalent annual cost at 35 years for the zinc systems would still be less than that for the other systems. From the findings of the performance evaluation in Chapter 6, it appears highly unlikely that the titanium mesh with overlay and the sprayed titanium would reach a 35-year service life. The 5-year annual cost assumed for the re-installation of zinc was the annual cost for the lowest service life computed.

Table 7.3: Equivalent annual costs for anode systems

	Equivalent Annual cost ($)			
	Bent			
	19	**20**	**21**	**22**
Service life (years)	**Impressed Sprayed Zn**	**Impressed Sprayed Ti**	**Impressed Ti Mesh**	**Sacrificial Sprayed Zn**
5				1,024
10	1,559	13,549	3,275	598
15	1,202	10,447	2,525	
20		8,982	2,171	
25		8,164	1,973	
30		7,669	1,854	
35		7,346	1,776	
40		7,136		

Table 7.4: Equivalent annual costs for anode systems per unit area

Service life (years)	Equivalent Annual cost ($/100ft^2)			
	Bent			
	19	20	21	22
	Impressed Sprayed Zn	Impressed Sprayed Ti	Impressed Ti Mesh	Sacrificial Sprayed Zn
5				78
10	118	1,026	248	598
15	91	791	191	
20		680	164	
25		618	150	
30		581	140	
35		556	135	
40		541		

The zinc systems were more cost effective than the sprayed titanium and titanium mesh with overlay anode systems for the Queen Isabella Causeway, based on the results of the simplified comparative analysis. A definitive selection could not be made between the impressed current and the sacrificial zinc systems. The reasons for this were the uncertain service lives of the two systems, the limited time the cathodic protection systems had been in service, the difficulty in assigning accurate cost figures to certain elements in the cost equation, and the comparable cost effectiveness in the simplified economic analysis presented.

7.4 CONCLUSIONS FROM DURABILITY AND COST ANALYSIS

Findings from the preliminary performance evaluation presented in Chapter 6 should impact the durability of the systems studied. Disbondment of the sprayed titanium was observed in the performance evaluation. The low conductivity of the sprayed titanium could result in accelerated electrochemical aging of the anode. In the case of the titanium mesh with overlay anode, premature and progressive delamination of the overlay was observed. No observations that could potentially impact durability were made of the sprayed zinc systems in the preliminary performance evaluation.

For comparison purposes, the estimated initial costs unique to each system were computed. The initial cost per unit area for the sprayed titanium anode in Bent 20 was \$71/ft^2 (\$760/m^2). This is equivalent to 4 times the cost of the titanium mesh with overlay anode in Bent 21, 10 times the cost of the impressed current sprayed zinc anode in Bent 19, and 35 times the cost of the sacrificial sprayed zinc anode in Bent 22. The sacrificial sprayed zinc anode system in Bent 22 had the lowest cost per unit area at \$2/ft^2 (\$22/m^2).

For the purpose of the simplified economic analysis, a range of service lives was determined. The range for the titanium mesh with overlay and the sprayed titanium system was from 10 years to the highest estimate in the literature.

On the basis of the simplified economic analysis, the sprayed zinc systems were more cost effective than the sprayed titanium and titanium mesh with overlay anode systems for the Queen Isabella Causeway. A definitive selection could not be made between the impressed current and the sacrificial zinc systems based on the simplified economic analysis. The reasons for this were the uncertain service lives of the different systems, the limited time the cathodic protection systems had been in service, the difficulty in assigning cost figures to certain elements in the cost equation, and the comparable cost effectiveness in the simplified economic analysis.

The cost of installation for the sacrificial sprayed zinc system should be less than that for the impressed current system. The service life of the sacrificial zinc system should be less than that of the impressed current zinc system, given that the impressed current system can bypass the increasing anode resistance with time from the development of zinc corrosion products.

Although the costs of monitoring and maintenance were not considered in the simplified economic analysis, they should not be overlooked. The costs of monitoring and maintenance were expected to be higher for impressed current systems than for sacrificial systems, insofar as the risks associated with lack of or poor monitoring were higher for impressed current systems.

CHAPTER 8. CONCLUSIONS AND RECOMMENDATIONS

8.1 CONCLUSIONS

8.1.1 Pre-installation Condition Evaluation

- In the pre-installation condition evaluation, a very strong correlation was found among the existence of cracks, construction joints or spalls, and chloride contents and half-cell potentials indicative of corrosion activity.
- Because the footings were in the splash/evaporation zone, they were found to be in worse condition than the tie beams. At the footings, more indications of corrosion activity were found in the south footings than in other footings. This excess was due to the prevailing south wind and wave action in the area. At the tie beams, the construction joint was responsible for the deterioration, as evidenced by the existence of cracks and high chloride contents. It was observed that at times of severe weather the cast-in-place portion of the tie beam was subjected to seawater spray from waves striking the footings.
- Overall, the structure was visually in good condition but potentially in poor condition, as evidenced by the chloride content and half-cell potential condition indicators. The condition of this structure made it an ideal candidate for cathodic protection.

8.1.2 Field Installation

- The application of the titanium mesh with overlay requires adequate surface preparation in bridge substructures with vertical or overhead surfaces or with complicated geometries. A clean concrete surface with exposed aggregate of the appropriate density and profile should be specified. Otherwise, no bond between the overlay and the concrete substrate will be achieved.
- Sprayed zinc and titanium can conform to any type of surface. While sprayed zinc and the titanium mesh with overlay have color similar to the surrounding concrete, titanium has a dark gold color with blue tints.
- The highest productivity in the installation of the anodes in the Queen Isabella Causeway was achieved for the sprayed zinc. The productivity was somewhat less for the sprayed titanium and substantially less for the titanium mesh with overlay.

8.1.3 Performance Evaluation

Control Members

- From the visual inspection, delamination survey, and half-cell potential surveys of the control members, it was evident that the progression of the deterioration was fairly

rapid. This rapid progress of the deterioration was observed over a period of approximately 1 year.

- There was a significant difference between the permeability obtained in the precast and cast-in-place portions of the tie beam for the untreated control bent. The difference in permeability could have created a macrocell between the areas of high and low permeabilities in the proximity of the construction joint. This macrocell would have exacerbated the deterioration process at this location.

Protected Members

- There were no signs of concrete deterioration in any of the bents protected with cathodic protection 9 months after installation. This observation confirmed the effectiveness of cathodic protection in arresting corrosion-induced concrete deterioration.
- Significant deterioration was observed in some of the anode materials. The sprayed titanium exhibited widespread minor disbondment of the anode material. The titanium mesh with overlay evidenced delaminations of the overlay. The increase in delaminated areas of the overlay over time was very significant.
- The current density for the sprayed titanium was higher compared with the other impressed current systems. This difference was due to the low conductivity of the sprayed titanium anode and the consequent higher applied current. This condition probably resulted in accelerated electrochemical aging of the anode. Another indication of the low conductivity of the sprayed titanium system was the very low depolarization potentials for the reference cell that was located farthest from either of the two positive connections.
- The impressed current sprayed zinc exhibited adequate depolarization. The titanium mesh with overlay had consistently the highest depolarization values. Considering the sacrificial nature of the system, the galvanic sprayed zinc exhibited high depolarization values.
- The current readings for the sacrificial sprayed zinc readings were variable. The variability correlated well with changes in dew point between February and mid-April. Between mid-April and June, the correlation was not as good. A cyclic behavior for the current output during the course of a day was observed between mid-April and June. The higher temperatures and the solar radiation during the daytime hours could have resulted in drying of the concrete and, consequently, a decrease in the current output for the galvanic zinc.

Assessment of Methods for Evaluation

- From the rectifier and system component evaluation of the cathodic protection systems, it was gathered that the methods to evaluate cathodic systems take the form of guidelines from a variety of sources. There is not a single updated source for information on how to evaluate cathodic protection systems.

- The benefit from the use of null probes was found to be extremely limited. The use of null probes for assessment of cathodic protection performance should be limited to checking reversal or changes in the millivolt drop as the system is energized or de-energized. Limited information can be obtained from the magnitude of the changes in millivolt drop. The benefit from the use of null probes was also found questionable for the energization of the cathodic protection systems, because polarity reversed with the first current increment.

8.1.4 Durability and Cost Analyses

- For comparison purposes, the estimated initial costs unique to each system were computed for the systems installed at the Queen Isabella Causeway. The initial cost per unit area for the sprayed titanium anode was \$71/ft^2 (\$760/m^2). This is equivalent to 4 times the cost of the titanium mesh with overlay anode, 10 times the cost of the impressed current sprayed zinc anode, and 35 times the cost of the sacrificial sprayed zinc anode. The sacrificial sprayed zinc anode system had the lowest cost per unit area at \$2/ft^2 (\$22/m^2).
- On the basis of the simplified economic analysis, the sprayed zinc systems were more cost effective than the sprayed titanium and titanium mesh with overlay anode systems for the Queen Isabella Causeway. A definitive selection could not be made between the impressed current and the sacrificial zinc systems based on the simplified economic analysis.
- The cost of installation for the sacrificial sprayed zinc system should be less than that for the impressed current system. The service life of the sacrificial zinc system should be less than that of the impressed current zinc system, because the impressed current system can bypass the increasing anode resistance with time from the development of zinc corrosion products. The costs of monitoring and maintenance were expected to be higher for impressed current systems than for sacrificial systems, because the risks associated with lack of or poor monitoring were higher for impressed current systems.

8.2 RECOMMENDATIONS

8.2.1 Recommendations for Future Research

The testing program described in Chapter 6 should be continued for at least 3 years. The frequency of the field evaluations could be decreased to two field evaluations per year.

Future research could determine the impact of the cathodic protection systems installed in the tie beams and footings of the Queen Isabella Causeway on other structural elements of the bridge substructure. The possibility of development of corrosion cells between protected and unprotected members of the structures could be studied. The deterioration of the batter piles and the columns should be monitored. The impact of the installation of bulk zinc anodes to protect the batter piles should be evaluated if the cathodic

protection systems installed result in deterioration of the batter piles. Electrical continuity between the reinforcing steel in the columns and the reinforcing steel in the tie beams and footings will result in some level of protection at elevations in the proximity of the tie beams. The extent of such protected areas in the columns could be evaluated.

8.2.2 Cathodic Protection System Selection for the Queen Isabella Causeway

On the basis of the evaluations of the condition of the existing structure, the field installation, the performance, and the durability and cost analysis, the sacrificial sprayed zinc was the recommended cathodic protection system type for a full-scale installation at the Queen Isabella Causeway. The primary reasons for this selection rested on the installation simplicity, adequate performance to date, and both lower installation and projected costs with respect to any of the impressed current systems. The limitation of this system is the relatively short service life compared to impressed current systems. It is important to recognize that the recommendation of the sacrificial sprayed zinc system is preliminary because it is based on the limited 9-month performance evaluation. Continued monitoring could lead to a modification of this recommendation.

It is recommended that other types of cathodic protection systems, such as clamp-on systems or sprayed aluminum zinc, be applied in a few bents as part of a potential full-scale installation at the Queen Isabella Causeway. In this way, the performance of these sacrificial cathodic protection systems could be evaluated alongside the sacrificial sprayed zinc and the impressed current systems installed at the Queen Isabella Causeway.

8.2.3 Guidelines for Full-Scale Installation

Guidelines for the design, installation, monitoring, and maintenance were provided for the recommended cathodic protection system type. The purpose of these guidelines was to develop a cost-effective rehabilitation strategy for a potential full-scale rehabilitation of the tie beams and footings of the Queen Isabella Causeway using sacrificial sprayed zinc.

System Design. The sacrificial sprayed cathodic protection system should be applied to the top and sides of the footings, the cast-in-place portion of the tie beam, and a 2-ft (0.60-m) band of the tie beam extending beyond the construction joint into the precast section. Figure 8.1 presents a schematic diagram with the recommended areas for installation of the sacrificial sprayed zinc cathodic protection system. The combination of a footing, the cast-in-place portion of the tie beam that rested on it, and the 2-ft (0.60-m) band of the precast tie beam extending beyond the construction joint was designated a cathodic protection unit. Under this designation, every protected bent consisted of three cathodic protection units. The approximate total surface area of the three cathodic protection units in a typical bent was approximately 940 ft^2 (87 m^2). This represented approximately a 30 percent surface area reduction with respect to the 1,320 ft^2 (123 m^2) per bent that were protected as part of this study.

As found in the pre-installation condition evaluation and the performance evaluation of the control members, the tie beams were in better condition than the footings. The cast-in-

place portion of the tie beam was more prone to deterioration than the precast portion, as it had higher permeability. Moreover, at times of severe weather, the cast-in-place portion of the tie beam was subjected to seawater spray from waves striking the footings. In addition, in the presence of a corrosion cell created by permeability differentials between the precast and cast-in-place sections of the tie beams, the anodic portion would be in need of protection. The condition of the tie beam and the potential deterioration was such that cathodic protection was required in the cast-in-place portion of the tie beam. In addition, the 0.61-m (2-ft) protected band in the precast section adjacent to the construction joints was also protected to account for the unabated penetration of chlorides and moisture through the construction joint.

Sacrificial zinc is highly dependent on moisture to deliver adequate current outputs. Being in the splash/evaporation zone, the footings received adequate moisture. The tie beams were for the most part under an atmospheric influence; accordingly, the current density produced by the sacrificial sprayed zinc in this portion of the tie beam would not be very significant. Because the precast portion of the tie beam had higher resistivity than the cast-in-place section, spraying zinc in this area would result in even lower current densities. Thus, the benefits from the application of sprayed zinc on the entire surface of the tie beam could not be justified.

Installation. There were a total of 141 bents of similar geometry to the six that were studied as part of this project. Potentially, an area of up to approximately 130,000 ft^2 (12,300 m^2) of sprayed zinc could be applied under the recommended scheme. Because of the potential large area of application, economies of scale could be enjoyed with a planned full-scale installation at the Queen Isabella Causeway. Industrializing the installation process of the cathodic protection systems should be essential to reducing installation costs. This should not only be contemplated in the construction process but in the design specifications as well.

The main work items of such an installation would be concrete removal, sandblasting surface preparation, continuity testing and corrections, connections and instrumentation, concrete repairs, and zinc spraying. The method of zinc application should be arc-spray. The largest possible diameter wire should be used so as to maximize the productivity of the zinc spraying operation.

The application for every cathodic protection unit should be performed from a barge rather than from a scaffold. In a full-scale installation, providing a scaffold for every bent to be protected would not be cost-effective. Work barges could be used for sandblasting, zinc spraying, and storage of materials. Owing to the geometry of this structure and the location of the areas recommended for protection, which were in the vicinity of the footings, much of the work can be performed from the footings.

It is imperative for the sake of safety and the environment that the appropriate enclosure systems to mitigate the negative impacts of the zinc application be designed. Because of the similar geometry of every cathodic protection unit, it would be possible to build re-usable enclosure systems extending from the barge work to the different cathodic protection units.

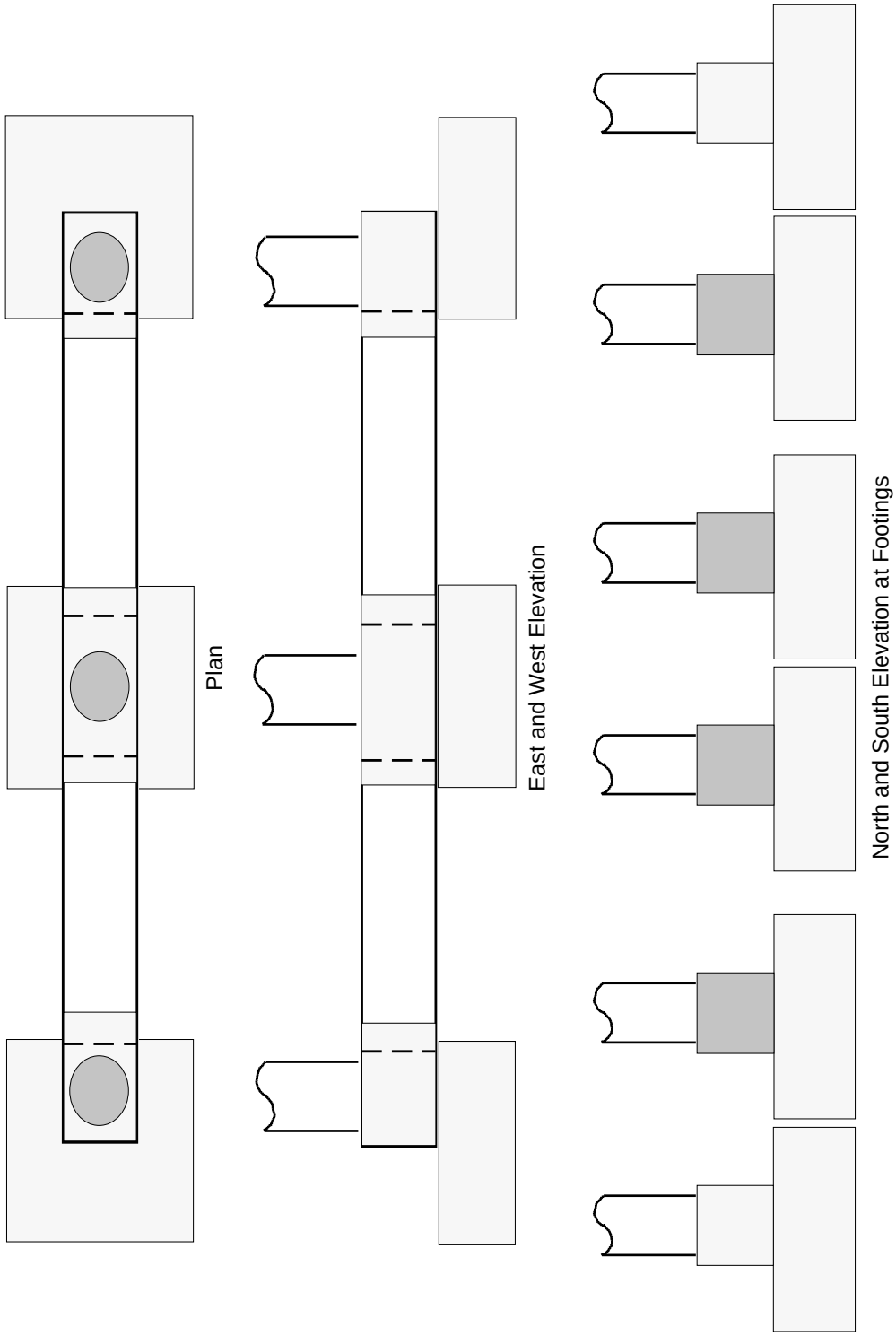

Figure 8.1: Recommended surface areas for sacrificial sprayed zinc installation

Installation Costs. Based on the costs for installation for an ongoing project in the Florida Keys, the cost of installation at the Queen Isabella Causeway was estimated. The reference project is the Seven Mile Bridge in Marathon, Florida. The Seven Mile Bridge is part of US 1 in the Florida Keys. Construction of the bridge was completed in 1979. The bridge has 266 bents, an overall length of 6.8 mi (10.9 km), and a deck width of 36 ft (10.9 m) and consisting of two travel lanes. The substructure consists of 36-in. (0.91-m) diameter columns, which terminate in drilled shafts and struts between each column pair. The reinforcement is epoxy coated.

The ongoing rehabilitation project at the Seven Mile Bridge involved the columns and struts in the bridge substructure. The main work items of the installation were concrete removal, sandblasting surface preparation, continuity testing and corrections, repair with latex-modified concrete, and zinc spraying. No instrumentation was installed at the Seven Mile Bridge.

The similarities between the installation at the Seven Mile Bridge and a potential installation at the Queen Isabella Causeway were that both bridge substructures were in a marine environment and that both structures involved minor zinc spraying applications at numerous locations for a large total area. As part of the ongoing rehabilitation project at the Seven Mile Bridge, 150 locations were sprayed with zinc for a total of 3,000 ft^2 (279 m^2), which is equivalent to an average of 200 ft^2 (18.5 m^2) per location (Ref 38). Each cathodic protection unit at the Queen Isabella Causeway was approximately 300 ft^2 (27.9 m^2).

The unit costs in the Seven Mile Bridge were used to calculate the costs for the potential installation at the Queen Isabella Causeway. Three unit costs were used for pricing and payment of the installation work at the Seven Mile Bridge (Ref 38). The first cost was the unit cost of concrete removal. The second unit cost was the cost for concrete repairs, sandblasting, and continuity corrections. The third cost was the cost of zinc spraying. The unit costs used for calculation of cost per bent at the Queen Isabella Causeway are presented in Table 8.1 (Ref 38).

The areas for concrete removal and repair were calculated for the untreated control bent. It was assumed that the total area for concrete removal and repair was the sum of the spalled and the delaminated areas. The total concrete removal and repair area was estimated to be 20 ft^2 (1.9 m^2) based on the findings of the fourth evaluation for Bent 24 presented in Chapter 6. For the purpose of the cost calculation for the patch repairs, it was assumed that the repairs would be performed to a depth of 5 in. (102 mm).

The installation cost per bent was estimated to be $34,000, which is equivalent to $11,000 per cathodic protection unit. The total cost of full-scale installation for the 141 bents would be approximately $4,800,000. These costs did not include the cost of the instrumentation.

Monitoring. Simplifying the monitoring process of the cathodic protection would be essential. Monitoring would involve measuring current for every cathodic protection unit. A fraction of the cathodic protection units would be instrumented with embedded reference cells to perform depolarization testing. By correlating measured current of instrumented cathodic protection units with level of protection from the depolarization testing, a good

measure of the level of protection could be obtained for uninstrumented cathodic protection units.

Table 8.1: Estimated costs for installation using recommended system

Work Item	Seven Mile Bridge		Queen Isabella Causeway	
	Unit	**Unit Cost ($)**	**Estimated Quantity**	**Cost ($)**
Concrete removal	ft^2	140	20	2,800
Sandblasting, continuity corrections, connections and repair with LMC	ft^3	400	8	3,200
Zinc spraying	ft^2	30	940	28,200
Total Cost per Bent				34,000
Total Cost per Cathodic Protection Unit				11,000
Total Cost for Full-Scale Installation (141 Bents)				4,800,000

A junction box should be installed in every cathodic protection unit. The junction box should have the terminals and wires to measure current and, where applicable, conduct polarization decay testing.

To measure current in all cathodic protection units, a shunt across the positive and negative connections should be installed. Current should be measured as the millivolt drop across the shunt. In a fraction of the cathodic protection units, embedded reference cells should be installed. The reference cell and reference cell ground wires should be routed to the junction box for each cathodic protection unit. At the connection of the positive and negative connection for each cathodic protection unit, an on/off switch should be installed to connect and disconnect the system for the purpose of measuring instant-off potentials.

Monitoring should be performed at least once a year by measuring current in all the cathodic protection units and performing polarization decay testing where applicable. Testing would be performed from a boat, and the equipment required would be a standard digital voltmeter.

Maintenance. Maintenance for the recommended type of system would be simple relative to other types of cathodic protection systems. The main problem would be corrosion of the terminals and connections within the junction box. Because the terminals and connections would be in a marine environment, the terminals should be replaced periodically.

From the visual inspection and the monitoring data, the timing of an eventual reapplication of the sprayed zinc could be determined. The reapplication would involve sandblasting for removal of the existing zinc coating and respraying of the zinc coating.

8.3 CATHODIC PROTECTION FOR MARINE BRIDGE SUBSTRUCTURES IN TEXAS

The simplicity of galvanic sprayed zinc lends itself to easier implementation for those beginning to venture into cathodic protection of bridge substructures. The recommendation is contingent upon the installation of this system for marine bridge structures in the tidal or splash/evaporation zones and upon acceptable future performance of this system at the Queen Isabella Causeway.

In spite of this recommendation, every bridge substructure should be considered on a case-by-case basis and all the possible rehabilitation strategies, including different types of cathodic protection systems, should be evaluated for every candidate bridge substructure. Cathodic protection might not always be the most cost-effective strategy for rehabilitation of a given corrosion-deteriorated concrete bridge substructure in a marine environment. It is important, however, to consider cathodic protection as an alternative rehabilitation strategy, especially because cathodic protection is the only rehabilitation strategy capable of stopping the mechanism of deterioration.

Sacrificial systems should be the focus of future development and research in the area of cathodic protection of bridge substructures in marine environments. The development of new anode materials or the development of additives or alloys that extend the life of the existing systems should be considered.

The focus of full-scale installations and future research should be on the application and development of cathodic protection systems that are not only cost-effective solutions for arresting corrosion, but also simple to install, monitor, and maintain. This type of development and application would foster the adoption of cathodic protection as a valuable tool for extending the service life of concrete bridge substructures in marine environments in the state of Texas.

APPENDIX A: PRE-INSTALLATION CONDITION EVALUATION CORROSION POTENTIAL MAPPING

Bent 19

19

-146 -253 -344 -211 -241 -174 -267 -166 -159 -196 -273 -117

Tie Beam

-230 -271 -310 -350

North Footing

-208 -248 -241 -226

Center Footing

-241 **-385** -291 **-369**

South Footing

East Side

North

-209 -315 -288 -237 -255 -237 -247 -171 -181 -225 -279 -156

Tie beam

-316 **-477** -342 -315

North Footing

-250 -271 -262 -225

Center Footing

-266 -322 **-441** -330

South Footing

West Side

Bent 19 (continued)

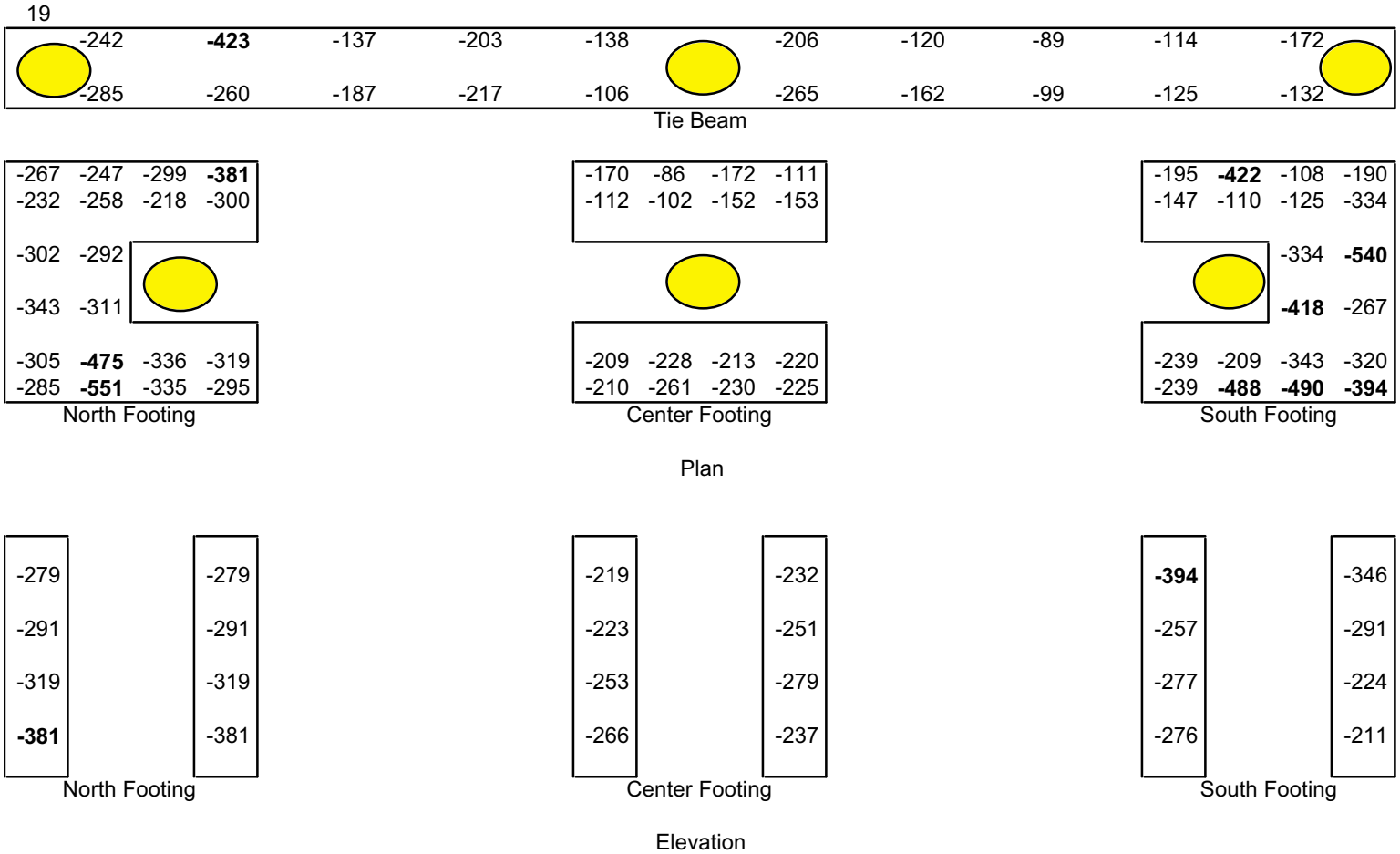

Bent 20

20

-272 -102 -50 -191 -4 -24 -55 -34 -12 -12

Tie Beam

-181 -138 -133 -217

North Footing

-96 -122 -173 -130

Center Footing

-145 -135 -125 -130

South Footing

East Side

North

-255 -145 -92 -41 -53 -78 -87 -93 -44 -30 -273 -117

Tie beam

-102 -139 -135 -145

North Footing

-67 -137 -205 -130

Center Footing

-128 -118 -107 -105

South Footing

West Side

Bent 20 (continued)

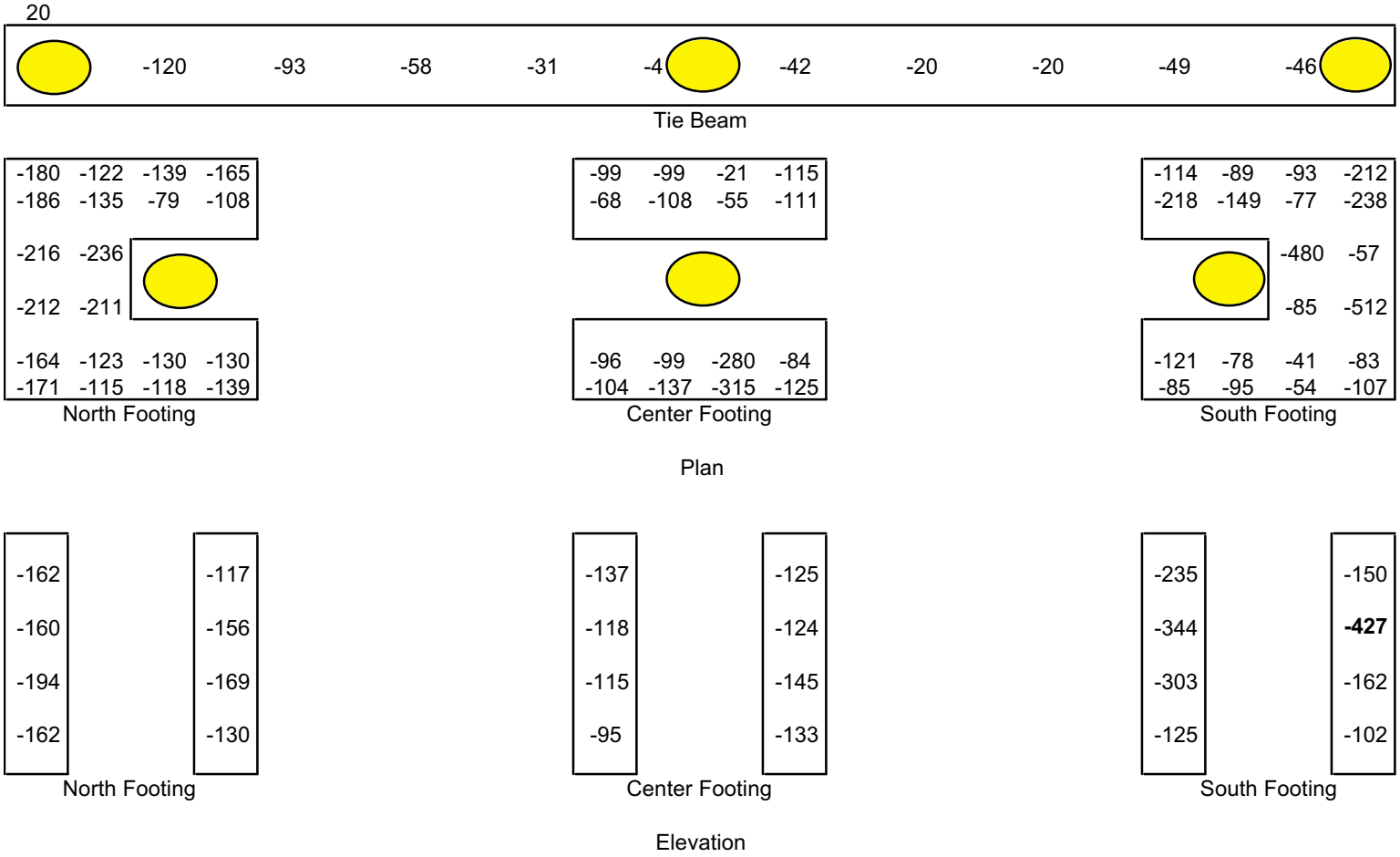

Bent 21

21

-36 -133 -130 -65 -34 -15 -66 -140 -143 -134 -134 -313

Tie Beam

-160 -148 -123 -141

North Footing

-65 -109 -136 -146

Center Footing

-370 **-361** -159 -155

South Footing

East Side

North

-83 -301 -177 -45 -40 -51 -133 -204 -112 -134 -107 -16

Tie beam

-121 -112 -87 -93

North Footing

-387 -236 -137 -127

Center Footing

-112 -130 -163 -148

South Footing

West Side

Bent 21 (continued)

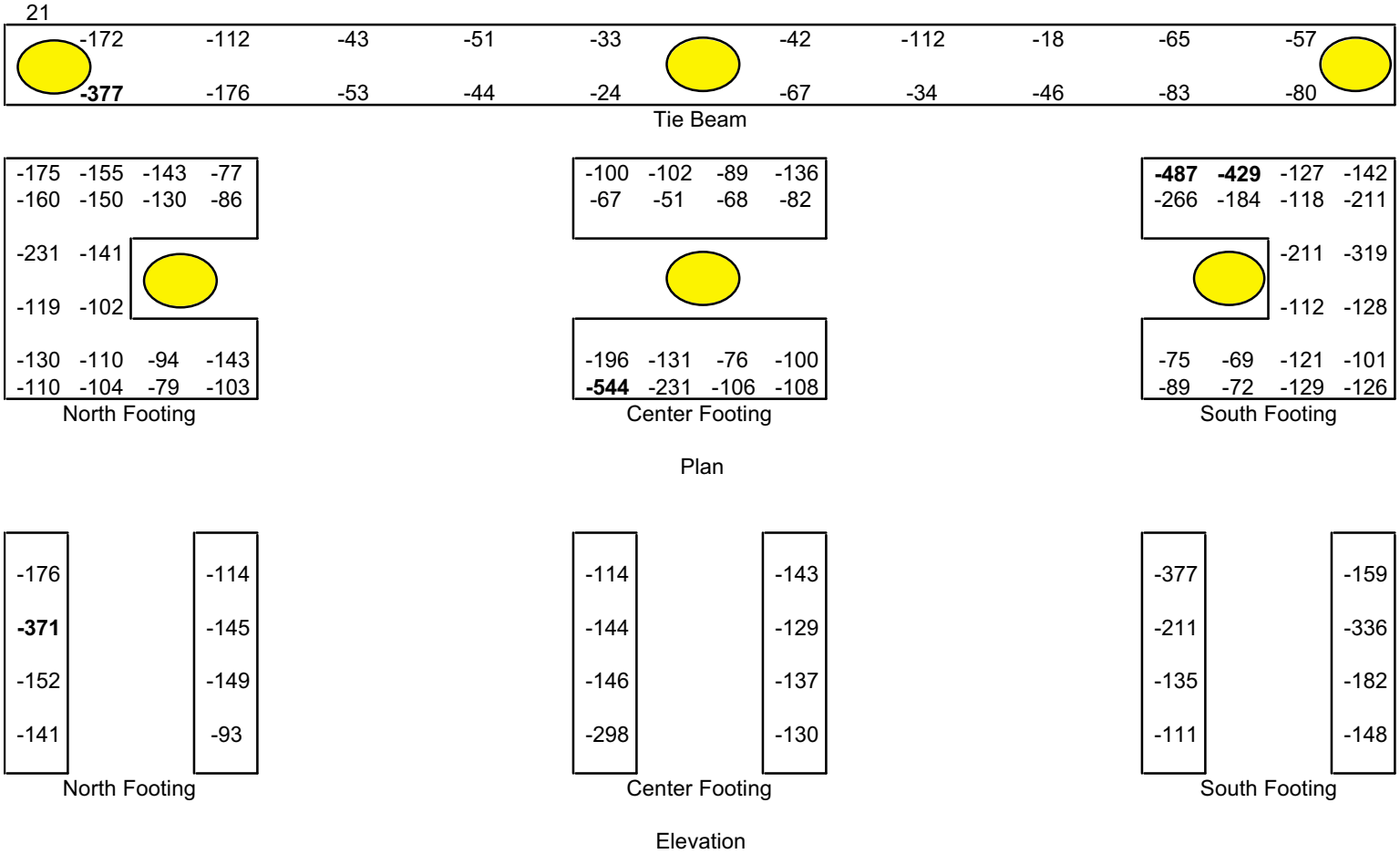

Bent 22

22

-31 -255 -155 -50 -124 -52 -156 -107 -61 -167 -147 -6

Tie Beam

-211 -170 -118 -120

North Footing

-134 -160 -195 -208

Center Footing

-226 -244 -204 -225

South Footing

East Side

North

-17 -198 -161 -89 -111 -93 -129 -134 -106 -155 67 25

Tie beam

-98 -50 -77 -183

North Footing

-154 -177 -303 -313

Center Footing

-134 -128 -142 -115

South Footing

West Side

Bent 22 (continued)

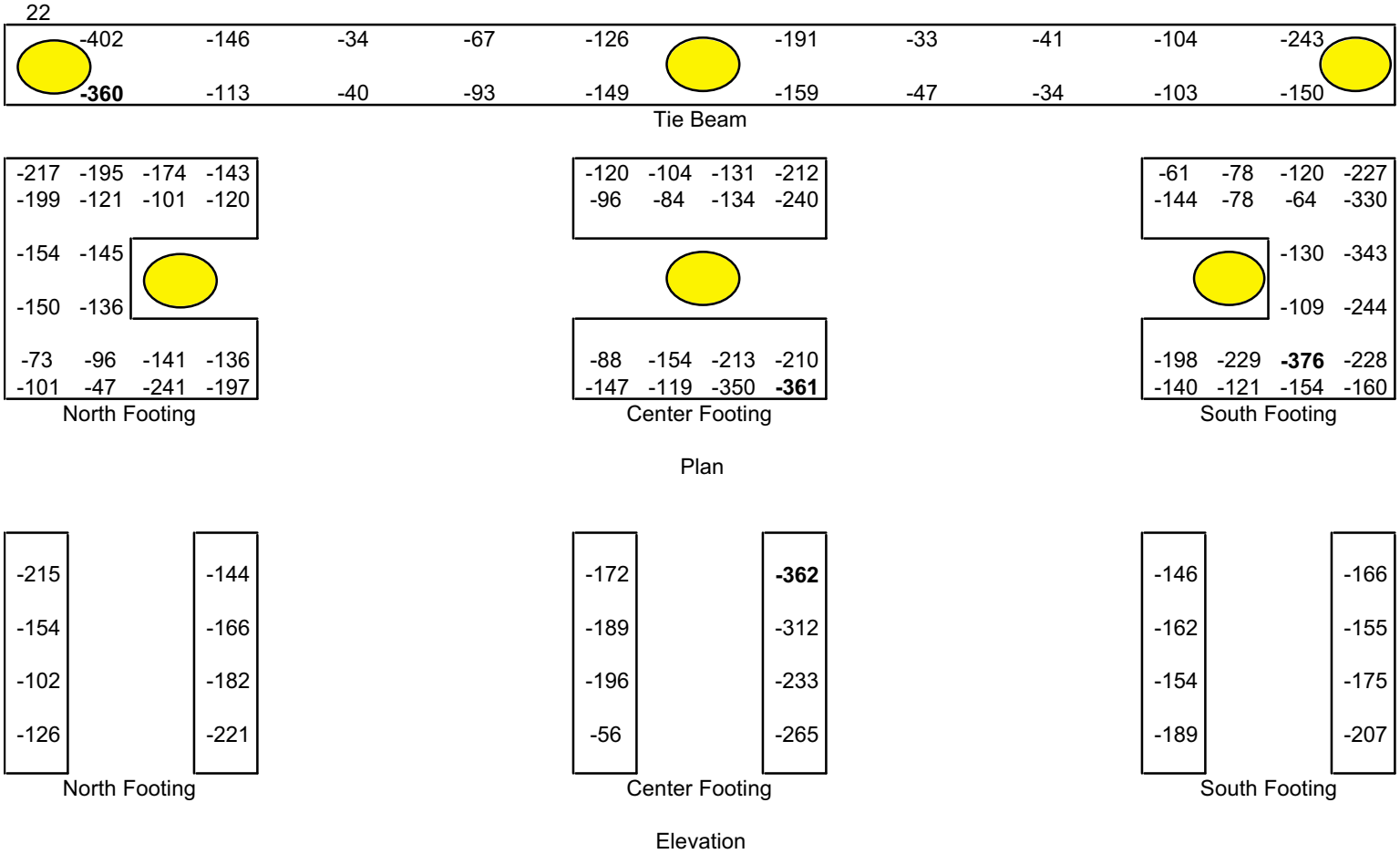

Bent 23

23

-7 -138 -199 -76 -106 -69 -75 -85 -73 -116 -90 -15

Tie Beam

-191 -168 -152 -125

North Footing

-210 -305 -309 -266

Center Footing

-112 -140 -129 -187

South Footing

East Side

North

-22 -172 -197 -108 -115 -81 -110 -107 -35 -149 -77 -5

Tie beam

-114 -125 -141 -140

North Footing

-247 -320 -236 -187

Center Footing

-184 -189 -222 -212

South Footing

West Side

Bent 23 (continued)

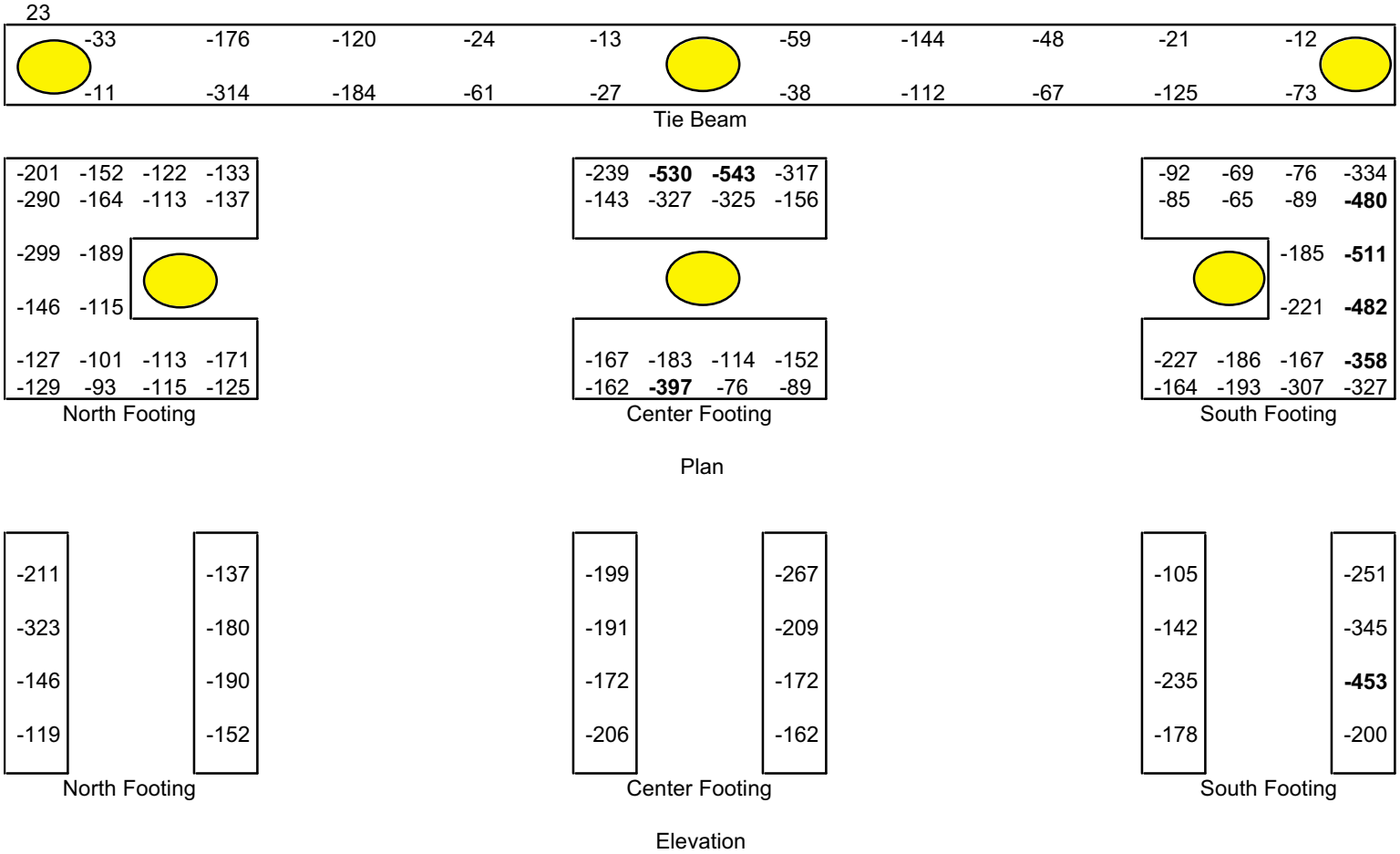

Bent 24

24

-74 -144 -41 -74 -111 -60 -35 -273 -97 -123 -2 -10

Tie Beam

-173 -184 -180 -163

North Footing

-120 -170 -161 -122

Center Footing

-282 -324 -196 -207

South Footing

East Side

North

-79 -210 -141 -101 -183 -129 -192 -130 -125 -223 -124 -20

Tie beam

-241 -243 -244 -200

North Footing

-264 -38 -220 -191

Center Footing

-188 -187 -173 -137

South Footing

West Side

Bent 24 (continued)

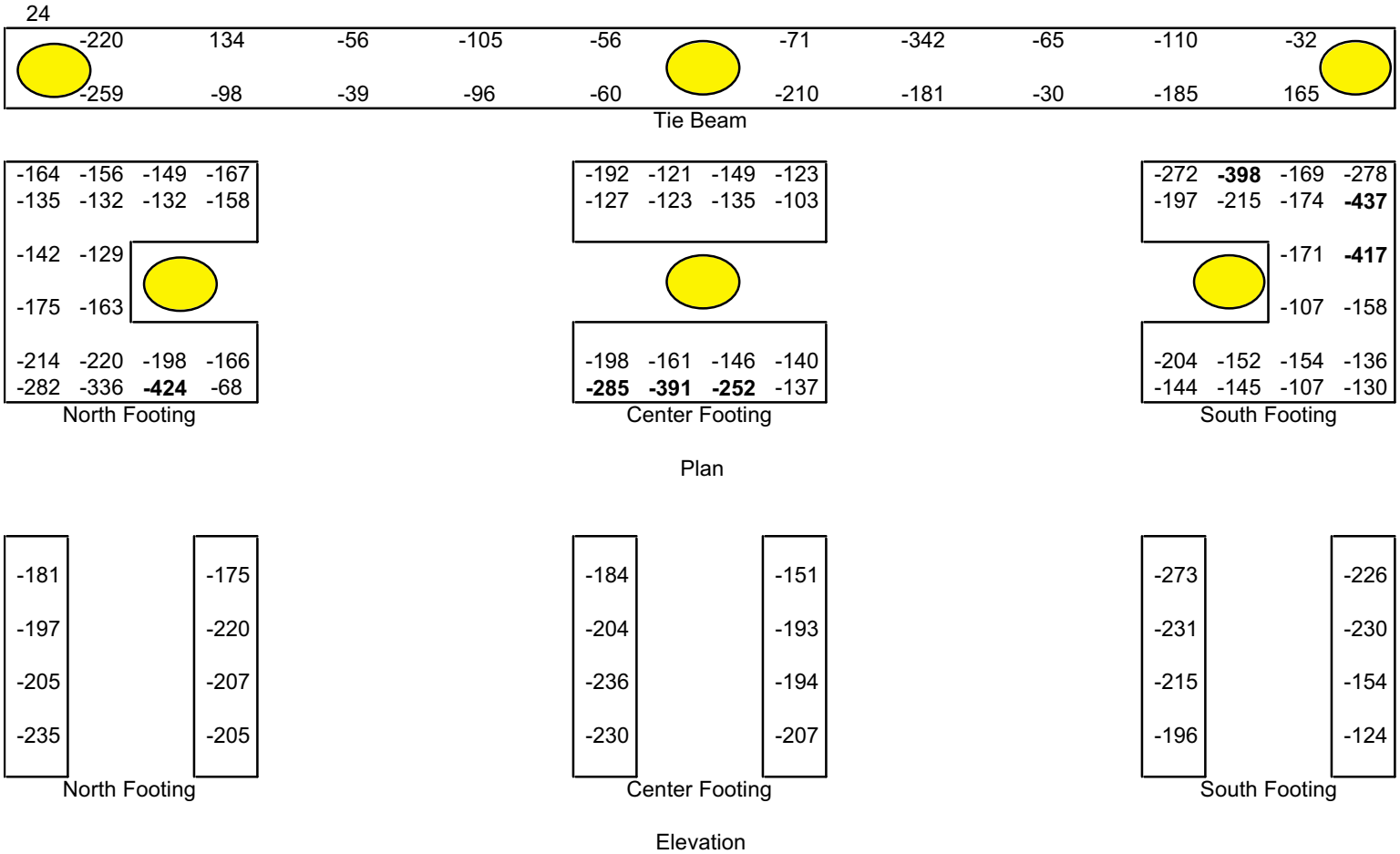

APPENDIX B: ENERGIZATION POLARIZATION DEVELOPMENT TESTING

Polarization Testing Zone 1

Current mA	Voltage V	RC-1 MV	RC-2 MV	RC-3 mV	NP-1 V	NP-2 V
0	0.0	1	-213	-307	-0.04	-0.16
414	3.1	27	-276	-361	0.40	0.30
600	3.8	30	-297	-378	0.60	0.50
800	5.3	57	-317	-391	0.70	0.70
1200	7.4	12	-351	-424		
1500	11.1		-366	-454		
1800	12.8		-415	-481		

Polarization Testing Zone 2

Current mA	Voltage V	RC-1 MV	RC-2 MV	RC-3 mV	NP-1 V	NP-2 V
0	0.0	-420	-320	-325	-0.70	-3.95
528	4.0	-431	-368	-371	-0.07	1.40
800	5.8	-434	-365	-378	1.20	3.40
1000	7.5	-419	-363	-372	1.60	5.30
1200	9.1	-434	-381	-387		
1500	12.2	-462	-400	-387		
1800	14.4	-447	-421	-407		
2200	16.4	-456	-451	-424		
2600	17.6	-466	-461	-439		
3000	19.8	-472	-491	-443		

Polarization Testing Zone 3

Current mA	Voltage V	RC-1 mV	RC-2 MV	RC-3 mV	NP-1 V	NP-2 V
0	0.0	-107	-243	-138	0.11	-2.29
480	4.0	-247	-251	-275	0.50	1.60
600	5.6	-290	-347	-308	0.60	2.20
800	7.1	-314	-323	-326	0.80	3.50
1000	9.0	-354	-348	-350		
1500	12.8	-407	-381	-373		
1800	15.1	-467	-427	-410		

APPENDIX C: FIELD EVALUATION CORROSION POTENTIAL MAPPING

Bent 23 Second Evaluation

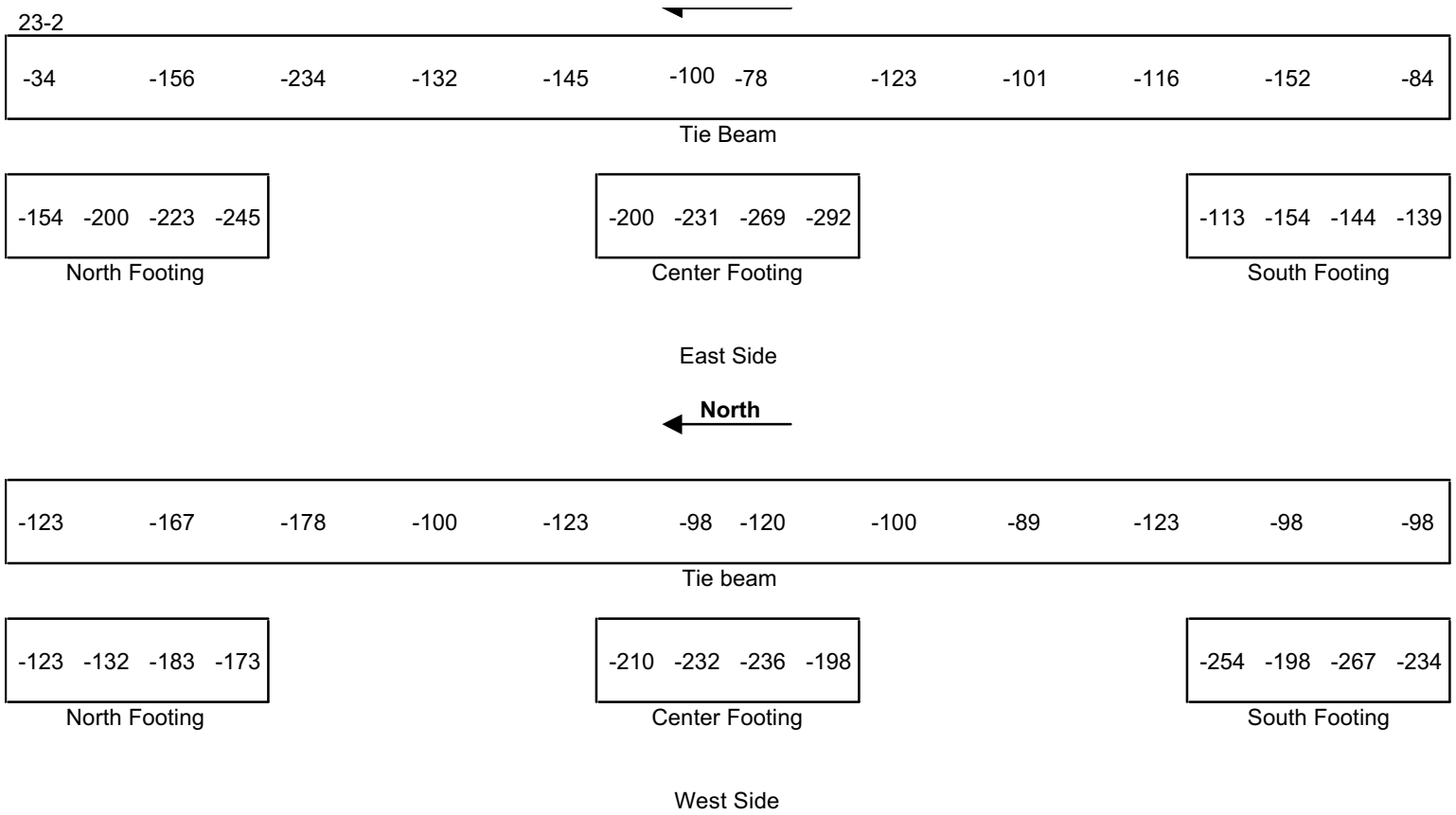

Bent 23 Second Evaluation (continued)

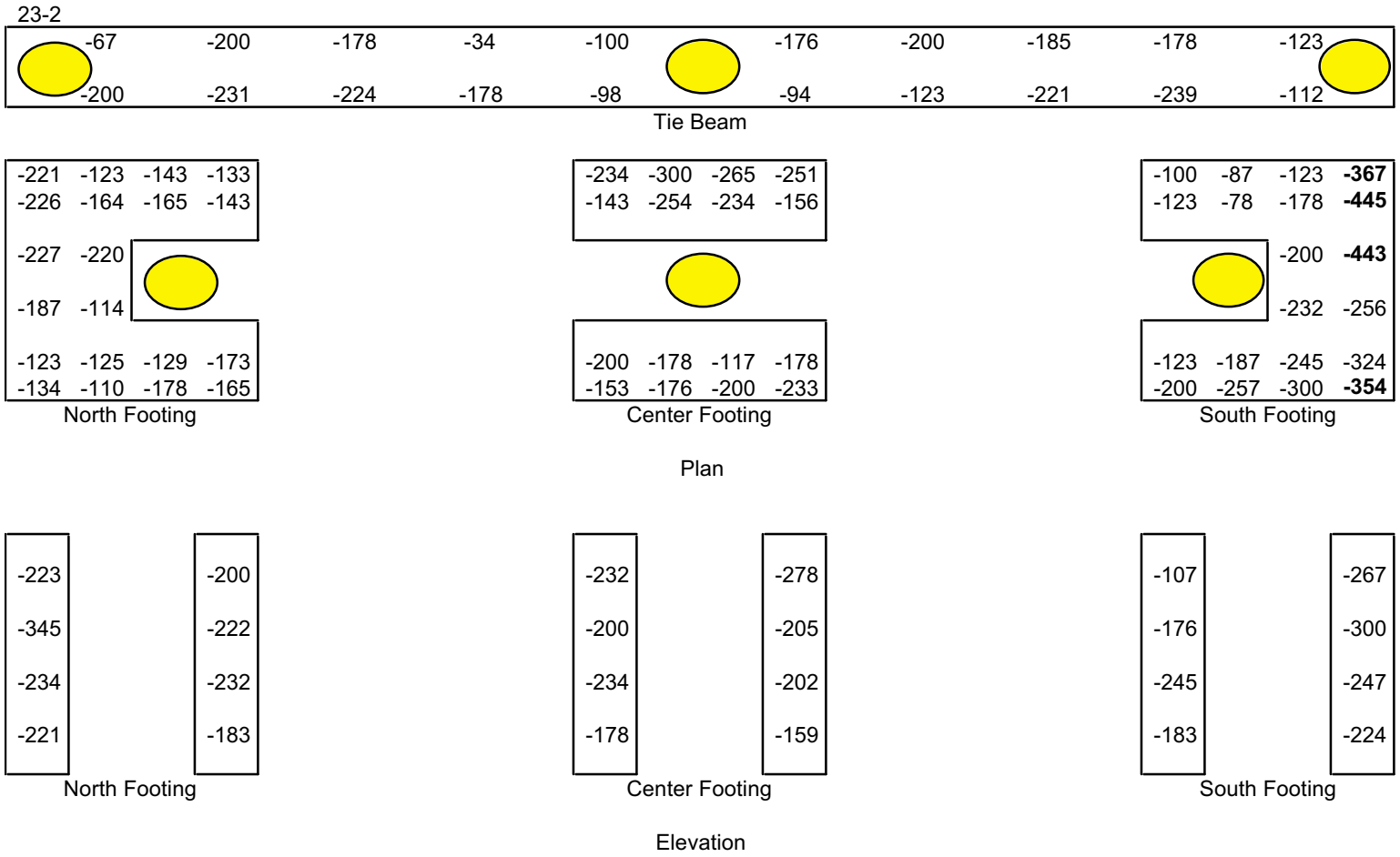

Bent 24 Second Evaluation

24-2

-174 -243 -156 -89 -101 -78 -66 -245 -107 -132 -55 -61

Tie Beam

-187 -188 -180 -178

North Footing

-178 -200 -268 **-352**

Center Footing

-278 -324 -184 -200

South Footing

East Side

North

-99 -234 -123 -67 -34 -156 -209 -145 -144 -217 -178 -56

Tie beam

-228 -67 -53 -89

North Footing

-185 -245 -257 -207

Center Footing

-200 -198 -267 -149

South Footing

West Side

Bent 24 Second Evaluation (continued)

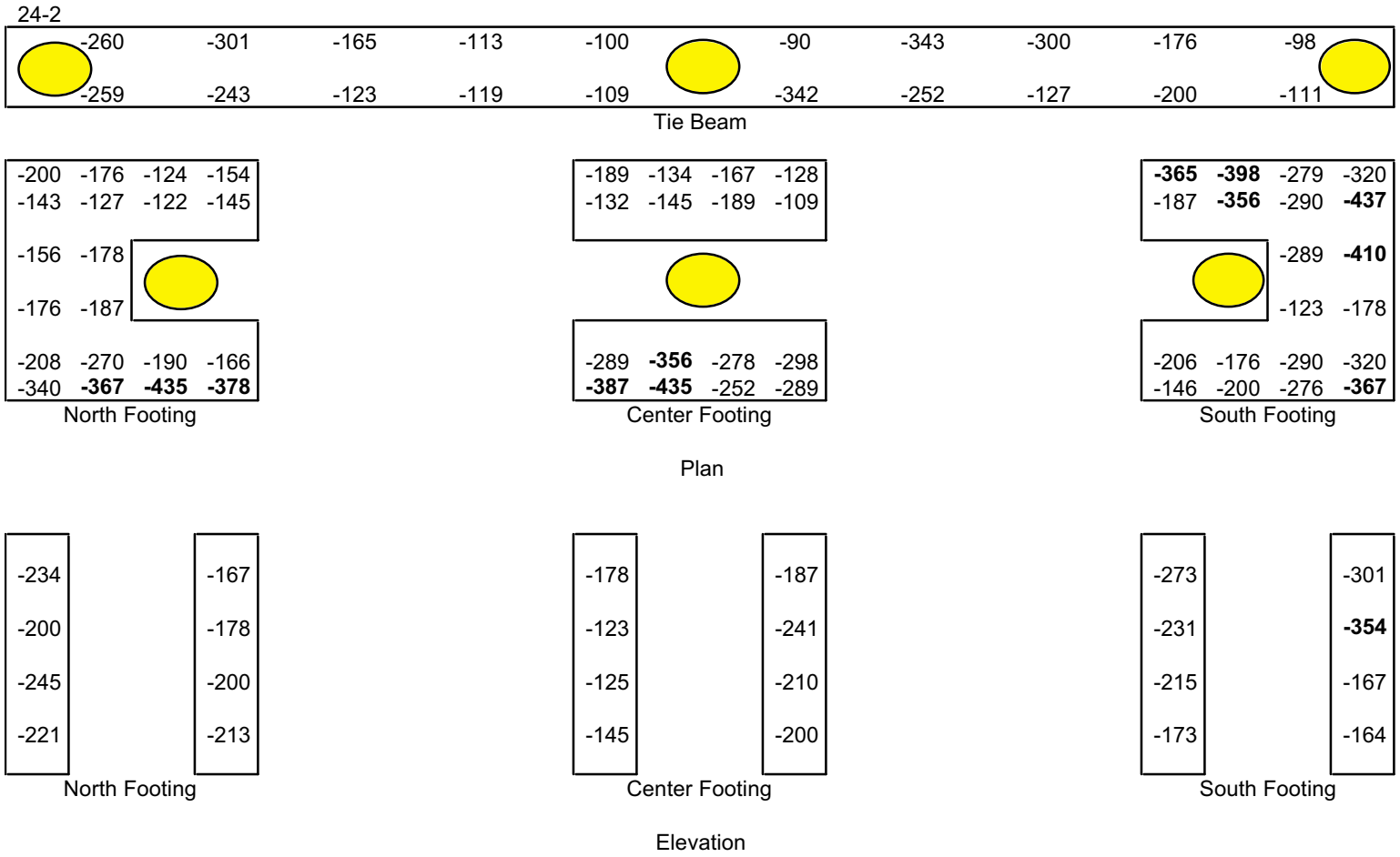

Bent 23 Fourth Evaluation

23-4

-69 -123 -180 -156 -167 -92 -96 -143 -121 -150 -167 -100

Tie Beam

-167 -201 -253 -223

North Footing

-187 -223 -218 -301

Center Footing

-200 -123 -143 -198

South Footing

East Side

North

-129 -123 -200 -132 -145 -100 -109 -112 -114 -107 -117 -101

Tie beam

-154 -145 -178 -165

North Footing

-203 -243 -278 -209

Center Footing

-265 -239 -266 -248

South Footing

West Side

Bent 23 Fourth Evaluation (continued)

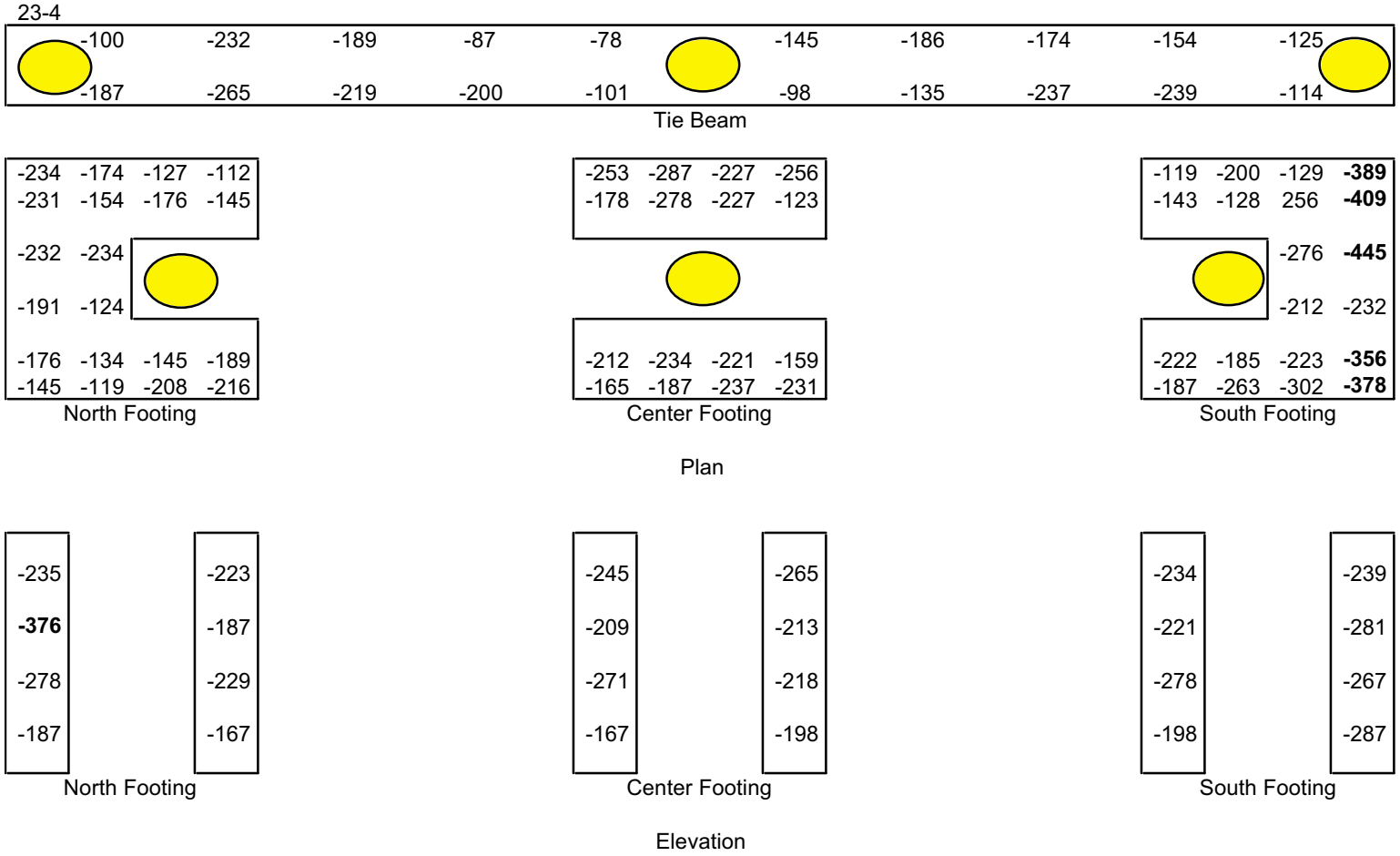

Bent 24 Fourth Evaluation

24-4

-168	-231	-176	-101	-127	-111	-128	-257	-110	-143	-87	-69

Tie Beam

-209	-221	-176	-179	-189	-210	-276	-256	-298	-329	-123	-218
North Footing				Center Footing				South Footing			

East Side

North

-134	-254	-101	-126	-29	-178	-251	-211	-165	-227	-185	-100

Tie beam

-234	-123	-28	-90	-176	-227	-278	-189	-237	-298	-265	-189
North Footing				Center Footing				South Footing			

West Side

Bent 24 Fourth Evaluation (continued)

24-4

-237	-324	-200	-107	-98	-97	**-356**	-321	-256	-76
-254	-278	-175	-128	-110	-328	-246	-138	-210	-123

Tie Beam

-209	-198	-112	-179
-145	-129	-165	-178
-176	-198		
-208	-201		
-232	-290	-229	-251
-329	**-378**	**-401**	**-351**

North Footing

-227	-178	-179	-134
-145	-168	-209	-127
-309	-309	-287	-310
-398	**-401**	-213	-299

Center Footing

-401	**-378**	**-367**	-300
-351	-278	-323	**-401**
		-289	**-410**
		-154	-201
-221	-197	-301	-348
-123	-201	-234	**-389**

South Footing

Plan

-264	-185
-176	-176
-265	-213
-231	-221

North Footing

-176	-200
-145	-221
-167	-221
-164	-207

Center Footing

-263	-307
-221	**-381**
-276	-287
-165	-167

South Footing

Elevation

APPENDIX D: FIELD EVALUATION CORROSION RATE DATA

Corrosion Rate Bent 24 Second Evaluation

Location	Corrosion Rate mA/ft^2
North end of tie beam at precast section	3.83
North end of tie beam at cast-in-place section	2.50
Northwest corner of north footing	1.25
Northeast corner of north footing	1.71
Southeast corner of north footing	1.20
West side of center footing	5.82

Corrosion Rate Bent 24 Fourth Evaluation

Location	Corrosion Rate mA/ft^2
North end of tie beam at precast section	3.02
North end of tie beam at cast-in-place section	2.48
Northwest corner of north footing	2.22
Northeast corner of north footing	2.08
Southeast corner of north footing	1.49
West side of center footing	6.00

APPENDIX E: FIELD EVALUATION CHLORIDE CONTENT

Chloride Contents Second Evaluation

Location	Steel Depth in.	Cl Sample Depth, in.	Cl Ion Content lbs/yd^3	Cl Ion Content ppm
Bent 19	3.55	0.5	16.51	4217
Top West Side		1.0	9.19	2347
Center Footing		1.5	6.62	1691
		2.0	3.74	955
		2.5	2.43	621
		3.0	1.89	483
		3.5	1.24	317
		4.0	1.39	355
Bent 20	4.00	0.5	11.90	3040
Top West Side		1.0	6.93	1770
Center Footing		1.5	4.45	1137
		2.0	2.34	598
		2.5	1.15	294
		3.0	1.27	324
		3.5	0.95	243
		4.0	0.99	253
Bent 21	3.75	0.5	13.38	3418
Top West Side		1.0	12.03	3073
North Footing		1.5	6.13	1566
		2.0	4.43	1132
		2.5	2.15	549
		3.0	1.78	455
		3.5	1.46	373
		4.0	1.29	330

Chloride Contents Second Evaluation (continued)

Location	Steel Depth In.	Cl Sample Depth, in.	Cl Ion Content, lbs/yd^3	Cl Ion Content, ppm
Bent 22 Top West Side North Footing	3.70	0.5	20.68	5282
		1.0	11.12	2840
		1.5	6.27	1602
		2.0	4.76	1216
		2.5	2.98	761
		3.0	1.87	478
		3.5	1.79	457
		4.0	1.63	416
Bent 24 Top West Side North Footing	3.50	0.5	9.41	2404
		1.0	6.40	1635
		1.5	2.34	598
		2.0	2.55	651
		2.5	1.98	506
		3.0	2.09	534
		3.5	1.64	419
		4.0	1.52	388

APPENDIX F: FIELD EVALUATION AS-FOUND CONDITIONS

As-Found Conditions First Evaluation

Zone	Voltage Output, V		Current Output, A		Current Density	Back emf
	Rectifier	External	Rectifier	External	mA/ft^2	V
1	16.8	16.87	1.5	1.52	1.15	0.92
2	20.2	20.36	3.1	3.08	2.33	1.76
3	16.0	16.10	1.5	1.52	1.15	1.44
4				0.24	0.18	

As-Found Conditions Second Evaluation

Zone	Voltage Output, V		Current Output, A		Current Density	Back emf
	Rectifier	External	Rectifier	External	mA/ft^2	V
1	15.2	15.22	1.5	1.48	1.12	0.56
2	19.6	19.72	3.1	3.02	2.29	2.00
3	15.8	15.84	1.5	1.54	1.17	1.64
4				0.46	0.35	

As-Found Conditions Third Evaluation

Zone	Voltage Output, V		Current Output, A		Current Density	Back emf
	Rectifier	External	Rectifier	External	mA/ft^2	V
1	15.4	15.52	1.7	1.71	1.30	1.24
2	19.8	19.97	3.0	2.96	2.24	2.04
3	16.2	16.30	1.6	1.57	1.19	1.64
4				0.27	0.20	

As-Found Conditions Fourth Evaluation

Zone	Voltage Output, V		Current Output, A		Current Density	Back emf
	Rectifier	External	Rectifier	External	mA/ft^2	V
1	17.4	17.52	1.6	1.66	1.26	0.96
2	19.3	19.44	3.0	2.97	2.25	1.92
3	15.7	15.77	1.5	1.50	1.14	1.56
4				0.31	0.23	

APPENDIX G: FIELD EVALUATION ELECTRICAL CONTINUITY DATA

Electrical Continuity First Evaluation

Zone	Items Checked	DC ohm Normal	DC ohm Reversed	DC V	Check
1	Anode to SG	1.860 M	1.359 M	0.195	No
	RC-1 G to SG	unstable	unstable	unstable	
	RC-2 G to SG	0.3	21.6	0.003	No
	RC-3 G to SG	0.4	21.4	0.003	No
	RC-1 G to RC-2 G	unstable	unstable	unstable	
	RC-1 G to RC-3 G	unstable	unstable	unstable	
	RC-2 G to RC-3 G	14.8	14.8	0.000	No
	NP-1 to SG	0.691M	0.604 M	0.079	No
	NP-1 G to SG	0.717 M	0.623 M	0.082	No
	NP-2 to SG	17.5	20.7	0.004	No
	NP-2 G to SG	7.5	10.9	0.006	No
2	Anode to SG	3.879 M	OL	OL	No
	RC-1 G to SG	6.2	12.9	0.001	No
	RC-2 G to SG	6.2	13.0	0.001	No
	RC-3 G to SG	5.4	13.9	0.001	No
	RC-1 G to RC-2 G	15.2	15.2	0.000	No
	RC-1 G to RC-3 G	14.4	16.2	0.000	No
	RC-2 G to RC-3 G	14.4	16.2	0.000	No
	NP-1 to SG	16.9	21.5	0.000	No
	NP-1 G to SG	12.9	6.0	0.001	No
	NP-2 to SG	9.8	30.1	0.003	No
	NP-2 G to SG	6.5	15.0	0.000	No
3	Anode to SG	7.08 M	-2.929 M	OL	No
	RC-1 G to SG	4.4	15.6	0.002	No
	RC-2 G to SG	4.5	15.7	0.002	No
	RC-3 G to SG	4.5	15.7	0.002	No
	RC-1 G to RC-2 G	15.9	15.9	0.000	No
	RC-1 G to RC-3 G	15.9	15.9	0.000	No
	RC-2 G to RC-3 G	16.0	16.0	0.000	No
	NP-1 to SG	4.4	15.6	0.002	No
	NP-1 G to SG	4.3	15.6	0.002	No
	NP-2 to SG	9.1	28.0	0.003	No
	NP-2 G to SG	2.0	16.5	0.002	No

Note: Continuity check based on the presently accepted criteria.

Electrical Continuity Second Evaluation

Zone	Items Checked	DC ohms Normal	DC ohms Reversed	DC V	Check
1	Anode to SG	-2.991 M	7.44 M	-0.526	No
	RC-1 G to SG	OL	OL	unstable	
	RC-2 G to SG	22.9	-1.5	0.003	No
	RC-3 G to SG	22.9	-1.5	0.003	No
	RC-1 G to RC-2 G	unstable	unstable	unstable	
	RC-1 G to RC-3 G	unstable	unstable	unstable	
	RC-2 G to RC-3 G	14.6	14.6	0.000	No
	NP-1 to SG	-60.6	0.472 K	0.039	No
	NP-1 G to SG	187.6 M	0.376 K	0.040	No
	NP-2 to SG	15.6	22.0	0.001	No
	NP-2 G to SG	11.8	5.9	0.000	No
2	Anode to SG	-1.991 K	2.243 M	0.226	No
	RC-1 G to SG	7.5	11.1	0.000	No
	RC-2 G to SG	11.1	7.6	0.000	No
	RC-3 G to SG	6.9	11.9	0.001	No
	RC-1 G to RC-2 G	14.9	15.0	0.000	No
	RC-1 G to RC-3 G	10.7	20.3	0.001	No
	RC-2 G to RC-3 G	14.4	15.7	0.000	No
	NP-1 to SG	21.4	16.8	0.000	No
	NP-1 G to SG	6.8	11.7	0.001	No
	NP-2 to SG	17.6	33.6	0.002	No
	NP-2 G to SG	22.9	10.3	0.001	No
3	Anode to SG	2.980 K	-1.5	0.225	No
	RC-1 G to SG	16.2	3.4	0.001	No
	RC-2 G to SG	3.3	16.4	0.002	No
	RC-3 G to SG	16.4	3.5	0.001	No
	RC-1 G to RC-2 G	15.6	15.8	0.000	No
	RC-1 G to RC-3 G	15.7	15.7	0.000	No
	RC-2 G to RC-3 G	15.9	15.9	0.000	No
	NP-1 to SG	26.2	13.1	0.001	No
	NP-1 G to SG	3.2	16.3	0.002	No
	NP-2 to SG	29.9	6.5	0.003	No
	NP-2 G to SG	30.0	6.5	0.003	No

Electrical Continuity Second Evaluation (continued)

Zone	Items Checked	DC ohm Normal	DC ohm Reversed	DC V	Check
4	Anode to SG	16.3	16.3	0.000	No
	RC-1 G to SG	16.2	16.2	0.000	No
	RC-2 G to SG	16.4	16.3	0.000	No
	RC-3 G to SG	16.4	16.3	0.000	No
	RC-1 G to RC-2 G	16.2	16.3	0.000	No
	RC-1 G to RC-3 G	16.2	16.3	0.000	No
	RC-2 G to RC-3 G	16.3	16.2	0.000	No
	NP-1 to SG	31.9	16.4	0.062	No
	NP-1 G to SG	9.7	19.9	0.002	No
	NP-2 to SG	25.8	23.3	0.000	No
	NP-2 G to SG	12.7	17.6	0.001	No

Note: Continuity check based on the presently accepted criteria.

Electrical Continuity Third Evaluation

Zone	Items Checked	DC ohm Normal	DC ohm Reversed	DC V	Check
1	Anode to SG	4.01 K	8.24 M	0.560	No
	RC-1 G to SG	13	5.7	0.001	No
	RC-2 G to SG	-2.1	24	-0.003	No
	RC-3 G to SG	-2.1	24	-0.003	No
	RC-1 G to RC-2 G	25.7	6.8	0.003	No
	RC-1 G to RC-3 G	25.7	6.8	0.003	No
	RC-2 G to RC-3 G	14.8	15.0	0.000	No
	NP-1 to SG	-57.5 K	0.699 M	-0.080	No
	NP-1 G to SG	-51.5 K	280	-0.067	No
	NP-2 to SG	1.18 M	-0.951	0.131	No
	NP-2 G to SG	12.3	6.2	0.001	No
2	Anode to SG	26.71 M	-38.63 K	-0.901	No
	RC-1 G to SG	12.1	7.3	0.001	No
	RC-2 G to SG	12.2	7.3	0.001	No
	RC-3 G to SG	13.0	6.4	0.001	No
	RC-1 G to RC-2 G	15.3	15.4	0.000	No
	RC-1 G to RC-3 G	14.4	16.4	0.000	No
	RC-2 G to RC-3 G	14.5	16.4	0.000	No
	NP-1 to SG	1.59 K	0.980 K	0.042	No
	NP-1 G to SG	6.0	13.1	-0.000	No
	NP-2 to SG	-40 K	0.442 M	-0.052	No
	NP-2 G to SG	10.7	20.2	-0.001	No
3	Anode to SG	2.22 M	-1.53 M	-0.225	No
	RC-1 G to SG	19.2	0.9	0.003	No
	RC-2 G to SG	19.5	1.0	0.003	No
	RC-3 G to SG	19.5	1.0	0.003	No
	RC-1 G to RC-2 G	15.9	16.3	0.000	No
	RC-1 G to RC-3 G	15.9	16.2	0.000	No
	RC-2 G to RC-3 G	16.0	16.3	0.000	No
	NP-1 to SG	2.3 K	2.7 K	-0.003	No
	NP-1 G to SG	0.9	19.3	-0.002	No
	NP-2 to SG	-51.1 K	0.573 M	-0.006	No
	NP-2 G to SG	0.2	18.8	-0.002	No

Electrical Continuity Third Evaluation (continued)

Zone	Items Checked	DC ohm Normal	DC ohm Reversed	DC V	Check
4	Anode to SG	16.5	16.5	0.000	No
	RC-1 G to SG	16.7	16.5	0.000	No
	RC-2 G to SG	16.8	16.5	0.000	No
	RC-3 G to SG	16.8	16.8	0.000	No
	RC-1 G to RC-2 G	16.6	16.7	0.000	No
	RC-1 G to RC-3 G	16.5	16.7	0.000	No
	RC-2 G to RC-3 G	16.6	16.7	0.000	No
	NP-1 to SG	380	0.810 K	-0.023	No
	NP-1 G to SG	16.5	167	0.000	No
	NP-2 to SG	16.6	16.8	0.000	No
	NP-2 G to SG	0.770	0.430 K	0.014	No

Note: Continuity check based on the presently accepted criteria.

Electrical Continuity Fourth Evaluation

Zone	Items Checked	DC ohms Normal	DC ohms Reversed	DC V	Check
1	Anode to SG	3.1 K	6.24 M	0.456	No
	RC-1 G to SG	12	5.7	0.001	No
	RC-2 G to SG	-1.8	24	-0.003	No
	RC-3 G to SG	-1.7	24	-0.003	No
	RC-1 G to RC-2 G	22.3	6.8	0.003	No
	RC-1 G to RC-3 G	25.7	6.9	0.003	No
	RC-2 G to RC-3 G	14.6	15.0	0.000	No
	NP-1 to SG	-57.5 K	0.733 M	-0.080	No
	NP-1 G to SG	-51.5 K	276	-0.067	No
	NP-2 to SG	1.18 M	-0.951	0.131	No
	NP-2 G to SG	12.3	6.7	0.001	No
2	Anode to SG	26.71 M	-38.63 K	-0.901	No
	RC-1 G to SG	12.1	7.3	0.001	No
	RC-2 G to SG	12.4	7.1	0.001	No
	RC-3 G to SG	13.0	6.4	0.001	No
	RC-1 G to RC-2 G	15.2	15.6	0.000	No
	RC-1 G to RC-3 G	14.4	15.3	0.000	No
	RC-2 G to RC-3 G	14.5	16.4	0.000	No
	NP-1 to SG	1.59 K	0.980 K	0.004	No
	NP-1 G to SG	6.0	13.1	-0.000	No
	NP-2 to SG	-40 K	0.441	-0.052	No
	NP-2 G to SG	10.5	20.8	-0.001	No
3	Anode to SG	1.98M	-1.43M	-0.225	No
	RC-1 G to SG	19.2	0.9	0.003	No
	RC-2 G to SG	19.5	1.0	0.003	No
	RC-3 G to SG	19.5	1.0	0.003	No
	RC-1 G to RC-2 G	15.9	16.3	0.000	No
	RC-1 G to RC-3 G	13.2	16.2	0.000	No
	RC-2 G to RC-3 G	16.0	16.3	0.000	No
	NP-1 to SG	2.1K	2.7 K	-0.003	No
	NP-1 G to SG	0.9	19.3	-0.002	No
	NP-2 to SG	-51.1 K	0.	-0.006	No
	NP-2 G to SG	0.2	18.8	-0.002	No

Electrical Continuity Fourth Evaluation (continued)

Zone	Items Checked	DC ohms Normal	DC ohms Reversed	DC V	Check
4	Anode to SG	16.5	16.5	0.000	No
	RC-1 G to SG	17.9	16.5	0.000	No
	RC-2 G to SG	16.5	16.5	0.000	No
	RC-3 G to SG	16.8	16.8	0.000	No
	RC-1 G to RC-2 G	16.6	16.9	0.000	No
	RC-1 G to RC-3 G	16.5	16.7	0.000	No
	RC-2 G to RC-3 G	16.6	16.7	0.000	No
	NP-1 to SG	376	0.810 K	-0.023	No
	NP-1 G to SG	16.5	167	0.000	No
	NP-2 to SG	18.9	16.8	0.000	No
	NP-2 G to SG	0.770	0.430 K	0.014	No

Note: Continuity check based on the presently accepted criteria.

APPENDIX H: FIELD EVALUATION AC RESISTANCE DATA

AC Resistance First Evaluation

Zone	Element Tested	AC Resistance, ohm
1	Anode to SG	5.5
	RC-1 to RC-1 G	10 K
	RC-2 to RC-2 G	3.4 K
	RC-3 to RC-3 G	1.7 K
	NP-1 to NP-1 G	11
	NP-2 to NP-2 G	11
2	Anode to SG	4.6
	RC-1 to RC-1 G	870
	RC-2 to RC-2 G	420
	RC-3 to RC-3 G	10 K
	NP-1 to NP-1 G	11
	NP-2 to NP-2 G	11
3	Anode to SG	4.6
	RC-1 to RC-1 G	1.7 K
	RC-2 to RC-2 G	10 K
	RC-3 to RC-3 G	10 K
	NP-1 to NP-1 G	11
	NP-2 to NP-2 G	11

AC Resistance Second Evaluation

Zone	Element Tested	AC Resistance, ohm
1	Anode to SG	6
	RC-1 to RC-1 G	8 K
	RC-2 to RC-2 G	3 K
	RC-3 to RC-3 G	1.4 K
	NP-1 to NP-1 G	10
	NP-2 to NP-2 G	10
2	Anode to SG	4.5
	RC-1 to RC-1 G	1.5 K
	RC-2 to RC-2 G	510
	RC-3 to RC-3 G	11 K
	NP-1 to NP-1 G	10
	NP-2 to NP-2 G	10
3	Anode to SG	4.6
	RC-1 to RC-1 G	2 K
	RC-2 to RC-2 G	11 K
	RC-3 to RC-3 G	11 K
	NP-1 to NP-1 G	10
	NP-2 to NP-2 G	10
4	RC-1 to RC-1 G	10 K
	RC-2 to RC-2 G	10.1 K
	RC-3 to RC-3 G	2.5 K
	NP-1 to NP-1 G	10
	NP-2 to NP-2 G	10

AC Resistance Third Evaluation

Zone	Element Tested	AC Resistance, ohm
1	Anode to SG	3.2
	RC-1 to RC-1 G	4.2 K
	RC-2 to RC-2 G	3.1 K
	RC-3 to RC-3 G	1.7 K
	NP-1 to NP-1 G	720
	NP-2 to NP-2 G	2 K
2	Anode to SG	4.5
	RC-1 to RC-1 G	1.6 K
	RC-2 to RC-2 G	520
	RC-3 to RC-3 G	11 K
	NP-1 to NP-1 G	900
	NP-2 to NP-2 G	530
3	Anode to SG	4.4
	RC-1 to RC-1 G	2.5 K
	RC-2 to RC-2 G	10 K
	RC-3 to RC-3 G	10 K
	NP-1 to NP-1 G	2.3 K
	NP-2 to NP-2 G	300
4	Anode to SG	15.0
	RC-1 to RC-1 G	3.3 K
	RC-2 to RC-2 G	11 K
	RC-3 to RC-3 G	2.4 K
	NP-1 to NP-1 G	440
	NP-2 to NP-2 G	490

AC Resistance Fourth Evaluation

Zone	Element Tested	AC Resistance, ohm
1	Anode to SG	6.9
	RC-1 to RC-1 G	4 K
	RC-2 to RC-2 G	3.2 K
	RC-3 to RC-3 G	2.8 K
	NP-1 to NP-1 G	9.5
	NP-2 to NP-2 G	9.5
2	Anode to SG	4.4
	RC-1 to RC-1 G	4.9 K
	RC-2 to RC-2 G	510
	RC-3 to RC-3 G	9 K
	NP-1 to NP-1 G	9.5
	NP-2 to NP-2 G	9.4
3	Anode to SG	4.5
	RC-1 to RC-1 G	2.6 K
	RC-2 to RC-2 G	9 K
	RC-3 to RC-3 G	9 K
	NP-1 to NP-1 G	9.6
	NP-2 to NP-2 G	9.8
4	Anode to SG	0.52
	RC-1 to RC-1 G	9.1 K
	RC-2 to RC-2 G	9 K
	RC-3 to RC-3 G	9 K
	NP-1 to NP-1 G	9.2
	NP-2 to NP-2 G	9.4

APPENDIX I: FIELD EVALUATION NULL PROBE DATA

Null Probe Testing First Evaluation

Zone	mV Drop Across 10-ohm Resistor				Current Density, mA/ft^2 steel			
	NP-1		NP-2		NP-1		NP-2	
	On	Off	On	Off	On	Off	On	Off
1	0.3	-1.0	2.2	0.0	0.2	-0.6	1.2	0.0
2	6.2	-0.5	18.0	-1.3	3.4	-0.3	10.0	-0.7
3	1.1	0.0	7.7	0.7	0.6	0.0	4.3	0.4
4	1.1		0.7		0.6	0.0	0.4	0.0

Null Probe Testing Second Evaluation

Zone	mV Drop Across 10-ohm Resistor				Current Density, mA/ft^2 steel			
	NP-1		NP-2		NP-1		NP-2	
	On	Off	On	Off	On	Off	On	Off
1	1.1	-0.1	2.9	0.0	0.3	-0.1	0.8	0.0
2	5.7	0.0	12.7	0.5	1.6	0.0	3.5	0.1
3	1.3	0.0	7.9	0.0	0.4	0.0	2.2	0.0
4	2.8	0.0	1.0	0.0	0.8	0.0	0.3	0.0

Null Probe Testing Fourth Evaluation

Zone	MV Drop Across 10-ohm Resistance				Current Density, mA/ft^2 steel			
	NP-1		NP-2		NP-1		NP-2	
	On	Off	On	Off	On	Off	On	Off
1	0.4	-0.5	2.3	0.3	0.1	-0.2	0.6	0.1
2	6.1	0.1	12.5	2.1	1.7	0.1	3.5	0.6
3	1.3	0.2	1.0	0.0	0.4	0.1	0.3	0.0
4	2.4	1.0	0.7	0.5	0.7	0.5	0.2	0.2

APPENDIX J: FIELD EVALUATION POLARIZATION DECAY TESTING

Polarization Decay Testing First Evaluation

Zone	Instant-Off mV			Static Potential, mV 4-hr			Depolarization, mV 4-hr		
	RC-1	RC-2	RC-3	RC-1	RC-2	RC-3	RC-1	RC-2	RC-3
1	U	-572	-640	-30	-351	-442		221	198
2	-720	-660	-512	-675	-492	-394	45	168	118
3	-500	-460	-516	-142	-320	-237	358	140	279

Notes:
U: unstable

Polarization Decay Testing Second Evaluation

Zone	Instant-Off mV			Static Potential, mV 1-hr			2.5-hr			4-hr		
	RC-1	RC-2	RC-3	RC-1	RC-2	RC-3	RC-1	RC-2	RC-3	RC-1	RC-2	RC-3
1	U	-512	-620	U	-445	-490	U	-430	-475	U	-420	-464
2	-808	-748	-332	-794	-554	-420	-778	-531	-392	-768	-518	-374
3	-528	-608	-404	-166	-403	-331	-151	-374	-301	-145	-354	-282
4	-310	-390	-354	-200	-327	-248	-203	-319	-240	-245	-295	-228

Notes:
U: unstable

Polarization Decay Testing Second Evaluation (continued)

Zone	Depolarization, mV								
	1-hr			2.5-hr			4-hr		
	RC-1	RC-2	RC-3	RC-1	RC-2	RC-3	RC-1	RC-2	RC-3
1		67	130		82	145		92	156
2	14	194	*	30	217	28	40	230	46
3	362	205	73	377	234	103	383	254	122
4	110	63	106	107	71	114	65	95	126

Notes:

*: 1-hr static potential in lieu of instant-off potential for calculation of depolarization potential

Polarization Decay Testing Third Evaluation

Zone	Instant-Off mV			Static Potential, mV								
				15-min			30-min			1-hr		
	RC-1	RC-2	RC-3	RC-1	RC-2	RC-3	RC-1	RC-2	RC-3	RC-1	RC-2	RC-3
1	140	-580	-528	-219	-510	-498	-232	-494	-490	-238	-481	-478
2	-748	-748	-184	-819	-622	-422	-816	-609	-408	-811	-591	-388
3	-520	-600	-444	-225	-441	-345	-200	-426	-379	-173	-403	-355
4	-510	-380	-323	-405	-333	-266	-394	-327	-257	-382	-321	-248

Polarization Decay Testing Third Evaluation (continued)

Zone	Static Potential, mV											
	2-hr			3-hr			4-hr			17.5-hr		
	RC-1	RC-2	RC-3	RC-1	RC-2	RC-3	RC-1	RC-2	RC-3	RC-1	RC-2	RC-3
1	-228	-460	-464	-218	-443	-452	-201	-426	-435	-88	-363	-379
2	-805	-570	-367	-800	-558	-353	-795	-550	-342	-753	-479	-279
3	-154	-376	-327	-148	-359	-310	-143	-347	-296	-127	-260	-209
4	-380	-304	-227	-356	-292	-213	-284	-286	-207	-56	-280	-184

Polarization Decay Testing Third Evaluation (continued)

Zone	Depolarization, mV											
	15-min			30-min			1-hr			2-hr		
	RC-1	RC-2	RC-3	RC-1	RC-2	RC-3	RC-1	RC-2	RC-3	RC-1	RC-2	RC-3
1	*	70	30	-13	86	38	-19	99	50	-9	120	64
2	*	126	*	3	139	14	8	157	34	14	178	55
3	79	159	99	320	174	65	347	197	89	366	224	117
4	177	47	57	116	53	66	128	59	75	130	76	96

Notes:

*: 15-min static potential in lieu of instant-off potential for calculation of depolarization potential

Polarization Decay Testing Third Evaluation (continued)

Zone	Depolarization, mV								
	3-hr			4-hr			17.5-hr		
	RC-1	RC-2	RC-3	RC-1	RC-2	RC-3	RC-1	RC-2	RC-3
1	1	137	76	18	154	93	131	217	149
2	19	190	69	24	198	80	66	269	143
3	372	241	134	377	253	148	393	340	235
4	154	88	110	226	94	116	454	100	139

Polarization Decay Testing Fourth Evaluation

Zone	Instant-Off, mV					
	Manual			Peak Hold		
	RC-1	RC-2	RC-3	RC-1	RC-2	RC-3
1	-145	-615	-543	-160	-496	-488
2	-730	-663	-444	-524	-684	32
3	-472	-445	-539	-472	-248	-116
4	-390	-328	-311			

Polarization Decay Testing Fourth Evaluation (continued)

Zone	Static Potential, mV											
	15-min			30-min			1-hr			2-hr		
	RC-1	RC-2	RC-3	RC-1	RC-2	RC-3	RC-1	RC-2	RC-3	RC-1	RC-2	RC-3
1	-333	-515	-515	-330	-505	-509	-322	-491	-501	-310	-475	-491
2	-712	-550	-391	-709	-535	-378	-703	-515	-358	-696	-491	-334
3	-216	-407	-374	-192	-393	-358	-171	-374	-337	-155	-350	-310
4	-316	-280	-250	-310	-272	-239	-302	-261	-227	-284	-250	-214

Polarization Decay Testing Fourth Evaluation (continued)

Zone	Static Potential, mV								
	3-hr			4-hr			22-hr		
	RC-1	RC-2	RC-3	RC-1	RC-2	RC-3	RC-1	RC-2	RC-3
1	-303	-465	-483	-296	-457	-477	-225	-366	-415
2	-691	-482	-322	-688	-476	-315	-650	-384	-241
3	-150	-338	-293	-146	-327	-282	-119	-253	-202
4	-276	-244	-206	-267	-240	-201	-266	-228	-180

Polarization Decay Testing Fourth Evaluation (continued)

Zone	Depolarization, mV											
	15-min			30-min			1-hr			2-hr		
	RC-1	RC-2	RC-3	RC-1	RC-2	RC-3	RC-1	RC-2	RC-3	RC-1	RC-2	RC-3
1	*	100	28	3	110	34	11	124	42	23	140	52
2	18	113	53	21	128	66	27	148	86	34	172	110
3	256	38	165	280	52	181	301	71	202	317	95	229
4	74	48	61	80	56	72	88	67	84	106	78	97

Notes:
*: 15-min static potential in lieu of instant-off potential for calculation of depolarization potential

Polarization Decay Testing Fourth Evaluation (continued)

Zone	Depolarization, mV								
	3-hr			4-hr			22-hr		
	RC-1	RC-2	RC-3	RC-1	RC-2	RC-3	RC-1	RC-2	RC-3
1	30	150	60	37	158	66	108	249	128
2	39	181	122	42	187	129	80	279	203
3	322	107	246	326	118	257	353	192	337
4	114	84	105	123	88	110	124	100	131

REFERENCES

1. Federal Highway Administration (FHWA), 1991 Report to Congress, June 1991.

2. FHWA, "1991 Status of the Nation's Highways and Bridges: Conditions, Performance and Capital Investments Requirements," July 1991.

3. Scheffey, C. F., "Bridge Deck Deterioration — A 1981 Perspective," FHWA Memorandum, FHWA Office of Research, December 31, 1981.

4. Emmons, P. H., and Vaysburd, A. M., "Corrosion Protection in Concrete Repair: Myth and Reality," *Concrete International*, Vol. 19, No. 3, March 1997, pp. 47–56.

5. Bennett, J. E., Bushman, J. B., Clear, K. C., Kamp, R. N., and Swiat, W. J., "Cathodic Protection of Concrete Bridges: A Manual of Practice," Strategic Highway Research Program (SHRP), SHRP-S-372, 1993.

6. American Concrete Institute Standard 222R85, "Corrosion of Metals in Concrete," ACI International, Detroit, Michigan, 1985.

7. Broomfield, J. P., "Corrosion of Steel in Concrete: Understanding, Investigation and Repair," E & FN Spon, 1997.

8. Weyers, R. E., Prowell, B. D., Sprinkel, M. M., and Vorster, M., "Concrete Bridge Protection, Repair and Rehabilitation Relative to Reinforcement Corrosion: A Methods Application Manual," SHRP, SHRP-S-360, 1993.

9. Berkeley, K. G. C., and Pathmanaban, S., "Cathodic Protection of Reinforcement Steel in Concrete," Butterworths & Co. Ltd., 1990.

10. Vaca Cortes, E., "Electrochemical Procedures to Rehabilitate Corroded Concrete Structures," master's thesis, The University of Texas at Austin, May 1993.

11. Carello, R. A., Parks, D. M., and Apostolos, J. A., "Development, Testing and Field Application of Metallized Cathodic Protection Coatings on Reinforced Concrete Substructures," FHWA, FHWA/CA/TL-89-04, 1989.

12. Gu, P., Beaudoin, J. J., Tumidajski, P. J., and Mailvaganam, N. P., "Electrochemical Incompatibility of Patches in Reinforced Concrete," *Concrete International*, Vol. 19, No. 8, August 1997, pp. 68–72.

13. Eltech Research Corporation, "Cathodic Protection of Reinforced Concrete: Bridge Elements: A State-of-the-Art Report," SHRP, SHRP-S-337, 1993.

14. Jones, D. A., *Principles and Prevention of Corrosion*, Prentice Hall, Upper Saddle River, NJ, 1996.

15. Nash, P. T., Parker, H. W., and Feingold, R. W., "Cathodic Protection for Reinforced Concrete Bridge Deck — Big Spring," Texas Tech University, Research Study No. 1-10-85-500, 1994.

16. Han, M. K., Snyder, M. J., Simon, P. D., Davis, G. O., and Hindin, B., "Cathodic Protection of Concrete Bridges Components," Quarterly Report SHRP-87-C-102B, April 1989.

17. Manning, D. G., and Schell, H. C., "Early Performance of Eight Experimental Cathodic Protection Systems at the Burlington Bay Skyway Test Site," Transportation Research Record No. 1041, 1985, pp. 23–32.

18. Martin, B. L., and Bennett, J. E., "An Activated Titanium Mesh Anode for the Cathodic Protection of Reinforcing Steel in Concrete," Paper No. 147, National Association of Corrosion Engineers International Corrosion 87, 1987.

19. Kessler, R. J., and Powers, R. J., "Update on Cathodic Protection of Reinforcing Steel in Concrete Marine Substructures," Paper No. 326, National Association of Corrosion Engineers International Corrosion 93, 1993.

20. Perenchio, W. F., Landgren, J. R., and West, R. E., "Cathodic Protection of Concrete Bridge Substructures," Transportation Research Board, National Cooperative Highway Research Program (NCHRP) Report No. 278, 1985.

21. Kundjapur, M., "Cathodic Protection of a Reinforced Concrete Bridge Substructure Using Conductive Paint System Anodes," Paper No. 371, NACE International Corrosion 89, 1989.

22. Bennett, J. E., Schue, T. J., and McGill, G. E., "A Thermal Sprayed Titanium Anode for Cathodic Protection of Reinforced Concrete Structures," Paper No. 504, NACE International Corrosion 95, 1995.

23. Kessler, R. J., and Powers, R. G., "Zinc Metallizing for Galvanic Cathodic Protection of Steel Reinforced Concrete in a Marine Environment," Paper No. 324, NACE International Corrosion 90, 1990.

24. McGill, G. E., Cramer, S. D., Bullard, S. J., Covino, Jr., B. S., and Holcomb, G. R., "Field Application of an Arc-Sprayed Titanium Anode for Cathodic Protection of Reinforcing Steel in Concrete," Interim Report, Oregon Department of Transportation, FHWA, 1996.

25. Funahashi, M., Daily, S. F., and Young, W. T., "Performance of Newly Developed Sprayed Anode Cathodic Protection System," Paper No. 254, NACE International Corrosion 97, 1997.

26. Scannell, W. T., Sohanghpurwala, A. A., Powers, R. G., and Hartt, W. H., "Cathodic Protection of Prestressed Concrete Bridge Pilings in a Marine Environment," Paper No. 305, NACE International Corrosion 94, 1994.

27. Kessler, R. J., Powers, R. G., and Lasa, I. R., "Cathodic Protection Using Zinc Sheet Anodes and an Ion Conductive Gel Adhesive," Paper No. 234, NACE International Corrosion 97, 1997.

28. *Standard Method of Sampling and Testing for Total Chloride Ion in Concrete and Concrete Raw Materials,* AASHTO Designation T 260 (1993), American Association of State Highway and Transportation Officials.

29. *Selecting and Specifying Concrete Surface Preparation for Sealers, Coatings and Polymer Overlays,* Guideline No. 03732 (1996), International Concrete Repair Institute.

30. *Guide for the Protection of Steel with Thermal Sprayed Coatings of Aluminum and Zinc and their Alloys and Composites,* ANSI/AWS C2.18-93 (1993), American Welding Society.

31. "Electrical Indication of Concrete's Ability to Resist Chloride Ion Penetration," AASHTO Designation T 277 (1993), American Association of State Highway and Transportation Officials.

32. "Guide Specification for Cathodic Protection of Concrete Bridge Decks," AASHTO-AGC-ARTBA, Task Force #29, July 1993.

33. Islam, M., Scannell, W. T., Sohanghpurwala, A. A., and Gonzalez, A., "Evaluation of a Cathodic Protection System — Wavecus Hill Road Bridge Over I-395, Norwich, Connecticut," CONCORR Inc., 1997.

34. *Cathodic Protection of Reinforcing Steel in Atmospherically Exposed Concrete Structures*, NACE Standard RP0290-90, Item 53072, NACE International, 1990.

35. Draft, CEN European Standard, "Cathodic Protection of Steel in Concrete, Part I: Atmospherically Exposed Concrete."

36. Saguez, A. A., and Powers, R. G., "Low-Cost Sprayed Zinc Galvanic Anode for Control of Corrosion of Reinforcing Steel in Marine Bridge Substructures," SHRP, Contract No. SHRP-88-ID024, 1994.

37. Covino, B. S., Cramer, S. D., Bullard, S. J., Holcomb, G. R., and Collins, W. K., "Consumable and Non-Consumable Thermal Spray Anodes for Impressed Current Cathodic Protection of Reinforced Concrete Structures," Paper No. 658, NACE International Corrosion 98, 1998.

38. Personal Communication with Mr. Gary Peters, Senior Project Engineer, Matrices, Inc., August 28, 1998, Marathon, FL.

39. American Welding Society. Zinc Thermal Coatings for Reinforced Concrete.